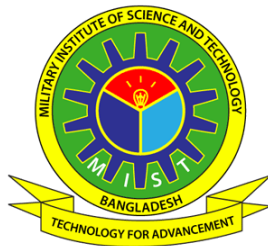


Effect of Back Surface Layer Material on Efficiency of Dual Junction Photovoltaic Solar Cell

A thesis submitted to the Department of EECE, MIST
in partial fulfillment of the requirements
for the degree of
**Bachelor of Science in Electrical, Electronic and Communication
Engineering**

by
TAHMIDA HASNAT FERDOUS: 201416033
FATEMA TUZ ZOHRA: 201416036
TASIN NUSRAT: 201416038



**Department of Electrical, Electronic and Communication Engineering
(EECE)**

**Military Institute of Science and Technology
(MIST)**

**Mirpur Cantonment, Dhaka, Bangladesh
December, 2017**

The thesis titled “Effect of Back Surface Layer Material on Efficiency of Dual Junction Photovoltaic Solar Cell” submitted by TAHMIDA HASNAT FERDOUS: 201416033, FATEMA TUZ ZOHRA: 201416036, TASIN NUSRAT: 201416038, Session: 2016-2017 has been accepted as satisfactory in partial fulfillment of the requirements for the degree of BACHELOR OF SCIENCE IN ELECTRICAL, ELECTRONIC AND COMMUNICATION ENGINEERING on December, 2017.

APPROVAL OF THE SUPERVISOR

Yeasir Arafat

Associate Professor

Department of Electrical, Electronic and Communication Engineering
BUET, Dhaka-1205, Bangladesh.

DECLARATION

It is hereby declared that this thesis or any part of it has not been submitted elsewhere for the award of any degree or diploma.

Signatures of candidates

(TAHMIDA H. FERDOUS)

(FATEMA TUZ ZOHRA)

(TASIN NUSRAT)

DEDICATION

To Our Parents

ABSTRACT

Effect of Back Surface Layer Material on Efficiency of Dual Junction Photovoltaic Solar Cell

TAHMIDA HASNAT FERDOUS, FATEMA TUZ ZOHRA, TASIN NUSRAT

Single junction Si solar cell is the most convenient and cost-effective photovoltaic cell but has restriction in the efficiency. Globally in this field, everyone is trying to utilize renewable energy and introduced the upgraded model of solar cell – multi-junction solar cell. The comparison between the single junction solar cell and the multi-junction solar cell and also designing the model of an effective cell is the purpose of this thesis. The main focus is on the dual junction solar cell as the illustration of a multijunction solar cell. The entire analysis is done by TCAD simulation tool. Concentrating on the bandgap of the dual-junction solar cell, it found more effective in the comparison of the single junction solar cell. This thesis represents the improvement of InGaP-GaAs dual junction solar cell by introducing a new back surface material AlGaAs and also considering the doping concentration of wider bandgap InGaP. The findings of this thesis show that with a new BSF material (AlGaAs), InGaP-GaAs dual junction solar cell can reach 40.02% efficiency. This demonstrates that a significant amount of efficiency can be achieved by III-V multi-junction solar cell.

ACKNOWLEDGEMENTS

In this wonderful journey of intensive learning, at first and foremost we would like to express our sincere and heartfelt gratitude to our respected thesis supervisor Yeasir Arafat Sir, Associate Professor, Department of Electrical and Electronic Engineering, BUET, for his immense support, guidance and encouragement throughout the long period. We are grateful not only for supervising with initial guidance that opens the door for thesis but also introducing us with various software and inspiring us to learn them which can be used for lot of other purposes ahead. We are also thankful for the fact that his substantial amount of research and study in PV solar cell and hetero junctions inspired us to work in this particular area. So far we learnt a lot related to this topic due to his motivation. We are fortunate for his ever ready attitude to render help in his busy schedule of multiple important tasks.

During the work progress in thesis his insight was invaluable in clarifying issues regarding the use of TCAD simulation tools. Again we are fortunate to get his academic theory class on hetero junction and semiconductor and we are grateful for that as it helped a lot in our field of topic. We had great experience of pleasure and knowledge to work under his supervision for the accomplishment of this thesis dissertation. As a teacher and mentor he taught more than we can give credit for. We are also very grateful to our Department of EECE, MIST for its excellent curriculum and providing us with enriched faculty.

Above all we would like to thank Almighty to bless us with such a learned and knowledgeable supervisor and such parents of us for their profound support in the pursuit of this thesis and help us to go on with our educational success.

**TAHMIDA HASNAT FERDOUS
FATEMA TUZ ZOHRA
TASIN NUSRAT**

MIST, Dhaka

December, 2017

TABLE OF CONTENTS

DECLARATION	iii
DEDICATION	iv
ABSTRACT	v
ACKNOWLEDGEMENTS	vi
LIST OF TABLES	xii
LIST OF FIGURES	xiii
LIST OF ABBREVIATIONS	xviii
LIST OF SYMBOLS	xix
INTRODUCTION.....	01
CHAPTER ONE: PHOTOVOLATIC TECHNOLOGY.....	07
1.1 INTRODUCTION.....	07
1.2 HISTORY.....	07
1.3 WORKING PRINCIPLEOF PHOTOVOLATIC CELL.....	09
1.4 TYPES OF PHOTOVOLATIC TECHNOLOGY.....	11
1.4.1 Thin Film PV.....	11
1.4.2 Concentrated PV (CPV).....	12
1.5 MATERIALS DEVELOPMENT.....	14
1.6 THE NEXT GENERATION PHOTO VOLTAICS CELL.....	14
1.7 RECENT IMPROVEMENTS ON PHOTO VOLTAIC CELL.....	15
1.7.1 Improved Efficiency.....	15
1.7.2 Solar Fabrication Using Maximum Voltage from CdTe.....	16
1.7.3 Introducing Hot Solar Cell.....	16
1.7.4 Developing Home Systems in Bangladesh.....	18
1.7.5 Installation and Plans by BPDB.....	19

1.7.4	High Concentration Photovoltaic (HPCV) for Better Efficiency.....	19
1.7.7	New Solar Panel in Market 2017.....	20
1.8	CONCLUSION.....	21
CHAPTER TWO: FILL FACTOR AND EFFICIENCY OF SOLAR CELL.....		22
2.1	INTRODUCTION.....	22
2.2	THEORATICAL APPROACH.....	22
2.2.1	Equivalent Circuit.....	23
2.2.2	Short Circuit Current.....	24
2.2.3	Open Circuit Voltage.....	24
2.2.4	Maximum Power.....	25
2.2.5	Fill Factor.....	25
2.3	PRACTICAL APPROACH.....	25
2.3.1	Solar Area Mounting and Tracking (general process of improvement).....	26
2.3.2	Improving Solar Efficiency Using Simple Mirrors and Cooling Method.....	29
2.3.3	Improved Perovskite Solar Cell.....	31
2.3.4	High Efficient Ga-As-P Solar Cell.....	33
2.3.5	A Micro-scale Photo Voltaic Cell “Solar Glitter”.....	35
2.4	LATEST INNOVATIONS.....	37
2.4.1	Cool Earth Inflatable Solar Balloons.....	37
2.4.2	“Hairy” Thin Film Solar Cell.....	38
2.4.3	Moth Eyes Biomimicry for Solar Cell.....	39
2.4.4	Printed Solar Panel “Nanosolar”.....	39
2.4.5	Conversion of Infrared Light to Electricity.....	40
2.4.6	19.9% Efficient CIGS Solar Cell.....	40
2.4.7	CdTe Solar Panel.....	41
2.5	CONCLUSION.....	42

CHAPTER THREE: ANALYSIS TECHNIQUE.....	43
3.1 INTRODUCTION.....	43
3.2 OPERATING PRINCIPLE OF SOLAR CELL.....	43
3.3 RESEARCH WORK RELATED TO SOLAR DEVICES.....	44
3.3.1 Analytical Method.....	45
3.3.1.1 Solar cell parameters.....	45
3.3.1.2 Effect of Rs and Rsh Parameters.....	48
3.3.2 Effect of Temperature.....	52
3.4 SIMULATION ANALYSIS.....	55
3.4.1 Why We Need the Simulation.....	56
3.4.2 TCAD (Technology Computer Aided Design).....	57
3.4.2.1 TCAD Tools.....	57
3.4.2.2 TCAD simulation process.....	58
3.4.2.3 TCAD work flow.....	59
3.4.3 Parameters That Can be changed.....	60
3.5 EXPERIMENTAL ANALYSIS.....	61
3.5.1 For The Measurement of External Characteristics.....	62
3.5.2 Measurement in Different Wavelengths.....	64
3.5.3 For the Measurement of Internal Characteristics.....	65
3.5.4 Measurement of Electro-luminescence.....	68
3.6 RESULT FOUND FROM THESE METHODS.....	69
3.7 CONCLUSION.....	71
CHAPTER FOUR: TCAD SIMULATION SOFTWARE.....	72
4.1 INTRODUCTION.....	72
4.2 VIRTUAL WAFER WEB.....	74
4.3 SIMULATION for ELECTRICAL CHARACTERISTICS.....	74
4.3.1 Functions of The Simulator.....	75
4.3.2 Inputs and Outputs.....	76
4.4 MODEL EXTRACTOR.....	76
4.5 DEVICE EDITOR.....	78

4.6	VISUALIZATION TOOL.....	79
4.7	SIMULATION PROCEDURE OVERVIEW.....	80
4.7.1	Modes of Operation.....	80
4.7.2	Starting with Model Extractor.....	80
4.7.3	Syntax.....	81
4.7.4	Structure Specification.....	82
4.7.5	Result Analysis.....	86
4.7.6	Extract Description.....	87
4.8	CONCLUSION.....	88
	CHAPTER FIVE: TYPE OF SOLAR CELLS SELECTED FOR SIMULATION.....	89
5.1	INTRODUCTION.....	89
5.2	SILICON SOLAR CELL.....	89
5.3	WORKING PRINCIPLE.....	90
5.4	DUAL JUNCTION SOLAR CELL.....	92
5.5	PARAMETERS TO BE CONSIDERED.....	93
5.5.1	Lattice Match.....	93
5.5.2	Bandgap.....	94
5.5.2.1	Structure.....	96
5.5.2.2	Metal contacts.....	97
5.5.2.3	Window layer and back surface layer.....	97
5.5.2.4	Anti reflective (AR) coating.....	98
5.5.2.5	Tunnel junction.....	99
5.6	CONCLUSION.....	101
	CHAPTER SIX: RESULT AND DISCUSSION.....	102
6.1	INTRODUCTION.....	102
6.2	SINGLE JUNCTION SOLAR CELL.....	104
6.2.1	Boron doped silicon solar cell.....	104
6.2.2	Arsenic doped silicon solar cell.....	108
6.2.3	Phosphorus doped silicon solar cell.....	111

6.3	COMPARISON BETWEEN DIFFERENTLY DOPED SOLAR CELL.....	114
6.4	DUAL JUNCTION SOLAR CELL.....	115
6.4.1	InGaP-GaAs Dual Junction Solar Cell.....	116
6.4.2	AlGaAs-GaAs Dual Junction Solar Cell.....	117
6.5	InGaP-GaAs DUAL JUNCTION SOLAR CELL.....	120
6.5.1	Concentration Increasing.....	120
6.5.2	Concentration Decreasing.....	123
6.5.3	Changing Back Surface.....	126
6.5.4	Increasing Concentration for New BSF.....	128
6.5.5	Concentration Change for Wider Bandgap for New BSF.....	129
6.5.6	Concentration Change for Wider Bandgap for New BSF.....	130
6.6	CONCLUSION	132
	CHAPTER SEVEN: CONCLUSION AND RECOMMENDATION.....	133
7.1	CONCLUSION.....	133
7.2	RECOMMENDATION FOR FUTURE WORK.....	134
	REFERENCES.....	135

LIST OF TABLES

Name	Caption	Page
Table 1.1	Efficiencies achieved from HCPV	20
Table 2.1	Azimuth Angle by heading	26
Table 2.2	Change In Current, Voltage and Power With Respect To Concentration and Cooling	30
Table 2.3	Hourly Comparison of Three Methods	31
Table 3.1	TCAD Tools	57
Table 3.2	Typical physical parameters that can changed as input	60
Table 3.3	Typical layer parameters that can changed as input	61
Table 3.4	Confirmed single-junction terrestrial cell and sub module efficiencies measured under the global AM1.5 spectrum (1000 W/m) at 25°C	69
Table 3.5	Confirmed multiple-junction terrestrial cell and sub module efficiencies measured under the global AM1.5 spectrum (1000 W/m) at 25°C	70
Table 5.1	Bandgap of some semiconductor	94
Table 6.1	Important parameters for boron doped silicon solar cell	106
Table 6.2	Important parameters for arsenic doped silicon solar cell	109
Table 6.3	Important parameters for phosphorus doped silicon solar cell	112
Table 6.4	Efficiency for increasing concentration	123
Table 6.5	Efficiency for decreasing concentration	126
Table 6.6	Efficiency between new BSF & reference model	127
Table 6.7	Efficiency for both increasing & decreasing concentration of new BSF model	130
Table 6.8	Model proposed for highest efficiency	132

LIST OF FIGURES

Name	Caption	Page
Figure 1.1	The photoelectric effect	8
Figure 1.2	Formation of the photovoltaic device	9
Figure 1.3	(a) Layers of photo voltaic cell	10
	(b) Energy absorption of photo voltaic cell	
Figure 1.4	Diagram of a typical crystalline silicon solar cell	11
Figure 1.5	Thin-film PV	12
Figure 1.6	Concentrated-film PV	13
Figure 1.7	A Ga-As solar cell	15
Figure 1.8	Black carbon nano tubes sit on top of the absorber-emitter layer, collecting energy across the solar spectrum and converting it to heat	17
Figure 2.1	Incident light on a typical PN Solar Cell	23
Figure 2.2	Equivalent circuit for solar cell	24
Figure 2.3	Sun's position; Azimuth and Altitude	27
Figure 2.4	A 2-Axis Tracking system	28
Figure 2.5	Improving efficiency of Perovskite solar cell	32
Figure 2.6	Solar panel	33
Figure 2.7	Microsystems-enabled photovoltaics	35
Figure 2.8	Solar glitter	36
Figure 2.9	Solar balloons	37
Figure 2.10	A forest of GaAs nanowires growing on a silicon substrate.	38
Figure 2.11	X-Ray of solar panels arranged inspired by moth eyes	39
Figure 2.12	Nano solar	40

Name	Caption	Page
Figure 2.13	Electromagnetic spectrum	40
Figure 2.14	Cadmium Telluride Solar Panels	41
Figure 2.15	CdTe thin film morphology	42
Figure 3.1	Cross section of a solar cell	44
Figure 3.2	Standard equivalent circuit of single junction solar cell	46
Figure 3.3	General view of solar cell idealized curve	46
	Different mathematical models for PV module	
	a) ideal model	
Figure 3.4	b) Rs-model and	48
	c) Rp-model.	
Figure 3.5	Obtaining Resistances from the I-V Curve	50
Figure 3.6	Effect of shunt resistance on the current–voltage characteristics	50
Figure 3.7	Effect of series resistance on the I-V characteristics of a solar cell	51
Figure 3.8	Effect of temperature on I-V curve	52
Figure 3.9	I-V curve for different temperature	55
Figure 3.10	Simulation Work Flow	60
Figure 3.11	Experimental setup and schematic for the electric characteristics of solar panel	63
Figure 3.12	Characteristics of solar panel	64
Figure 3.13	Solar irradiance Vs wavelength curve	65
Figure 3.14	Internal characteristics of solar cell	66-67
Figure 3.15	Change of I-V characteristics curve with increasing incident light	67
Figure 3.16	(a) Schematic of the experimental setup (b) Schematic structure if the GaInp/GaAs/Ge - 3junction solar cell	68

Name	Caption	Page
	(c) Output of the experiment EL Vs current density curve	
Figure 4.1	TCAD software	73
Figure 4.2	Virtual Wafer Fabrication Environment	74
Figure 4.3	Flow of simulation	76
Figure 4.4	Model extractor Commands Menu	77
Figure 4.5	Device editor Base Window Display	78
Figure 4.6	Visualization tool output	79
Figure 5.1	Structure of silicon solar cell	90
Figure 5.2	Cross-sectional view of Si solar cell	91
Figure 5.3	Referenced model for Si solar cell	92
Figure 5.4	Graph for BandgapVs Lattice Constant	93
Figure 5.5	Irradiance on different bandgap cell	95
Figure 5.6	Design of multi-junction solar cell & the efficiency vsBandgap	96
Figure 5.7	Structure of multi-junction solar cell	97
Figure 5.8	(a) Layers and band diagram of a window layer. The surface recombination is reduced	98
	(b) Layers and band diagram of a BSF layer. The scattering of carriers is reduced.	
Figure 5.9	a) structure of MJ solar cell	99
	b) diode sequence of the junctions	
Figure 5.10	Layers and band diagram of the tunnel junction. Because the length of the depletion region is narrow and the band gap is high, electrons can tunnel	100
Figure 5.11	Reference model of dual junction solar cell	101
Figure 6.1	Summary of the analysis	103
Figure 6.2	I-V Characteristics Curve Boron Doped Silicon Solar Cell	105

Name	Caption	Page
Figure 6.3	I-V Characteristics Curve Boron Doped Silicon Solar Cell (mirrored for calculation)	105
Figure 6.4	P-V curve of Boron Doped Silicon Solar Cell	106
Figure 6.5	Graph of efficiency for different concentration	107
Figure 6.6	Graph of fill factor for different concentration	107
Figure 6.7	I-V characteristics of Arsenic doped Si solar cell	108
Figure 6.8	P-V characteristics of Arsenic doped Si solar cell	109
Figure 6.9	Efficiency for different concentration	110
Figure 6.10	Fill Factor for different concentration	110
Figure 6.11	I-V curve for phosphorus doped Si solar cell	111
Figure 6.12	P-V curve for phosphorus doped Si solar cell	112
Figure 6.13	Efficiency for different concentration	113
Figure 6.14	Fill factor for different concentration	113
Figure 6.15	Efficiency for different material doped Si solar cell	114
Figure 6.16	Fill factor for different material doped Si solar cell	115
Figure 6.17	Schematic diagram of InGaP-GaAs solar cell	116
Figure 6.18	I-V characteristic of InGaP-GaAs dual junction solar cell	116
Figure 6.19	P-V characteristic of InGaP-GaAs dual junction solar cell	117
Figure 6.20	Schematic diagram of AlGaAs-GaAs dual junction solar cell	117
Figure 6.21	I-V characteristics of AlGaAs-GaAs dual junction solar cell	118
Figure 6.22	P-V characteristics of AlGaAs-GaAs dual junction solar cell	118
Figure 6.23	Efficiency for different solar cell	119
Figure 6.24	Fill factor for different solar cells	119

Name	Caption	Page
Figure 6.25	I-V curve for high concentration	120
Figure 6.26	P-V curve for high concentration	121
Figure 6.27	I-V characteristics for higher concentration	121
Figure 6.28	P-V characteristics for higher concentration	122
Figure 6.29	I-V curve for decreasing concentration	123
Figure 6.30	P-V curve for decreasing concentration	124
Figure 6.31	I-V curve for lower concentration	124
Figure 6.32	P-V curve for lower concentration	125
Figure 6.33	I-V curve for new BSF	126
Figure 6.34	P-V curve for new BSF	127
Figure 6.35	I-V curve for increasing concentration in new BSF model	128
Figure 6.36	P-V curve for increasing concentration in new BSF model	128
Figure 6.37	I-V curve for decreasing concentration in new BSF model	129
Figure 6.38	P-V curve for decreasing concentration in new BSF model	129
Figure 6.39	I-V curve for new BSF high concentration of InGaP	130
Figure 6.40	P-V curve for new BSF high concentration of InGaP	131

LIST OF ABBREVIATIONS

PV	Photovoltaic
CPV	Concentrated PV
HCPV	High Concentration Photovoltaic
REN21	Renewable Energy Policy Network for 21 st Century
AC	Alternating Current
DC	Direct Current
AM	Air Mass
FF	Fill Factor
LM	Lattice Matched
E-L	Electro- luminescence
TCAD	Technology Computer Aided Design
IC	Integrated Circuit
VWF	Virtual Wafer Web
MJ	Multi junction
DJ	Double junction
B	Boron
As	Arsenic
P	Phosphorus
GaAs	Gallium Arsenide
SiGe	Silicon Germanium
CdTe	Cadmium telluride
GaAsP	Gallium Arsenide Phosphide
InGaP	Indium Gallium Phosphide
AlGaAs	Aluminium Gallium Arsenide
InAlGaP	Indium Aluminium Gallium Phosphide

LIST OF SYMBOLS

Symbols	Description
I	Current passing through the load
I_s	Saturation current
I_{pv}	Light current
I_{sc}	Short circuit current
I_{MP}	Maximum current in the load line
V_{oc}	Open circuit voltage
V_{MP}	Maximum voltage in the load line
U	Voltage
Φ_T	Thermal potential
P_{in}	Input power
P_{MP}	Power achieved from maximum value of both current & voltage
R_s	Series resistance
R_{sh}	Shunt resistance
A	Area
k	Boltzmann's constant, 1.38×10^{23} J/K
E_g	Bandgap energy
η	Efficiency
e, q	charge on an electron, 1.6×10^{-19} Coulombs
L	Minority carrier diffusion length
n_i	Intrinsic carrier concentration
N_A	Concentration of acceptor layer
N_D	Concentration of donor layer
T	Temperature

INTRODUCTION

In contrast to nonrenewable energy source the renewable sources are infinite, environmental friendly. Most renewable energy comes either directly or indirectly from the sun. Solar energy is a renewable free source of energy that is sustainable and totally inexhaustible, unlike fossil fuels that are finite. It is also a non-polluting source of energy and it does not emit any greenhouse gases when producing electricity. It is one of the most promising sources of energy due to its potential of energy independence through power provided by the sun. Sunlight or solar energy, can be used directly for heating and lighting homes and other buildings, for generating electricity, and for hot water heating, solar cooling, and a variety of commercial and industrial uses.

For the purpose of utilizing the renewable source of solar energy large solar cells also known as photovoltaic cells are used to power homes, are single cells grouped together and electrically connected and packaged in a frame. The PV effect was observed as early as 1839 by Alexandre Edmund Becquerel, and was the subject of scientific inquiry through the early twentieth century. In 1954, Bell Labs in the U.S. introduced the first solar PV device that produced a useable amount of electricity, and by 1958, solar cells were being used in a variety of small-scale scientific and commercial applications. The energy crisis of the 1970s saw the beginning of major interest in using solar cells to produce electricity in homes and businesses, but prohibitive prices (nearly 30 times higher than the current price) made large-scale applications impractical.

Industry developments and research in the following years made PV devices more feasible and a cycle of increasing production and decreasing costs began which continues even today.

The intensive use of these cells works by converting sunlight into electricity using semiconductors that absorb sunlight and create electricity through the transfer of

electrons. The PV cell is composed of semiconductor material, which combines some properties of metals and some properties of insulators. That makes it uniquely capable of converting light into electricity. When light is absorbed by a semiconductor, photons of light can transfer their energy to electrons, allowing the electrons to flow through the material as electrical current. This current flows out of the semiconductor to metal contacts and then makes its way out to power home and the rest of the electric grid. The cost of PV has dropped dramatically as the industry has scaled up manufacturing and incrementally improved the technology with new materials.

Most modern solar cells are made from either crystalline silicon or thin-film semiconductor material. Silicon cells are more efficient at converting sunlight to electricity, but generally have higher manufacturing costs. Thin-film materials typically have lower efficiencies, but can be simpler and less costly to manufacture. A specialized category of solar cells - called multi-junction or tandem cells - are used in applications requiring very low weight and very high efficiencies, such as satellites and military applications. All types of PV systems are widely used today in a variety of applications.

Many researches and analysis have been carried out in order to improve efficiency through practical and theoretical methods. Various types of photovoltaic cells such as silicon photovoltaics, polycrystalline thin-film photovoltaics, III-V compound photovoltaics are used recent technology. Thin-Film is a second generation solar cell that is made by depositing one or more thin layers, or thin film (TF) of photovoltaic material on a substrate, such as glass, plastic or metal.

Understanding how solar efficiency is measured helps to determine if we are getting the most from the system .The conversion efficiency of a photovoltaic (PV) cell, or solar cell, is the percentage of the solar energy shining on a PV device that is converted into usable electricity. Improving this conversion efficiency is a key goal of research and helps make PV technologies cost-competitive with conventional sources of energy.

Single junction solar cells have just one p-n junction, as against multi-junction solar cells which consist of more than one p-n junction and thus exhibit better efficiency. High-efficiency multi junction devices use multiple bandgaps, or junctions, that are tuned to absorb a specific region of the solar spectrum to create solar cells having improved efficiencies.. The limiting efficiency, known as the Shockley-Queisser limit, arises from the fact that the open-circuit voltage (V_{oc}) of a single-bandgap solar cell with non-concentrated sunlight is limited by the bandgap of the absorbing material and that photons with energies below the bandgap are not absorbed. Photons that have energies greater than the bandgap are absorbed, but the energy greater than the bandgap is lost as heat.

Multi junction devices use a high-bandgap top cell to absorb high-energy photons while allowing the lower-energy photons to pass through. A material with a slightly lower bandgap is then placed below the high-bandgap junction to absorb photons with slightly less energy (longer wavelengths). Typical multi junction cells use two or more absorbing junctions, and the theoretical maximum efficiency increases with the number of junctions. Early research into multi junction devices leveraged the properties of semiconductors comprised from elements in the III and V columns of the Periodic table, such as indium gallium phosphate (InGaP), gallium indium arsenide (GaInAs), and gallium arsenide (GaAs).

Within this context, the potential of designing a dual-junction cell to improve and boost the efficiency we will focus on working with back surface material of the cell which is the main aim of this thesis. We study the efficiency, fill factor of single and various dual junction solar cells by changing various parameters using TCAD simulation tools.

LITERATURE REVIEW

Electrical power is the driving source of the world. It has made the world faster and has made our life a lot easier. It is one of the important parameter that decides the development of any country. The more the resourceful a country in power generation the more developed that country is. From the early times till now there have been a massive variety of fuels used in electrical power generation. Coal and Oil were the primary elements which were used as fuels. In the last century due to the high environmental pollution these fuels were discouraged to use. Then the usage of natural gases were introduced which were less harmful to environment. With the rapid growth of civilization importance of electricity have extended to an unimaginable point. In order to cope up with that the natural resources of the earth is being decreased to an alarming rate. That's the point where the renewable energy sources are being focused.

Renewable resources can be used repeatedly and are also replaced without damaging the eco-logical balance of the environment. People are now trying to use this resource as much as they can because of their recycling facility. They are also eco-friendly. That's why all the governments are emphasizing on electricity generation based on renewable resource according to a study by Tyagi, Rahims and Selvaraj (2013). In this sector the PV technology as well as the solar devices covering a significant area. Tyagi, Rahims and Selvaraj (2013) have given us the clear view of how fast the PV technology is developing in their journal. According to them the annual growth rate of this industry is 35-40% per year. And we have also known that "Efficiency" is the prime parameter of this technology in order to survive the market. This is the reason a large number of researches are undergoing just to upgrade the efficiency of the solar devices. Their studies also give us the rough idea about the power generation by utilizing solar power. The numerical value is around 18GW to 27GW. From their study we came to know that the European countries are holding the first place in using solar energy. Meanwhile the developing countries in Asia are showing good improvement in installing PV modules.

There are a number of techniques introduced in order to increase the efficiency of photo-voltaic cells. The theoretical approaches are not as new as the practical approach. They follow the normal principle of p-n junctions. Primarily people have tried to capture as much as sunlight in order to get the maximum efficiency. But there comes the heating problem which ends up in enlarging the losses. There is also the atmospheric obstacle the cloudy weather. Usually the 2-axis tracking system, in which solar modules are directly pointed at the sun, improves the overall capture of solar energy by a given area of modules by 30–50% versus modules with a fixed tilt. But a study conducted by Kelly and Gibson (2009) shows that on sunny days the direct sunshine accounts for up to 90% of the total solar energy, with the other 10% from diffuse (scattered) solar energy. They have also found out the solution of this problem. According to them during overcast conditions, tilting a solar module or sensor away from the zenith reduces the irradiance relative to a horizontal configuration, in which the sensor or module is pointed toward the zenith (horizontal module tilt), and thus receives the highest amount of this isotropically-distributed sky radiation. Another important outcome of their study is during cloudy periods we show that a horizontal module orientation increases the solar energy capture by nearly 50% compared to 2-axis solar tracking during the same time period.

Apart from experimental setup their numerous research are going to improve the semiconductor material and layering used in solar devices. Perovskite solar cells are one kind of special tandem solar cells where efficiency up to 19% have been recorded where normal solar cells gives 15% efficiency at the highest. On the latest work done by Zhou and Yang (2017), they have claimed that by controlling the formation of the perovskite layer and careful choices of other materials, suppressing carrier recombination in the absorber, facilitated carrier injection into the carrier transport layers, and maintained good carrier extraction at the electrodes they have recorded a efficiency of 19.3% by applying reverse bias scan. Another research had done by Nayak, Dutta and Mishra (2015) leads us to a new way of efficiency improvement for multi-junction solar cells. According to their study by using a double layer BSF in other words by increasing the thickness of the BSF layer a significant rise of efficiency is being observed. Their study shows that a double layer BSF for top cell

with their varied thicknesses is investigated on GaInP/GaAs DJ solar cell using the computational numerical modelling TCAD tool Silvaco ATLAS. For this optimized cell structure, the maximum conversion efficiency is 34.52% (1 sun) and 39.15% (1000 suns).

For our assessment we shall analyse the most efficient solar device through simulation. We shall start our work by observing various characteristics of single junction solar cells. Then we shall expand our boundary to multi (dual) junction solar cells. For observing their different characteristics and also to calculate the important parameters we shall be using SILVACO as or TCAD tools. Silvaco is a very reliable simulator offering layout driven 3D process simulation, 3D device simulation, parallel SPICE circuit simulation etc. We shall be using Silvaco TCAD incorporating Deckbuild, Athena, Atlas, Devedit which is necessary for our efficiency parameter calculation. In order to operate this powerful simulator we shall be following the manuals available ATLAS User's Manual, ATHENA User guide and Manual with Examples etc. The video tutorial related to this simulator will be helpful as well.

CHAPTER ONE

PHOTOVOLTAIC TECHNOLOGY

1.1 INTRODUCTION

The basic of Photovoltaic (PV) materials and devices is it can convert sunlight into electrical energy and also does not store energy without a battery. It uses both direct and indirect isolation.

Photovoltaic panels are actually made of cells. One cell is actually a single PV device. Its size is comparatively very small and can produce one or two watts of power which is not enough to implant. So they are connected in chains for better power output that can be used as modules or panels.

For the establishment of a PV system the panels can be used individually, or we can connect few to form arrays. Either individual or arrays is then connected to the electrical grid. Whether the electric power is large or small, the PV system is developed such a way so that it can meet all the requirements.

1.2 HISTORY

In 1839, a French physicist, Edmund Bequerel, first observe the photoelectric effect. He noted that at the presence of light some materials would produce small amounts of electric current.

The whole PV technology is based on the photo electronic effect which is the invention of Albert Einstein, in 1905. In 1954 the world meet the first photovoltaic module which was just a solar battery. The first application was in spacecraft. In the 1960s, the space industry first use this technology to provide power. By this technology was established, as it was profitable it got the reliability, moreover the cost was also decreased. In 1970's the PV technology gained recognition as a power source for different non-space applications.

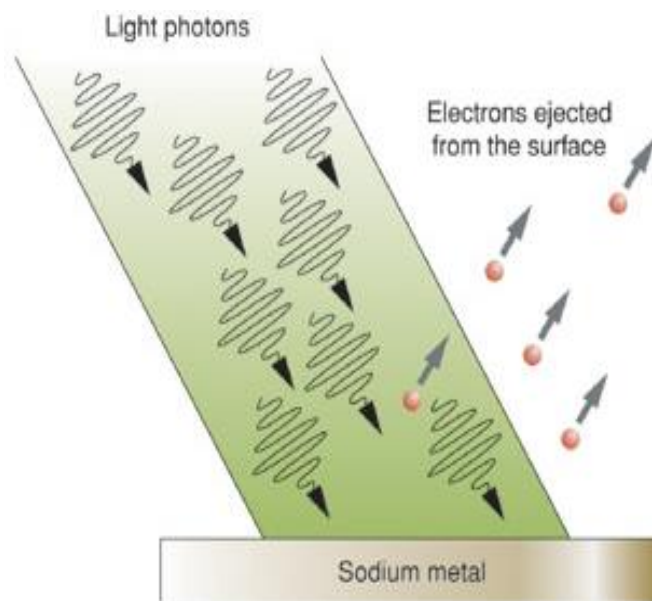


Figure 1.1 Photoelectric effect

Now this time the largest PV systems are located in California. The two most acknowledged power stations are the Solar Star PV power station which produces 550 megawatts. The Desert Sunlight Solar Farm another recognized station also reach the target of 550 megawatts.

1.3 WORKING PRINCIPLE of PHOTOVOLTAIC CELL

The operation of a basic photovoltaic cell is made of the same kinds of semiconductor materials, such as silicon. These are also called solar cell. The general structure for solar cells, is a thin semiconductor wafer. It is specially developed to form an electric field, positive on one side and negative on the other. The procedure is such a way that is:

- When light is emitted the photon strikes the solar cell the semiconductor is ionized and we got outer electrons as they were break free of their atomic bonds.
- It is the mechanism of semiconductor that the electrons are bound to flow in one direction.
- To form an electrical circuit the electrical conductors must be attached to the positive and negative sides.
- Thus we can capture the electrons in the form of an electric current. This electric current is actually the electricity which can be used to power system.

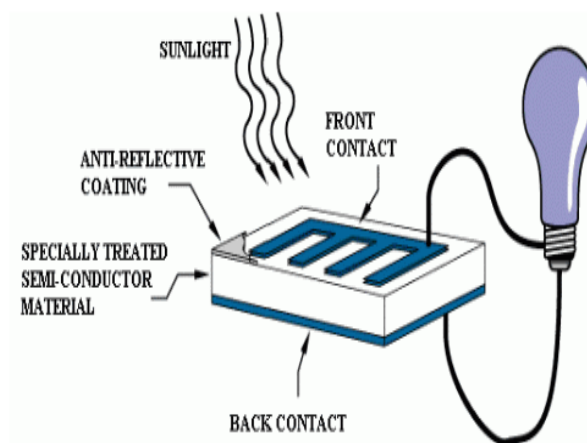
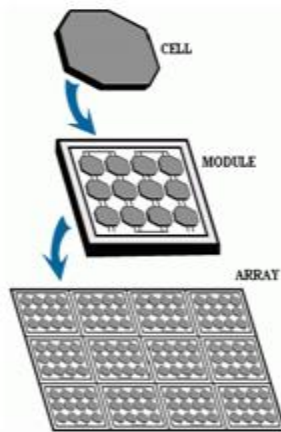
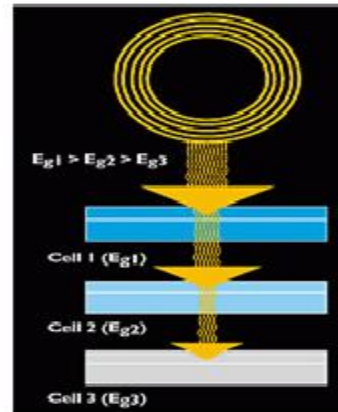


Figure 1.2 Formation of the photovoltaic device

- To form a photovoltaic module to supply electricity at a certain voltage a number of solar cells electrically connected to each other in chains and mounted a support structure or a plane.
- The voltage is commonly 12 volts and the current produced is directly dependent on the amount of light strikes the module.
- For the purpose of more electricity we need multiple modules as the larger the area, the more electricity will be produced. The modules can be wired together to form an array.
- These Photovoltaic modules can produce any required voltage and current combination. The modules or the arrays produce direct-current (dc) electricity. So the modules can be connected in both series and parallel arrangements which is highly beneficial for the system.



(a)



(b)

Figure 1.3 (a) Layers of photo voltaic cell (b) Energy absorption of photo voltaic cell[1]

But typically in case of another formation of solar cells like crystalline silicon solar cell are not 100% efficient in Diagram. It happened because of reflection. Some of the light spectrum is reflected back. Also there are some cases like infrared is too weak that it can't create electricity and again ultraviolet rays can't produce electricity, it rather creates heat energy [2].

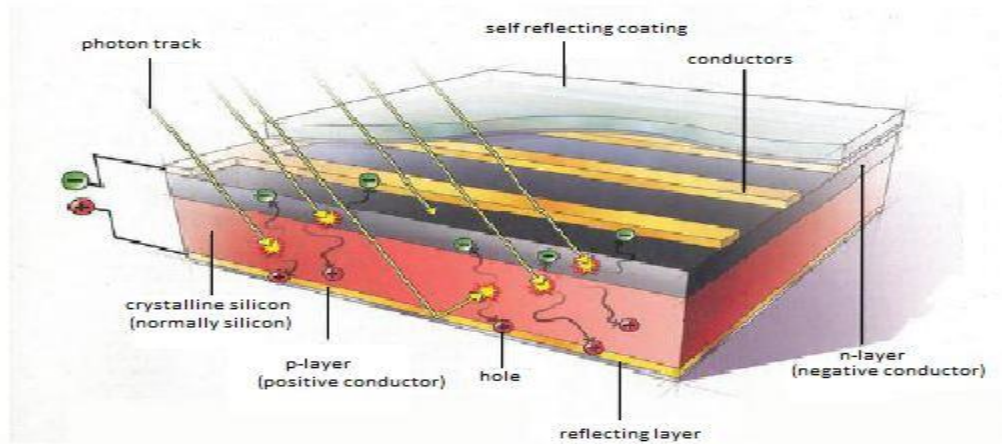


Figure 1.4 Diagram of a typical crystalline silicon solar cell

1.4 TYPES OF PHOTOVOLTAIC TECHNOLOGY

There are some other kinds of photovoltaic technology in addition to crystalline silicon. Here some of these are briefly described.

1.4.1 Thin-Film PV

Now-a-days it is one of the most fast growing technology. The motto of this PV is mainly become cost effective, cheaper than crystalline silicon modules. An important note is direct sunlight is not needed here. The formation of this PV panels is it can

convert sunlight into electricity. They do not require direct sunlight. The PV panels can generate energy regardless of where the light source is located. For this, they use solar trackers to fix or track the sun light.

The general procedure is to track the sun light from East to West during the day time. It is done by a single-axis array. The importance of this type is that it can provide 30%–40% more energy which is greater than a fixed array. Moreover output power is also more uniform. They use light sensors or computer programming so that unnecessary tracking movement can be avoided.[3]

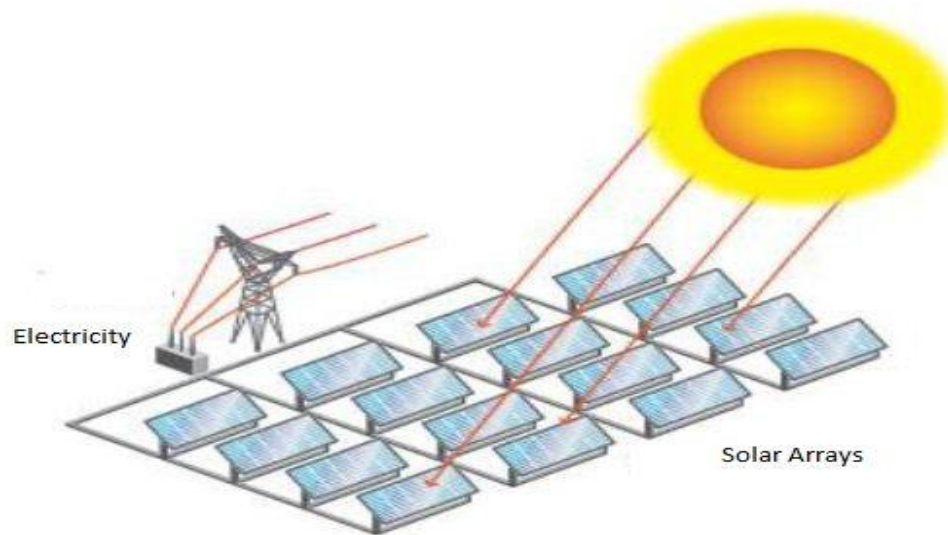


Figure 1.5 Thin-film PV

1.4.2 Concentrated PV (CPV)

These PV arrays are found in the desert southwest in the US. Its tracking system is more effective and for this technology direct sunlight is needed. The technology is quite complicated than thin-film technology, but this one is more efficient is higher than the previous one as we get more photons in this arrangement.

The basic of this technology is to use inexpensive materials like mirror or plastic lenses to track the sun energy and focus it onto PV solar cells. So this technology is cost efficient also. Another formation of it is multi-junction PV solar cell.

It is different from the thin-film modules. First of all it is highly beneficial than thin-film. It has also other good sides also. But this system needs vast space which is not available always.

The main reason for using CPV is to reduce the number of solar cell material. So that while decreasing the size and number of solar cell this technology can increase the power output.[4]

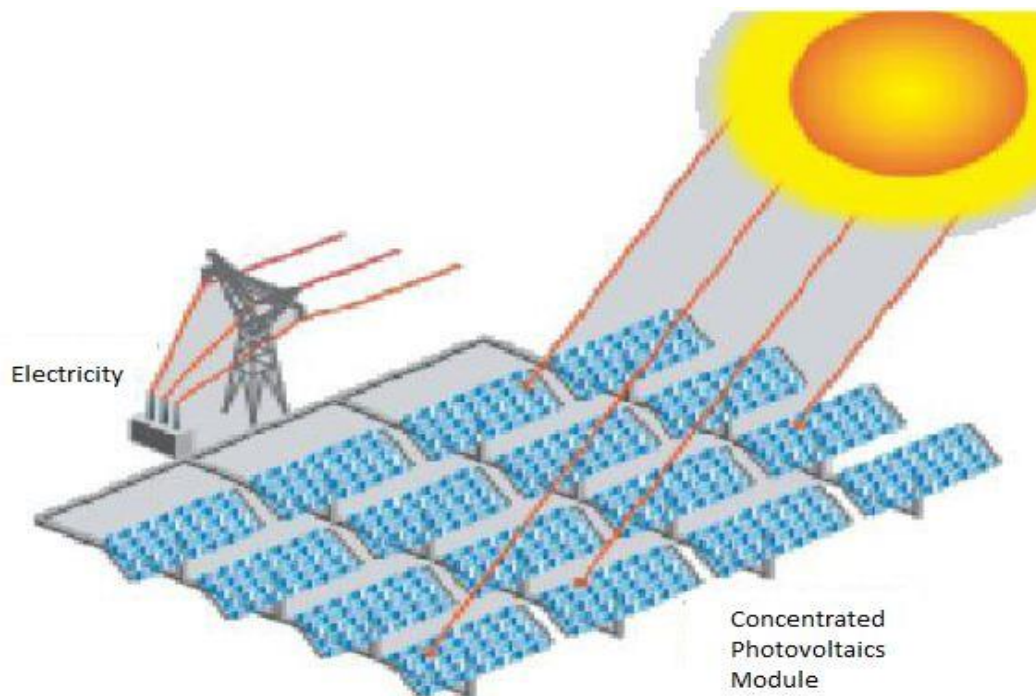


Figure 1.6 Concentrated-film PV

1.5 MATERIALS DEVELOPMENT

Photovoltaic performance is heavily dependent on the properties of materials. In particular, the active layers of solar cells require long carrier diffusion lengths and bulk material must be defect-free, surfaces and grain boundaries must be passivated. Fundamental materials research, of materials, grain boundaries, surfaces and passivating materials can always be justified in this context. Although it seems unlikely that any future developments of known materials can produce as tep-change in headline efficiencies, improvements in production yield or stability can be expected and research emphasis needs to be on materials produced by large-volume tools. An exceptional case for materials developments can be made for semiconductor in polymers, where the vast parameter space and inherent simplicity of device fabrication allows for considerable optimization and optimism. More complex ‘materials’ developments might also include the development of optical materials, plasmonic materials, quantum dots and bandgap-engineering materials.

1.6 THE NEXT GENERATION PHOTO VOLTAICS

The approach to photovoltaic is completely breaking the mold of previous solar cell technologies. By redefining the materials, architectures, and fabrication processes of solar cells, scientists aim to drastically reduce the cost and improve the efficiency of both inorganic and organic photovoltaic. Researchers are always trying to find newer combination of materials in order to make more efficient photovoltaics.

Latest technologies are also being invented. Now inorganic technology provides a process to make the most efficient solar materials (Gallium Arsenide) flexible and cost-effective for broader applications, while the organic photovoltaic technology focuses on developing the next generation of solar, unencumbered by today's limitations and burdensome cost structure.

The photovoltaics open an era of unlimited scope for energy source. Everyone from their respective position are trying heart and soul to make this renewable energy available for everyone. [5]

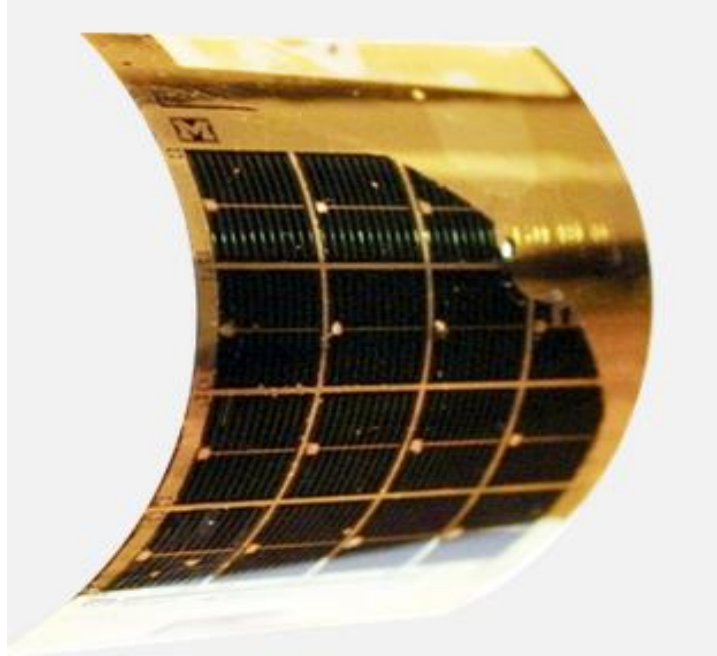


Figure 1.7 Ga-As solar cell

1.7 RECENT IMPROVEMENTS ON PV CELL

In today's fast expanding solar industry there are some constant improvements and innovations on solar technology in recent years.

1.7.1 Improved Efficiency:

Researchers at the Technion-Israel Institute of Technology have introduced a breakthrough technology in 2016 that improved the efficiency of photovoltaic cells

by nearly 70 percent which was a key for overcoming current technological limitations to utilizing solar power to meet the world's energy consumption demands. Their technology was based on an intermediate process that occurs between sunlight and the photovoltaic cell where the photoluminescence material used absorbs radiation from the sun which converts the heat and light from the sun into an "ideal" radiation, that illuminates the photovoltaic cell. As a consequence, higher conversion efficiency was ensured and the device's efficiency was increased from 30% to 50%. [6]

1.7.2 Solar Fabrication Using Maximum Voltage from CdTe:

Again Researchers of the U.S. Department of Energy's National Renewable Energy Laboratory in collaboration with Washington State University and the University of Tennessee have reached a critical milestone in solar cell fabrication. The work was based on improving the maximum voltage available from a cadmium telluride (CdTe) solar cell, overcoming a practical limit that has been pursued for six decades and ensured to ratchet up its efficiency. Silicon solar cell occupy the major portion in solar cell market with high manufacturing cost. Their work on CdTe offered a low cost alternative with better performance in hot, humid weather and under low light.

They placed a small number of phosphorus atoms on tellurium lattice sites and carefully formed ideal interfaces between materials with different atomic spacing to complete the solar cell which improved the CdTe conductivity and carrier lifetime each in terms of magnitude enabling the fabrication of CdTe solar cells with an open-circuit voltage that broke the 1-volt barrier for the first time. [7]

To ensure the purity the researchers mix, prepare and vacuum-seal the materials in an industry-standard clean room. The innovation provided electricity at lower cost than fossil fuels.

1.7.3 Introducing Hot Solar Cell:

One of the most recent researches in this year has been introduced by a team of MIT scientists termed as 'Hot Solar Cell'. It is based on converting heat to focused beams of light, a new solar device creating cheap and continuous power. The one of the most major drawbacks of photo-voltaics is the losses due to light falling on the cells. The source of the photo-voltaics is the sunlight which brings photon along with heat. This heat adds to the losses of the cells along with other losses. This heat is also a huge obstacle in usage of these cells in the hot countries. Because of the warm environment this cells cannot function work properly and the efficiency rate decreases along with the increament of losses. So this invention is a major step in increasing the flexibility of the photo-voltaics cell.[8]

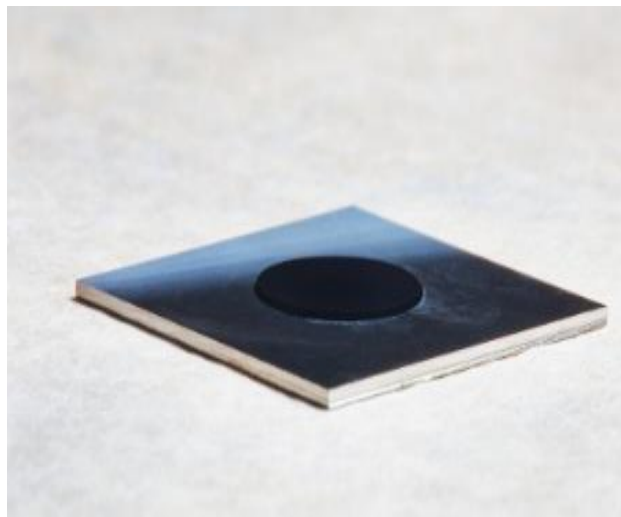


Figure 1.8 Black carbon nano tubes sit on top of the absorber-emitter layer, collecting energy across the solar spectrum and converting it to heat.

The focus is on building a different sort of solar energy device that uses inventive engineering and advances in materials science to capture far more of the sun's energy. The scheme is to first turn sunlight into heat and convert it back into light, but now focused within the spectrum that solar cells can use. While various researchers have been giving attention to solar thermo photovoltaic for years, the MIT device is the

first one to absorb more energy than its photovoltaic cell alone, demonstrating that the approach could dramatically increase efficiency.

The MIT device is still a crude and not fully processed prototype, operating at just 6.8 percent efficiency but with various enhancements it could be roughly twice as efficient as conventional photovoltaic.

The researchers are also exploring methods to utilize other strength of solar thermo photovoltaic. As heat is easier to store than electricity, it should be possible to divert excess amounts generated by the device to a thermal storage system that can be used to convert into electricity in the absence of shining sun.

If the researchers can incorporate a storage device and increase efficiency levels, the system could one day deliver clean, cheap and continuous solar power.

1.7.4 Developing Home System in Bangladesh:

The Statesman/ANN News Desk - A new report that shows Bangladesh is a world leader in the use of solar panels, "clean stoves" and biogas plants.[9]

With four million of the systems set up so far, the country is also at the forefront of nations using clean stoves and biogas plants, and promoting the cause of renewable energy that constitutes a fifth of the world's final power consumption as well as providing opportunities for people as a potential employment source.

Currently, 2.86 per cent of all power generated in the country comes from renewable energy, including solar power, according to power and energy ministry data.

The report noted that the complicated process of providing electricity access through grid extension alone is becoming obsolete, as new business models and technologies enables the development of off-grid markets.

According to the REN21 report, Bangladesh also emerged as 5th in installing clean cooking stoves with gradual increased use of the improved stoves. Five lakhs clean

cooking stoves were installed in 2014 in Bangladesh, which rose to seven lakhs the next year. Bangladesh reduced its import duty on improved stoves by 10 per cent, making the stoves more cost-competitive, the report observed.

According to the REN21 report, Bangladesh also emerged as 5th in installing clean cooking stoves with gradual improvements on stoves. The report also highlighted that Bangladesh belongs in the list of top five countries to have installed domestic biogas plants. The number of biogas plants stands at 45,610 in Bangladesh.

1.7.5 Installation and Plans by BPDB:

Bangladesh Power Development Board (BPDB) has also been installing solar based power plants in different areas of the country. BPDB installed 900 KW capacity grid connected Wind Plant at Muhuri Dam area of Sonagazi in Feni. Another project of 1000 KW Wind Battery Hybrid Power Plant at Kutubdia Island was completed in 2008 which consists of 50 Wind Turbines of 20 kW capacities each. [10]

BPDB has plans to setup 7.5 MW off Grid Wind-Solar Hybrid System with HFO/Diesel Based Engine Driven Generator in Hatiya Island, Noakhali. Apart from that, IDCOL has financed 9 bio-gas based power plants, having total capacity of 618 KW and two rice-husk based power plants having total capacity of 650 KW in the country.

1.7.6 High Concentration Photovoltaic (HCPV) for Better Efficiency:

HCPV is appropriate for areas having high direct normal irradiance. The light on small solar cells is focused by using concentrating optics. The standard Concentration level is above 400 suns. Various designs available in HCPV system for commercial purpose. High efficiencies are ensured.

Table1: Efficiencies achieved from HCPV[11]

Efficiencies	Lab Record	Commercial
Solar Cell	46%(ISE, Soitec, CEA)	38-43%
Mini module	43.4% (ISE)	N.A.
Module	38.9%(Soitec)	27-33%
System	N.A.	25-29%

1.7.7 New Solar Panel in Market 2017:

The solar panel manufacturers are developing solar panels to serve the purpose for both energy generation and aesthetic improved property for homeowners.[12]

Frameless solar panels

Many major manufacturers are producing frameless solar panels. Due to the lack of suitable mounting problem that can work without a frame the manufacturers are producing specialized mounting apparatus to match their frameless panels.

Clear solar panels

Glass solar panels are an innovative technology in various ways as in addition to being more visually attractive, glass panels are more durable than a typical silicon cell panel. These panels are significantly more resistant to fire hazard and also are less prone to erosion.

Tesla solar tiles

According to the demonstration at Tesla’s launch event, these solar tiles are significantly more durable than the standard roof materials commonly used nowadays. The solar roof product is designed to blend in with typical roof aesthetics and so will come in the following product lines: Tuscan glass, slate glass, textured glass and smooth glass tiles.

Product improvement: Double-sided solar panels

These type of panels can utilize sunlight through both surfaces of the panel. The simple assertion is that double-sided panels can capture light as it reflects off of the roof or ground surface below the panel. Due to the fact that the majority of roofs in the residential market are black, in order to maximize light reflection, the installers will typically paint a white border around the solar panel system before installation.

PV integration: solar panel with inverter

The concept of a solar panel plus inverter is a great innovation in the solar industry. The inverter installation and connection can add significant time to a typical rooftop installation. To solve this problem, innovative manufacturer is making inverters that are easily attachable to the back of the panel. The modules are schemed be manufactured with small inverters already in place on the back of the panel.

1.8 CONCLUSION

The importance of PV technology is on increase as a source of power energy. Because the driving energy of this system is the solar power, the most reliable form solar energy. The technology which was first launched successfully in the seventy's has come across a long distance making new improvements on its way. Various types of techniques were invented to make the PV technology highly efficient, sometimes changing the arrangements of the modules or by developing the element materials. This new technology has also been introduced lately. The most initial step was to install almost five lakhs solar driven cooking stoves in 2014. Recently necessary steps are being taken in order to add solar grids with the national grading system of the country. Different types of solar panels are now available here. We are very much hopeful about the bright future of PV technology in Bangladesh.

CHAPTER TWO

POWER FILL FACTOR EFFICIENCY OF SOLAR CELL

2.1 INTRODUCTION

The conversion efficiency of a solar cell is the ratio of the maximum output generated power to the input or incident power can be generalized by η . The main focus of any research on solar cell is to how the efficiency can be increased of the solar cells, so that the maximum usage of solar power can be possible. Solar is one of the most significant sources of energy. That's why importance of photovoltaic is on the rise. There are some of certain parameters by which the efficiency of solar cell can be influenced. A lot of research on is going on this aspect. Both theoretical and practical experiments are under process. Here we will describe both perspectives.

2.2 THEORATICAL APPROACH

When a solar cell is illuminated by sun-light, photons energy of the incident light is converted to direct current electricity through the process of photovoltaic effect of the solar cell. Incident light causes electron-hole pairs to be generated in the semiconductor and there is increase in the concentration of minority carriers in the depletion region. These photo-generated carriers cause the flow of photo-generated current, I-photons. When the junction is in the open-circuit condition, no net current can flow inside the p-n junction, thus the current resulting from the flux of photo-

generated and thermally generated carriers is balanced by the opposite recombination current.

If a load is connected between the electrodes of the illuminated p-n junction, some fraction of the photo-generated current will flow through the external circuit. The potential difference between the n-type and p-type regions will be lowered by a voltage drop over the load.

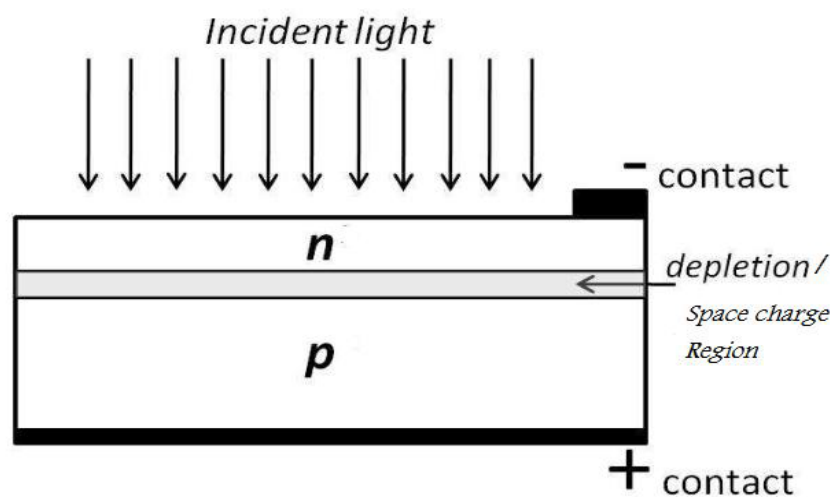


Figure 2.1 Incident light on a typical PN Solar Cell [2]

2.2.1 Equivalent Circuit

An equivalent circuit is an alternative way to represent any type of electrical system by means of various electrical elements like resistors, capacitors, inductors, diodes, transistors etc. It is not the actual arrangement of the system but gives a clear idea about the functions. It is the first step in designing and improvement of any electrical system. Here we are representing a solar cell through an equivalent circuit.

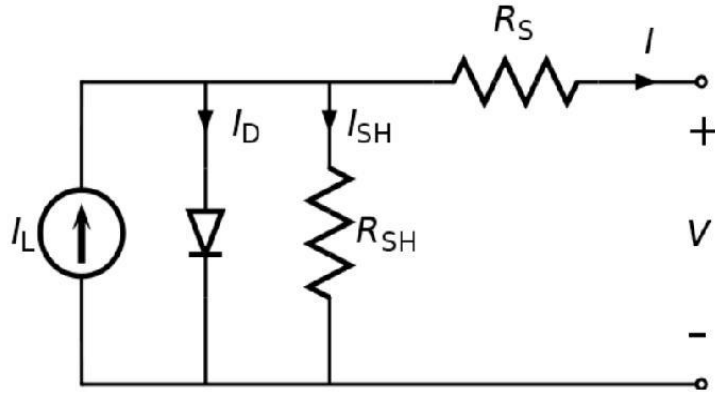


Figure 2.2 Equivalent circuit for solar cell

2.2.2 Short Circuit Current

This is the current that flows through the external circuit when the electrodes of a solar cell are short circuited. The short-circuit current is dependent on the incident photon flux density and the spectrum of the incident light.

For standard solar cell parameter measurements:

The spectrum is standardized to the AM1.5

For Ideal solar cell, $I_{sc} = I_{photon}$

And this is the maximum current delivery capacity of the solar cell at any given illumination level. The maximum ISC is found by the integration of the spectrum distributions from low wavelengths up to the maximum wavelength at which electron-hole pairs can be generated for a given semiconductor.

2.2.3 Open Circuit Voltage

The open-circuit voltage is the voltage at which no current flows through the external circuit; i.e. when the solar cell terminals are opened or not connected to a load. It is the maximum voltage that a solar cell can deliver under any given illumination. The

open circuit voltage depends on the photo-generated current density, I_{photon} and the saturation current I_0 . Also since the saturation current depends largely on the recombination in the solar cell, the open circuit voltage is a measure of the recombination in the device. For silicon solar cell, the maximum open circuit voltage is about 700mV.

2.2.4 Maximum Power

The maximum power can be determined by the maximum voltage and current. It can be symbolized as,

$$P_{MP} = V_{MP} * I_{MP}$$

2.2.5 Fill Factor

The fill factor FF is the ratio of the maximum power generated by the solar cell, to the product of the voltage open circuit V_{oc} and the short circuit current I_{sc} .

These three important parameters (V_{oc} , I_{sc} and FF) as described above are the most important factors that determine how efficient a solar cell is and are optimized for efficient solar cell design.

$$\text{Efficiency, } \eta = P_{MP}/P_{in}$$

2.3 PRACTICAL APPROACH

In the practical field it becomes difficult to get the perfect output. So scientists and researchers are working relentlessly to compress the loss and to gate a satisfactory output. There are different ways to increase the efficiency like- increasing the solar

concentration, rearrangement of solar panels maximizing the effective area, change of materials and many more. Here some of the processes are being discussed.

2.3.1 Solar Area Mounting and Tracking (general process of improvement):

The conversion efficiency of a solar panel is directly proportional to the amount of direct solar irradiance that is absorbed.

Irradiance is the amount of solar radiation that strikes the surface of a solar cell or panel and it is expressed in kW/m². The irradiance multiply by time is a measure of solar insulation. The peak sun hours is the number of hours per day when the solar insulation =1kw/m².

Solar energy absorption is also affected by the earth's distance from the sun and the earth tilt angle with respect to the sun. The angle between the true south and the point on the horizon directly below the sun is the Azimuth angle, measured in degrees east or west of true south. For south facing locations in the northern hemisphere, the default value is an azimuth angle of 180 degree. Increasing the azimuth angle maximizes afternoon energy production.

Table 2.1 Azimuth Angle by heading [13]

Heading	Azimuth angle (degree)
N	0 or 360
NE	45
E	90
SE	135
S	180
SW	225
W	270
NW	315

The sun's height above the horizon is its altitude. It changes based on time. Based on the sun's altitude changes, the tilt angle of a solar module with respect to the sun must be carefully considered during module or array installations.

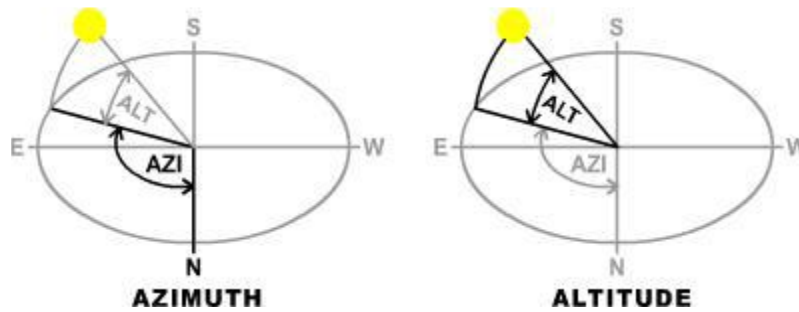


Figure 2.3 Sun's position; Azimuth and Altitude [14]

To make the solar system efficient we need to use the more sunlight at a time. But it can't possible to increase the amount of sunlight. But we can use the angle phenomenon to implant more sunlight in our panel. Tracking can be useful for this.

Solar Tracking

A solar tracker is a device that move or adjust the positional angle of solar photovoltaic panel towards the sun. The solar tracker mechanism will essentially increase the effectiveness of solar panels over a fixed solar array or panel.

Types of tracker:

- **Single axis**

Solar trackers can either have a horizontal or a vertical axis. The horizontal type is used in tropical regions where the sun gets very high at noon, but the days are short. The vertical type is used in high latitudes where the sun does not get very high, but 30 summer days can be very long. In concentrated solar power applications, single axis trackers are used with parabolic and linear Fresnel mirror designs.

- **Dual axis**

The Dual axis solar trackers have both a horizontal and a vertical axis and thus they can track the sun's apparent motion virtually at any angle. A dual axis tracker maximizes the total power output of solar array by keeping the panels in direct sunlight for the maximum number of hours per day.

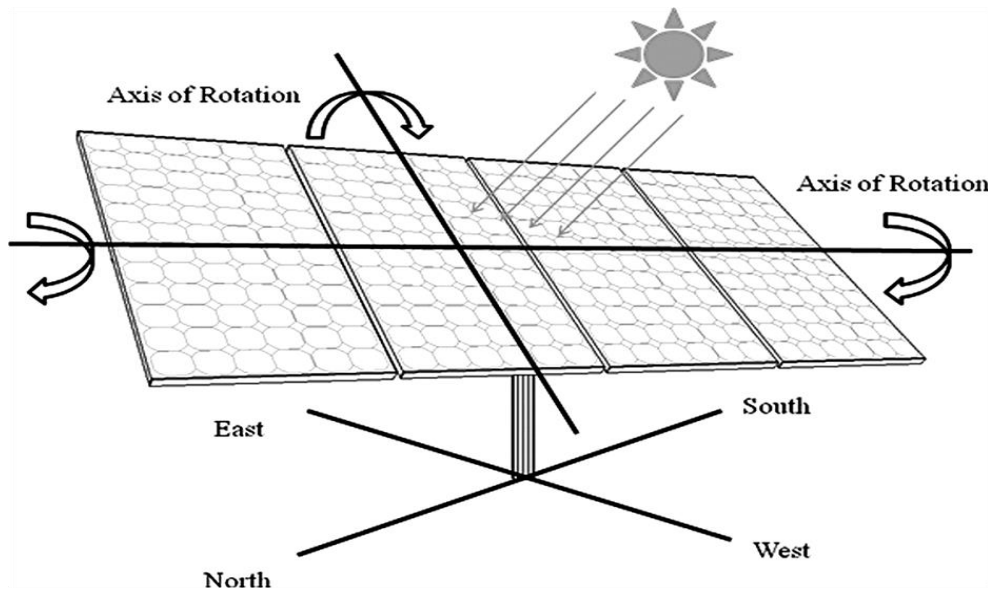


Figure 2.4 A 2-Axis Tracking system (It can move up to 270degree in the horizontal and 75 degree vertical)

Tracker Components:

Typical solar tracking system consists of mechanical parts.

- 1) Linear actuator with integrated dc or ac motor and gear.
- 2) An electronic parts like motor drive and controller.
- 3) Sun sensor
- 4) Power supply

The main problem occurs when most of the solar energy costs originate from the price of installing the panels and the land they sit on. It can contribute 20% of the

cost. So improvement of the solar cell is very important so that less number of array can produce more electricity.

2.3.2 Improving Solar Efficiency Using Simple Mirrors and Cooling Method

Under peak sunlight conditions, a typical commercial PV panel of surface area 160 cm² (25 inch²) will produce 2 watts peak power. If the intensity is 60 percent of peak it will produce about 1.2 watts. So intensity adds a lot to efficiency. Extensive research shows that output of a PV cell can be increased by two methods: fabrications and passive devices.

Efficiency of solar cell is greatly affected by the amount of solar irradiance. It is one of the most dynamic factors which change the solar array performance. Irradiance depends on geographical position, angle of sun to solar panel and amount of energy wasted by reflection from dust particles or from fog or clouds. Therefore change of irradiance means change of output performance of solar panel.

Based on the study of Akbarzadeh and Wadowaski, under concentrated solar radiation the performance of solar cell reduces 50% when its temperature rises from 46⁰C to 84⁰C.

Therefore, an efficient cooling system is quite essential to maximize solar cell's efficiency and to prevent the cell from degradation and damage.

The experimental approach of improving solar panel efficiency is based on readings were recorded during three bright sunny days of month April. A mono crystalline solar panel made of silicon semiconductor was used for this experiment. An iron made frame was designed with space for solar panel and for three mirrors.

The following table is giving information about how the performance measures of solar cell are changing with respect to change in environmental conditions which in this case are changing concentration and cooling step by step.

TABLE-2.2 Change In Current, Voltage and Power With Respect To Concentration and Cooling[15]

Voltage	Current	Power	Concentration
12.08	1.91	24.84	Without
15.02	1.92	28.828	1 mirror
15.43	1.93	29.625	Plus cooling
16.11	1.94	31.253	2 mirrors
16.50	1.94	32.001	Plus cooling
16.71	1.95	36.929	3 mirrors
16.91	2.23	37.709	Plus cooling

A. Without mirrors and without cooling

Though this method was practiced by most of the people from a very long time but now a days this method is almost losing its value due to its low efficiency. Solar irradiance, most of the time in this case is also around about 750w/m².

B. With mirrors and without cooling

Efficiency of solar panel can be increased by increasing solar irradiation on solar panel. In this case four mirrors were functioning at the same time. The output is also encouraging. Approximately, on average 32% efficiency was improved by this method.

C. With mirrors and with cooling

The output by using in this method is the better from the previous one as the result obtained from this method the power efficiency is the highest. As we know when the

electrons absorb sufficient heat energy they collide with each other and with other atoms thus producing free electrons.

TABLE -2.3 Hourly comparison of Three Methods [15]

Time	Without mirrors and cooling	With Mirrors and without cooling	Three mirrors plus cooling
9:00 AM	20.01	26.58	24.7756
10:00 AM	21.21	28.40	30.4433
11:00 AM	23.63	28.05	34.6399
12:00 PM	24.44	30.81	36.4188
01:00 PM	24.80	32.26	37.709
02:00 PM	23.44	29.94	35.5450
03:00 PM	20.22	29.34	30.0969
04:00 PM	19.02	27.56	26.0064

During these hours although solar panel is receiving same amount of solar energy from the sun as the method in section B but at the same time in this method cooling is removing away some of heat energy from the solar panel so making it less efficient than using mirror and without cooling method only for two hours. This method was approximately 20% more efficient than second one and 52% more efficient from the first one.

2.3.3 Improved Perovskite Solar Cell

Perovskite solar cells are potentially the most promising solar power technology for researchers right now. In 2009 its efficiency was of just 3.8 percent. Researchers from

Hong Kong Polytechnic University announced the development of perovskite-silicon tandem solar cells, with the world's highest conversion efficiency of 25.5 percent.[16]

Steps that increase the efficiency

A calibrated mix of solar cell materials would be ideal for energy absorption because different materials absorb different wavelengths for solar energy.

For instance, methyl ammonium lead tri-halide perovskite and silicon solar cells are a complementary pair. With the perovskite as a top layer, it can collect the short wavelength photons while the bottom silicon layer absorbs long wavelength photons.

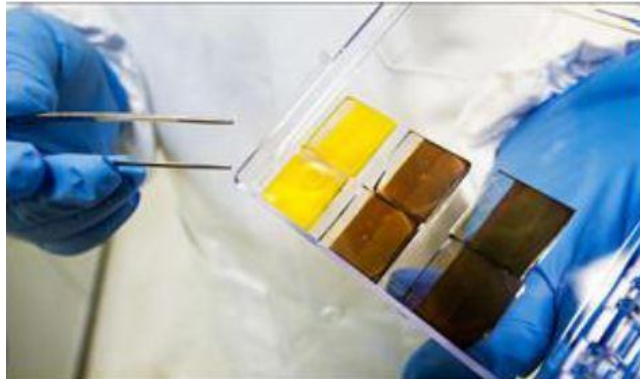


Figure 2.5 Improving efficiency of Perovskite solar cell

The efficiency can boost up by this hybrid cell, in three different steps:

1st step: A low temperature chemical method to lower the impact created by perovskite defects.

2nd step: A three-layer sandwich of molybdenum trioxide/gold/molybdenum trioxide, rendering it transparent, so light could penetrate to the bottom silicon layer.

3rd step: A rose petal-like film was placed as the top layer of the solar panel to capture even more light.

In this purpose the research is still going on for better fabrication and to improve the efficiency.

2.3.4 High Efficient Ga-As-P Solar Cell

We know different semiconductor materials, such as gallium arsenide and gallium phosphide have reached higher efficiencies than silicon. Till now most of the highest-efficiency solar cells have been made by layering different semiconductor materials on top of each other and fine-tuning them so that each can absorb a different slice of the electromagnetic spectrum.

These layered solar cells can reach theoretical efficiencies upward of 50% [6], but their very high manufacturing costs have relegated their use to niche applications, such as on satellites, where high costs are less important than low weight and high efficiency.



Figure 2.6 Solar panel

A group of comes with a proposal of MIT step cell, in contrast, can be manufactured at a fraction of the cost because a key component is fabricated on a substrate that can be reused. It is a solution of the costing of expensive materials.

The first step of this process is preparing the stem cell. The step cell is made by layering a gallium arsenide phosphide-based solar cell, consisting of a semiconductor material that absorbs and efficiently converts higher-energy photons, on a low-cost silicon solar cell. As silicon is one of the most abundant materials of the world.

Now let us focus on the layering of the cell. It is almost like a traditional junction solar cell with modification. The silicon layer is exposed, appearing like a bottom step. This intentional step design allows the top gallium arsenide phosphide (GaAsP) layer to absorb the high-energy photons (from blue, green, and yellow light) leaving the bottom silicon layer free to absorb lower-energy photons (from red light) not only transmitted through top layers but also from the entire visible light spectrum.

This team developed the GaAsP, by growing the semiconductor alloy on a substrate made of silicon germanium (SiGe). Gallium arsenide phosphide cannot be grown directly on silicon, because its crystal lattices differ considerably from silicon's, so the silicon crystals become degraded. Along with that mismatch in lattice constant there rises constrain force problem in crystal lattice. That's why the gallium arsenide phosphide on the silicon germanium provides a more stable base.

This highly efficient Ga-As-P solar cell may have many advantages but there is a problem regarding this. The silicon germanium under the GaAsP layer absorbs the lower-energy light waves before it reaches the bottom silicon layer and SiGe does not convert these low-energy light waves into current.

Here the step where the step cell idea is developed. The step cell concept is to improve cell in which the SiGe template is removed and re-used. So that we can create a solar cell in which Ga-As-P cell tiles are directly on top of a silicon cell. The step-cell allows for SiGe reuse since the GaAsP cell tiles can be under-cut during the transfer process.

The SiGe can be removed and reused repeatedly, which significantly reduces the manufacturing costs. Adding that one layer of the gallium arsenide phosphide can really boost efficiency of the solar cell but because of the unique ability to etch away the silicon germanium and reuse it, the cost will be also low.[17]

Though the idea is new currently at research level but it has opened a brand new dimension of thought on the field of high efficient solar cells.

2.3.5 A Micro-scale Photo Voltaic Cell “Solar Glitter”

Solar cells on the market today are most often made of crystalline silicon, used because of its high light-to-energy efficiency. Silicon is also the primary material used in semiconductors and computer electronics, which have seen a rapid decrease in cost over the past three decades. But unfortunately there has been no effect of that in the market. That’s why scientists have introduced a new product, a vial of liquid containing solar cells so small they look like bits of decorative glitter, which has earned them the nickname “solar glitter”.

Basic crystalline silicon solar cells are made from wafers of silicon roughly four to six inches squared and 200 microns thick. Each wafer makes a single cell, and the cells are lined up together to make solar panels that must be placed between plates of glass for handling, which makes the panel heavy.



Fig 2.7 microsystems-enabled photovoltaics

The researcher team is now using microsystems-enabled photovoltaics (MEPV) uses micro-design and micro-fabrication techniques to produce solar cells as small as 3-20 microns thick and 100-1000 microns wide. These PV cells are then placed or ‘printed’ onto a low-cost substrate with embedded contacts and micro lenses for focusing sunlight onto the cells. Moving to micro-scale PV cell sizes results in

distinct benefits at cell, module, and system levels, including reducing the amount of expensive semiconductors by 30 times while still achieving high efficiencies.[18]

They have also managed to cut up the solar silicon wafers into many smaller cells, between 100 and 750 microns squared, and thin them down to 10 to 20 microns thick. Individual cells cut from the same piece of silicon can be connected into single panels, but mounted in flexible, light-weight materials rather than glass. Eventually, this could mean solar cells in fabric, such as clothing or tents, and solar panels that fit a wide variety of surfaces and are easily relocated.



Figure 2.8 Solar glitter

To create solar glitter, a sticky polymer film with an interconnect pattern is applied to the top of the 200 micron thick wafer, and then pulled away, taking an array of new, 10 to 20 micron-thick solar cells with it. More than 90 percent of the light conversion takes place in the first 20 microns of a solar cell, so little efficiency is lost. After pulling off the top layer of the silicon wafer, the remaining silicon can be used to create more cells, cutting down on the cost of the material and leaving none to waste.

2.4 LATEST INNOVATIONS

Every single day we are getting introduced with latest idea and technology which is helping us to get one step closer to the higher efficiency in solar cells. All the inventions are different from each other, superior from each other in different prospects. But all of them are highly efficient and reliable.[19]

2.4.1 Cool Earth Inflatable Solar Balloons

Solar photovoltaic cells are still relatively expensive, so many companies are trying to find ways to reduce the PV surface area that they use. One way to do that is to use concentrators to direct more sunlight to smaller (but usually more efficient) solar panels. But even if it is possible, one have to still pay high costs for support materials and the concentrators themselves.



Figure 2.9 Solar balloons

That's the problems that Cool Earth is trying to solve with its inflatable solar collectors. The balloons themselves are said to be 400 times cheaper than a concentrator of the same size made of polished aluminum, and they can be mounted

on wires, reducing costs further. Maintenance is also easier: It can be repaired with tape, and replace one unit in about 15 minutes.

Solar balloons are very simple solar devices, in which solar energy is used to heat the air in the balloon by means of a black absorber. The absorber can either be on the surface or inside the balloon. The lighter hot air makes the balloon fly because of the Archimedes lift. Small scale solar balloons are common toys and can be easily built using a black polyethylene (PET) film for the balloon envelope: the black PET absorbs solar radiation and heats the internal air.

2.4.2 “Hairy” Thin Film Solar Cell

Nanotechnology has opened up new and promising possibilities to reduce the cost of PV cells and modules for bulk power generation as well as to improve the cell conversion efficiency. Researchers at McMaster University have succeeded in 'growing' light-absorbing nano wires made of high-performance photovoltaic materials on carbon-nano tube fabric in other words, hairy solar panels.

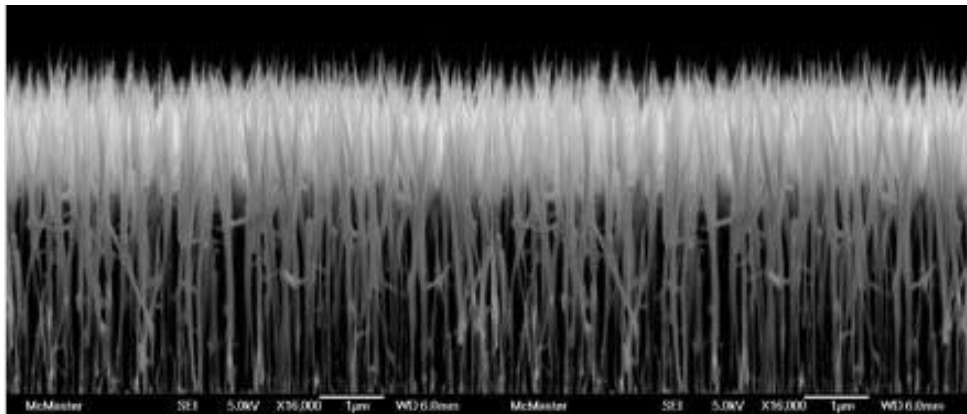


Figure 2.9 A forest of GaAs nano wires growing on a silicon substrate.

The aim is to produce flexible, affordable solar cells that, within five years, will achieve a conversion efficiency of 20%. Longer term, it's theoretically possible to achieve 40% efficiency.

2.4.3 Moth Eyes Biomimicry for Solar Cell

Silicon is reflective, so a lot of light that could be turned into electricity is bounced back and lost. Anti-reflective coating is used, but its effectiveness is limited and it has downsides too. So while looking for a solution, researchers noticed that moths have very non-reflective eyes ("most likely an evolutionary defense against nocturnal predators"). The moth-eye process creates panels that reflect less than 2% of light. That's a vast improvement over the 35 to 40% reflection rate seen without the anti-reflection coating layers.

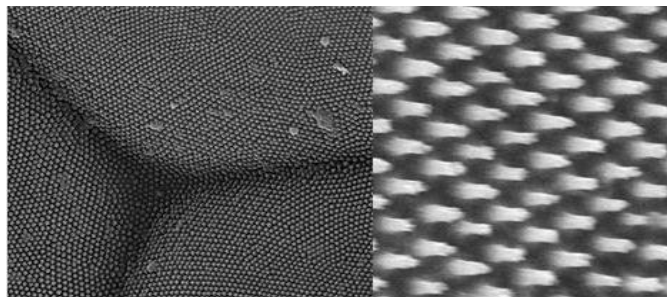


Figure 2.10X-Ray of solar panels arranged inspired by moth eyes.

2.4.4 Printed Solar Panel “Nanosolar”

Nanosolar (a company based in Palo Alto, California) uses an innovative technique to produce a kind of "solar film". To make the film, Nanosolar prints CIGS (copper-indium-gallium-selenium) onto a thin polymer using machines that look like printing presses. There is no costly silicon involved in the process, and, ultimately, a solar cell from Nanosolar will cost about one-fifth to one-tenth the cost of a standard silicon solar panel.

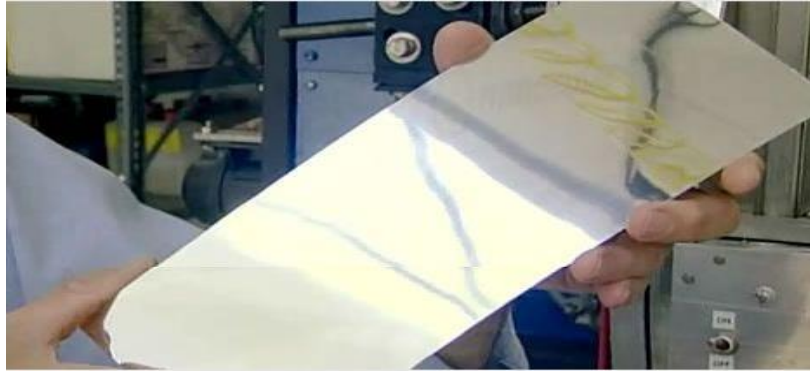


Figure 2.11 Nanosolar

2.4.5 Conversion of Infrared Light to Electricity

By adding titanium and vanadium into the semiconducting material of a solar panel, one can alter it so that it can use the infrared spectrum of light as well as the visible. Because of this, such solar panels have a theoretical absorption limit of 63%, which compares to about 40% for ordinary solar cells.

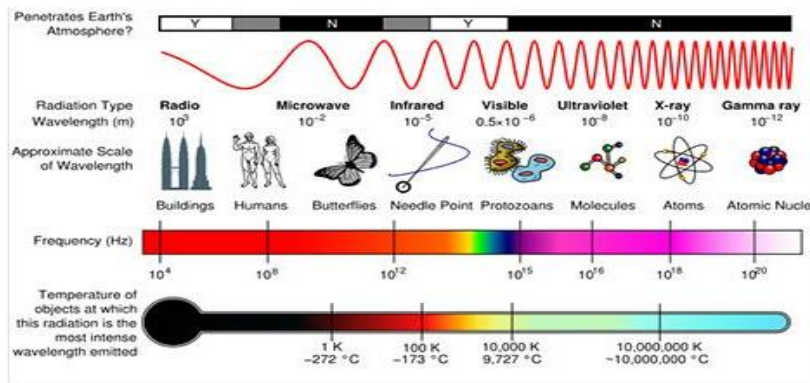


Figure 2.11 Electromagnetic spectrum

2.4.6 19.9% Efficient CIGS Solar Cell

A shortage of silicon in the past few years and the demand for thin and flexible panels has helped increase the focus on thin film solar recently, and a lot of progress is being

made. The US National Renewable Energy Laboratory (NREL) has created thin film solar panels that are very close to competing with their more traditional silicon-based cousins. "The copper indium gallium diselenide (CIGS) thin-film solar cell recently reached 19.9 percent efficiency in testing at the lab, setting a new world record."

2.4.7 CdTe Solar Panel

It is one of the most recent works in the field of photovoltaics. These highbred solar cells are combination of different materials. Solar panels made of Cadmium tellurium solar cells are very cheap. They can be manufactured in comparison to solar panels at less than \$1 per Watt,

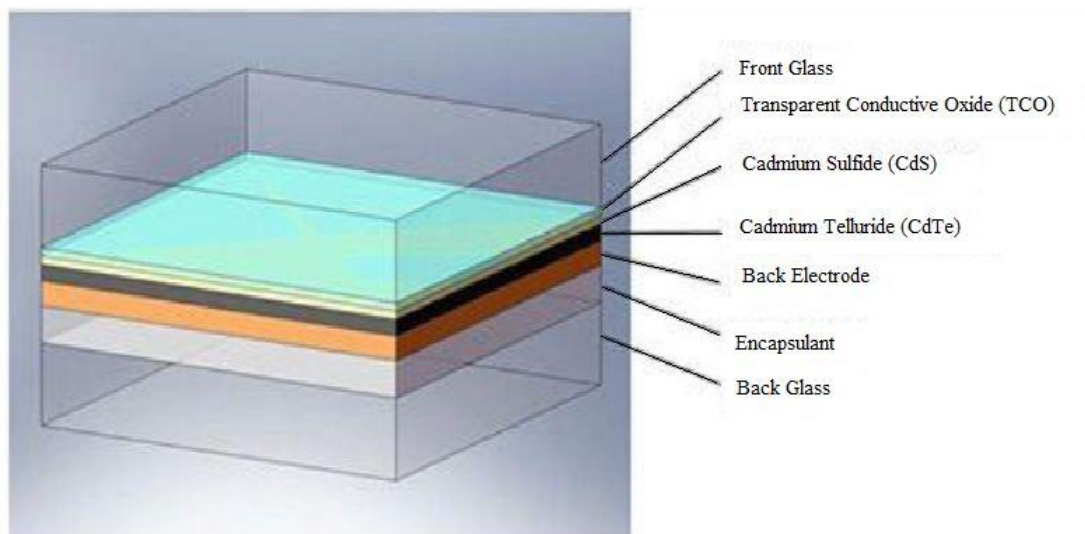


Figure 2.12 Cadmium Telluride Solar Panels

The energy band-gap of CdTe, at 1.45 eV is a good match to the solar spectrum and thus it enables conversion of more energy from the solar spectrum than the lower energy band-gap silicon (1.12 eV). Traditional solar modules become less efficient at converting solar energy into electricity as their cell temperatures increase [7].

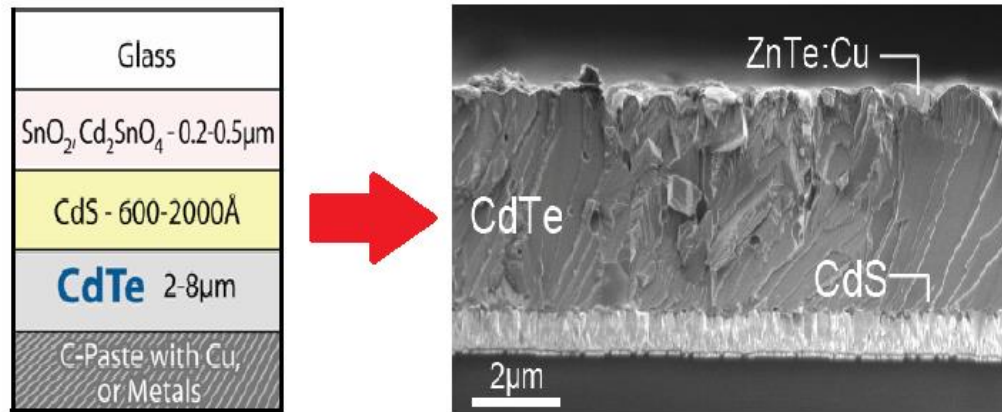


Figure 2.13 CdTe thin film morphology

However, the efficiency of CdTe is less susceptible to cell temperature increases, enabling CdTe solar modules to generate relatively more electricity under high ambient (and therefore high cell) temperatures. It also absorbs low and diffuse light and thus converts such light more efficiently to electricity under cloudy weather and dawn and dusk conditions where conventional cells operate less efficiently. As a result, under real world conditions CdTe will generally produce more electricity than a conventional solar module with similar power ratings [15].

2.5 CONCLUSION

The main aim of any idea, technology or system is to make it more and more efficient. Same goes for solar cell technology. A number of new methods are being invented and more are under research. Both theoretical and experimental approaches are there to fulfill the goal. The theoretical improvement works on the open circuit voltages (V_{oc}), short circuit voltages (I_{sc}), Fill factor etc. While the experimental approaches on solar mounting and tracking or using simple mirror methods in order to get the concentrated solar energy for higher output. Scientists and researchers are developing hybrid materials, bringing change in layer combination in multi-junction cell system. More innovative ideas are on their way to amaze us.

CHAPTER THREE

ANALYSIS TECHNIQUE

3.1 INTRODUCTION

For any kind of statement or calculation to any matter or information we need to analyze thoroughly on it. In order to get the perfect knowledge of anything it is very necessary to know every characteristics of it. On the basis of the analysis we get to think of the further procedure of improving way for efficiencies and usefulness. So in order to enhance the application of anything analysis is a must. There are a couple of ways for analysis techniques. At first we start on analysis theoretically as at first we must establish some sort of idea about the characteristics. Then comes to the practical part. In this case through some experimental setups we try to figure out the information for real and try to pick out the similarities and differences from the theoretical part. The experimental setup can be either software based or hardware based. But whatever the procedure analysis is must for acquiring deeper, correct and resourceful information on any subject or expression.

3.2 OPERATING PRINCIPLE OF SOLAR CELL

A solar cell is an electronic device which directly converts sunlight into electricity. Light shining on the solar cell produces both a current and a voltage to generate electric power. This process requires firstly, a material in which the absorption of light raises an electron to a higher energy state, and secondly, the movement of this higher energy electron from the solar cell into an external circuit. The electron then dissipates its energy in the external circuit and returns to the solar cell. A variety of materials and processes can potentially satisfy the requirements for photovoltaic

energy conversion, but in practice nearly all photovoltaic energy conversion uses semiconductor materials in the form of a $p-n$ junction.

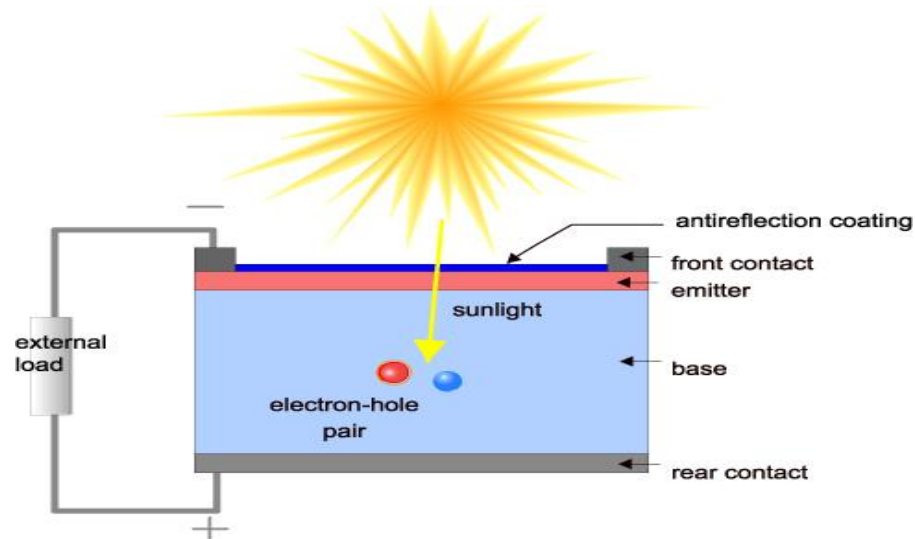


Figure 3.1 Cross section of a solar cell.

The basic steps in the operation of a solar cell are:

- the generation of light-generated carriers;
- the collection of the light-generated carries to generate a current;
- the generation of a large voltage across the solar cell
- The dissipation of power in the load and in parasitic resistances.

3.3 RESEARCH WORK RELATED TO SOLAR DEVICES

- Analytical method
- Simulation method
- Experimental method

These three methods are elaborated and discussed further with necessary explanation and figures.

3.3.1 Analytical Method

There are many models in the literature which represent the current voltage characteristics of solar cells incorporating many physical variables. The analytical methods are useful for different applications such as power extraction optimization, solar panels selection, efficiency calculations, many improvements and so on.

The efficiency of solar cells depends on a number of factors such as: the presence of series and shunt resistances; absorption of light in the surface layer; recombination of charge carriers in the volume of semiconductor or the area of spatial charge; heating in the presence of excessive photon energy; through passage of photons, etc. The series and shunt resistances are among the parameters that significantly affect the efficiency. The knowledge of these parameters is necessary for monitoring the quality and estimating the degree of perfection of solar cells.

3.3.1.1 Solar cell parameters

The illuminated Current-Voltage Characteristics of solar cell according to single-diode model of solar cell (Fig 3.2) can be characterized by the following expressions:

$$I = I_{pv} - I_s \left[\exp \left(\frac{U + IR_s}{n\varphi_T} \right) - 1 \right] - \frac{U + IR_s}{R_{sh}}$$

Where, I = current passing through the load;

I_{pv} = light current;

φ_T = thermal potential

$$\varphi_T = \frac{kT}{e}$$

T= temperature;

e = electron charge;

U = voltage;

I_s = saturation current;

R_s = series resistance & R_{sh} = shunt resistance;

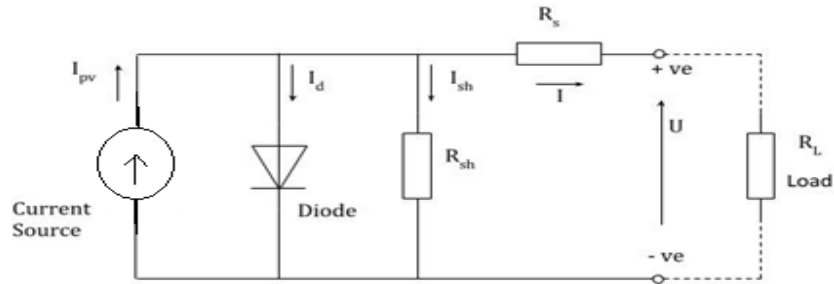


Fig3.2 Standard equivalent circuit of single junction solar cell

A solar cell equivalent circuit can be depicted according to the figure given above. During the operation, the efficiency of solar cells is reduced by the dissipation of power across internal resistances. These parasitic resistances can be modeled as a parallel shunt resistance (R_{sh}) and series resistance (R_s). For an ideal cell, R_{sh} would be infinite and would not provide an alternate path for current to flow, while R_s would be zero, resulting in no voltage drop and power loss before the load.

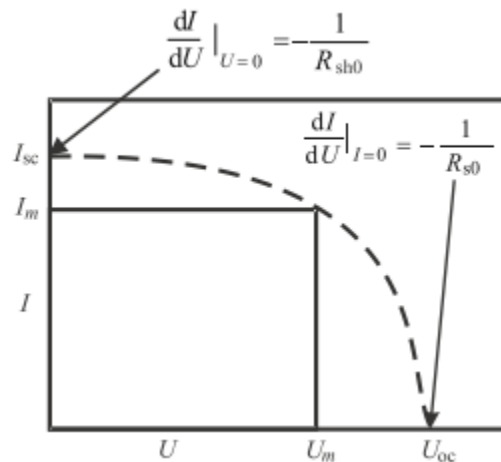


Fig 3.3 General view of solar cell idealized curve

Determination of the specified parameters (R_S , R_{sh} and I_S) is based on the precise determination of the location of three points of the experimental I-V curve, namely, the short-circuit current (I_{sc}), open-circuit voltage (U_{oc}), and maximum power (P_m). The availability of information on the location of three points on the curve makes it possible to calculate [16].

Dynamic resistance at the point of the short-circuit current,

At $I = I_{sc}$

$$R_{sh0} = - \left(\frac{dU}{dI} \right)$$

Dynamic resistance at the point of the open-circuit voltage,

At $U = U_{oc}$

$$R_{s0} = - \left(\frac{dU}{dI} \right)$$

Maximum current (I_m), maximum voltage (U_m), and maximum power (P_m),

$$P_m = I_m U_m$$

Parameters describing the solar cell current voltage characteristics can be obtained by using a system of nonlinear equations;

$$I_S e^{\left[\left(\frac{U_{oc}}{n\varphi_T} \right) - 1 \right]} - I_S e^{\left[\left(\frac{I_{sc} R_S}{n\varphi_T} \right) - 1 \right]} - I_{sc} \left(\frac{R_{sh} + R_S}{R_{sh}} \right) + \frac{U_{oc}}{R_{sh}} = 0$$

$$(R_{s0} - R_S) \left[\frac{1}{R_{sh}} + I_S \frac{1}{n\varphi_T} e^{\left(\frac{U_{oc}}{n\varphi_T} \right)} \right] - 1 = 0$$

$$(R_{sh0} - R_S) \left[\frac{1}{R_{sh}} + I_S \frac{1}{n\varphi_T} e^{\left(\frac{I_{sc} R_S}{n\varphi_T} \right)} \right] - 1 = 0$$

Proceeding with further calculations R_S and R can be calculated with the following expressions,

$$R_{sh} = \left[1 - e^{\left(\frac{I_{sc} R_S - U_{oc}}{n\varphi_T} \right)} \right] \frac{(R_{sh0} - R_S)(R_{s0} - R_S)}{e^{\left(\frac{I_{sc} R_S - U_{oc}}{n\varphi_T} \right)} (R_S - R_{sh0}) + (R_{s0} - R_S)}$$

$$R_s = \frac{R_{S0}(I_{sc}R_{sh0} - U_{oc}) + n\phi_T(R_{sh0} - R_{S0})}{(I_{sc}R_{sh0} - U_{oc})}$$

3.3.1.2 Effect of Rs and Rsh Parameters

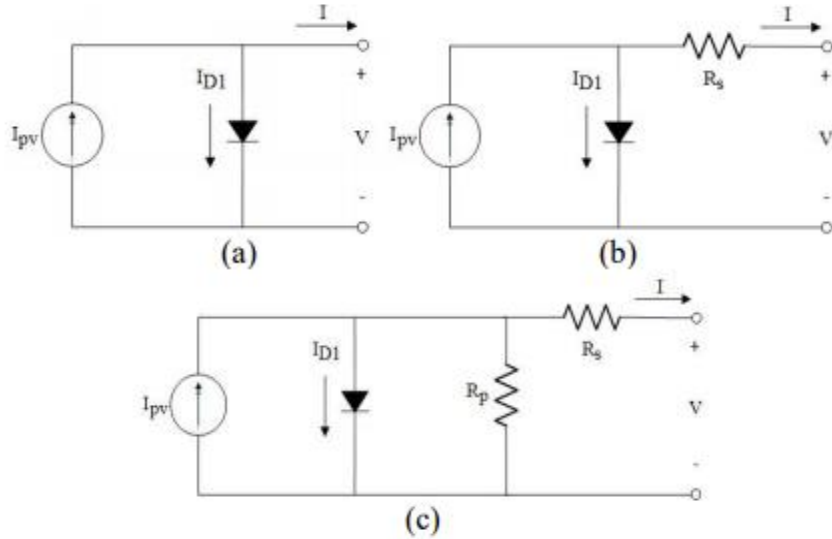


Fig 3.4 Different mathematical models for PV module a) Ideal model, b) R_s -model and c) R_p -model.

PV module models can be classified into three types: a) Ideal model, b) R_s -model and c) R_p -model. More accurate double-diode and three-diode models can be found respectively. These are complicated and not discussed here with details.[20]

R_s -model improves the ideal model by recognizing the series resistance (R_s) in solar modules, which basically depends on the contact resistance of the metal base with the p semiconductor layer, the resistances of the p and n bodies, the contact resistance of the n layer with the top metal grid, and the resistance of the grid. The values of PV current and voltage forming I-V curve are formed with the relationship that is given

by the following equation;

$$I = I_{pv} - I_o \left(e^{\frac{V+IR_s}{nN_sV_T}} - 1 \right)$$

Rp-model further improves the modeling accuracy by identifying shunt resistance (Rp) which exists mainly due to the leakage current of the p–n junction and depends on the fabrication method of the PV cell. It's I-V relationship is expressed as:

$$I = I_{pv} - I_d - \frac{V + IR_s}{R_p}$$

$$I_d = I_o \left(e^{\frac{V+IR_s}{nN_sV_T}} - 1 \right)$$

In the literature the expression can be approximated by the exponential relationship;

$$I_d \approx I_o e^{\frac{V+IR_s}{nN_sV_T}}$$

As we have seen previously photovoltaic cells can be modeled as a current source in parallel with a diode. When there is no light present to generate any current, the cell behaves like a diode. As the intensity of incident light increases, current is generated by the PV cell.

In an ideal cell, where R_{sh} is infinite and R_s is zero, the load current I is equal to the current I_l generated by the photoelectric effect minus the diode current I_D , according to the equation:

$$\begin{aligned} I &= I_l - I_D \\ &= I_l - I_s \left(e^{\frac{qV}{kT}} - 1 \right) \end{aligned}$$

Where

I_s = saturation current of the diode

q = charge on an electron, 1.6×10^{-19} Coulombs

k = Boltzmann's constant, 1.38×10^{23} J/K

T = cell temperature in degrees Kelvin

V = measured cell voltage that is either produced (power quadrant) or applied (voltage bias).

It is possible to approximate the series and shunt resistances, R_s and R_{sh} , from the slopes of the I/V curve at V_{oc} and I_{sc} , respectively.

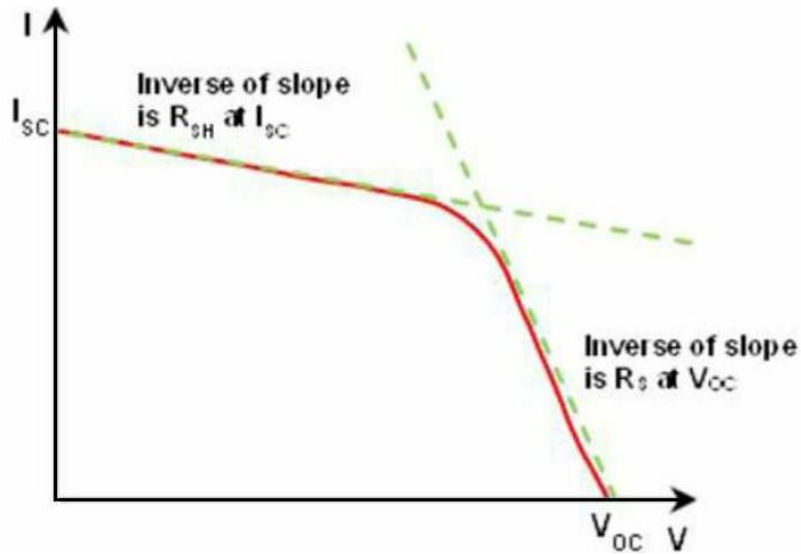


Fig 3.5 Obtaining Resistances from the I-V Curve

The resistance at V_{oc} , however, is at best proportional to the series resistance but it is larger than the series resistance. R_{sh} is represented by the slope at I_{sc} .

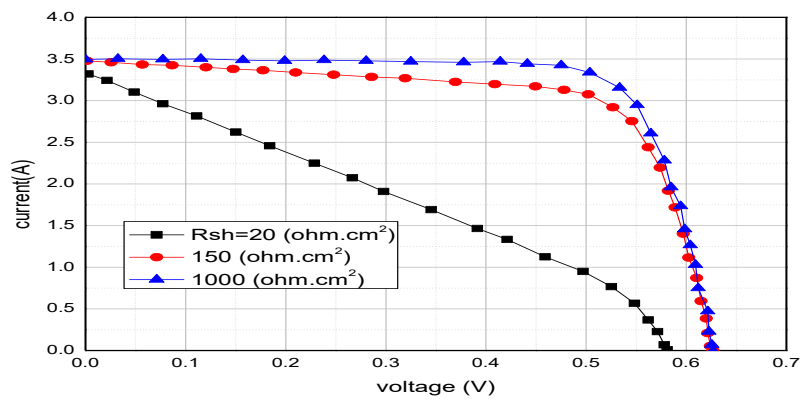


Fig 3.6 Effect of shunt resistance on the current–voltage characteristics[21]

As shunt resistance decreases, the current diverted through the shunt resistor increases for a given level of junction voltage. The result is that the voltage-controlled portion of the I-V curve begins to sag far from the origin, producing a significant decrease in the terminal current I and a slight reduction in V_{OC} . Very low values of R_{SH} will produce a significant reduction in V_{OC} . Much as in the case of a high series resistance, a badly shunted solar cell will take on operating characteristics similar to those of a resistor. These effects are shown for crystalline silicon solar cells in the I-V curves displayed in the figure to the right.

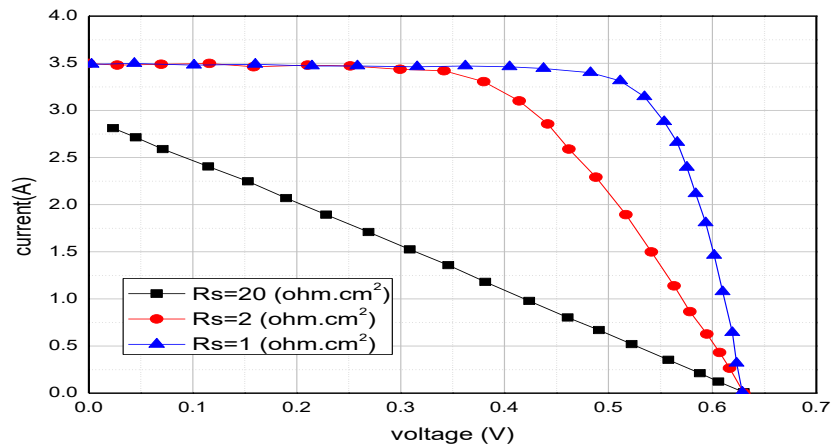


Fig3.7 Effect of series resistance on the I-V characteristics of a solar cell[21]

As series resistance increases, the voltage drop between the junction voltage and the terminal voltage becomes greater for the same current. The result is that the current-controlled portion of the I-V curve begins to sag toward the origin, producing a significant decrease in the terminal voltage V and a slight reduction in I_{sc} , the short-circuit current. Very high values of R_S will also produce a significant reduction in I_{sc} ; in these regimes, series resistance dominates and the behavior of the solar cell resembles that of a resistor. These effects are shown for crystalline silicon solar cells in the I-V curves displayed in the figure to the right.

Losses caused by series resistance are in a first approximation given by;

$$P_{loss} = V_{RS}I = I^2R_S$$

And increase quadratically with photo-current. Series resistance losses are therefore most important at high illumination intensities.

The equations that describe solar cell can be solved analytically or numerically. While the analytical equations are easier to solve by hand and give great insight into cell operation, they become difficult to solve as more factors of cell operation are included. In the past, it was common to re-write the equations slightly to simplify the solution to solve specific cases; however, such methods are time consuming.

3.3.2 Effect of Temperature

Solar cells are also sensitive to temperature like other semiconductor devices. Increase in temperature reduces the band gap of a semiconductor, thereby effecting most of the semiconductor material parameters. The decrease in the band gap of a semiconductor with increasing temperature can be viewed as increasing the energy of the electrons in the material. To break the bond lower energy is required. In the bond model of a semiconductor band gap, reduction in the bond energy also reduces the band gap. Therefore increasing the temperature reduces the band gap. In a solar cell, the parameter most affected by an increase in temperature is the open-circuit voltage[22]. The impact of increasing temperature is shown in the figure below.

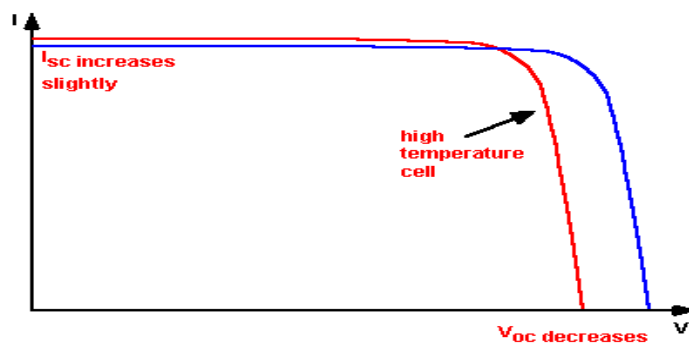


Fig 3.8 Effect of temperature on I-V curve

The open-circuit voltage decreases with temperature because of the temperature dependence of I_0 . The equation for I_0 from one side of a p-n junction is given by;

$$I_0 = qA \frac{Dn_i^2}{LN_D}$$

Where,

q = electronic charge

A = area;

D = diffusivity of the minority carrier given for silicon as a function of doping in the silicon material

L = minority carrier diffusion length;

N_D = doping; and

n_i = intrinsic carrier concentration given for silicon

In the above equation, many of the parameters have some temperature dependence, but the most significant effect is due to the intrinsic carrier concentration, n_i which depends on the band gap energy (with lower band gaps giving a higher intrinsic carrier concentration), and on the energy which the carriers have (with higher temperatures giving higher intrinsic carrier concentrations).

$$n_i^2 = 4 \left(\frac{2\pi kT}{h^2} \right)^3 (m_e m_h)^{3/2} \exp\left(-\frac{E_{G0}}{kT}\right) = BT^3 \exp\left(-\frac{E_{G0}}{kT}\right)$$

Where,

T = temperature;

h and k are constants given in the constants page;

m_e and m_h are the effective masses of electrons and holes respectively;

E_{G0} = band gap linearly extrapolated to absolute zero.

B = a constant which is essentially independent of temperature.

Substituting these equations back into the expression for I_0 , and assuming that the temperature dependencies of the other parameters can be neglected, gives the following expression,

$$I_0 = qA \frac{D}{LN_D} BT^3 \exp\left(-\frac{E_{G0}}{kT}\right) \approx B_1 T^\gamma \exp\left(-\frac{E_{G0}}{kT}\right)$$

Here B_1 is temperature independent constant. A constant, γ , is used instead of the number 3 to incorporate the possible temperature dependencies of the other material parameters. For silicon solar cells near room temperature, I_0 approximately doubles for every 10°C increase in temperature.

The impact of I_0 on the open-circuit voltage can be calculated by substituting the equation for I_0 into the equation for V_{oc} as shown below;

$$\begin{aligned} V_{oc} &= \frac{kT}{q} \ln\left(\frac{I_{sc}}{I_0}\right) \\ &= \frac{kT}{q} (\ln I_{sc} - \ln I_0) \\ &= \frac{kT}{q} \ln I_{sc} - \frac{kT}{q} \ln \left[B_1 T^\gamma \exp\left(-\frac{qV_{G0}}{kT}\right) \right] \\ &= \frac{kT}{q} \left(\ln I_{sc} - \ln B_1 - \gamma \ln T + \frac{qV_{G0}}{kT} \right) \end{aligned}$$

Where $E_{G0} = qV_{G0}$; assuming that $\frac{dV_{oc}}{dT}$ does not depend on $\frac{dI_{sc}}{dT}$, $\frac{dV_{oc}}{dT}$ can be found as,

$$\frac{dV_{oc}}{dT} = \frac{V_{oc} - V_{G0}}{T} - \gamma \frac{k}{q}$$

The above equation shows that the temperature sensitivity of a solar cell depends on the open circuit voltage of the solar cell, with higher voltage solar cells being less affected by temperature.

The short-circuit current, I_{sc} , increases slightly with temperature, since the band gap energy, E_g , decreases and more photons have enough energy to create electron-hole pairs.

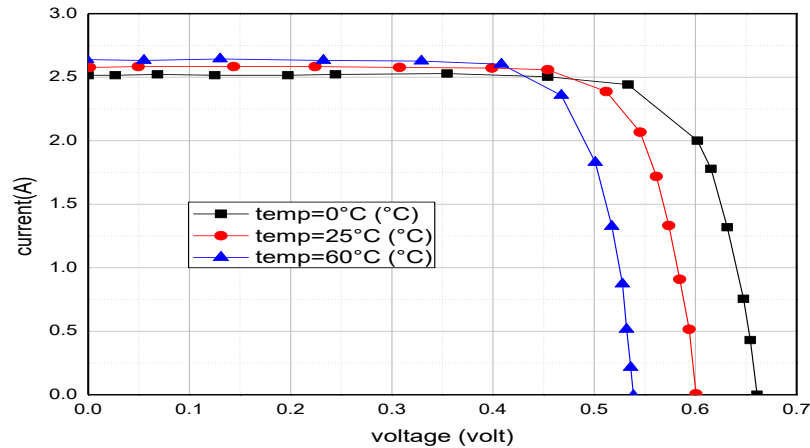


Fig 3.9 Effect of temperature on I-V curve

For the 1000 W/m^2 I-V curve, figure above shows the effect of cell temperature. As the temperature rises above 0°C , V_{oc} falls while I_{sc} gets slightly higher. However, the graph shows that the current at 16 V decreases because of the decrease of V_{oc} . Therefore, to get the maximum current output, modules should be mounted so that air can circulate around them freely to keep the cell cool. I-V curves are usually shown for the cell at the temperature of 25°C [23].

3.4 SIMULATION ANALYSIS

A solar simulator including artificial sun is a device that provides illumination approximating natural sunlight. The purpose of the solar simulator is to provide a controllable indoor test facility under laboratory conditions, used for the testing of solar cells, sunscreens, plastics and other materials and devices. The basic operation of a modeling program consists of setting up the model with user defined parameters, a generation of nodes to solve, then iterating to produce a solution that is consistent with all the nodes [24].

3.4.1 Why We Need the Simulation:

The continuous innovations of solar cell make the cells more and more complex. In this aspect we find that this improvement needs more experimental process and geometrical variables, 3D effects, complex light path, etc. It is impossible to design new cells without simulation. Too many experiments are needed to investigate design space, so without simulation it will be a great risk for optimum design.

The whole solar cell can in three basic parts:

- Cell
- module
- system

We can simulate these three and can get the benefits for all three aspects [24].

Cell Level:

- Maximize efficiency.
- Optimize geometric and process parameters.

Module Level:

- Minimize effect of interconnects on performance.
- Minimize impact of cell variation or degradation on module performance.
- Minimize interconnect losses.
- Evaluate effects of environmental variation.
- Light intensity and incidence angle.
- Temperature variation.

System Level:

- Maximize system level efficiency delivered to the grid, including inverter system.

- Given TCAD device design, physical parameters contributing to interconnect resistances can be extracted and a system-level model developed.
- From system cell level model, sweeps can be done to determine the effect of different cells widths on module performance.
- Allows for optimization of Maximum Power Point at a module.

3.4.2 TCAD (Technology Computer Aided Design):

Technology CAD is a branch of electronic design automation that models semiconductor fabrication and semiconductor device operation. This is a combination of process, device and circuit simulation and modeling tools. The goals start from the physical description of IC devices considering both the physical configuration and related device properties and build the links with broad range of physical and electrical behavior models device that supports device and circuit design.

3.4.2.1 TCAD tools:

Table 3.1 TCAD Tools[25]

Activities	Outcomes	Tools	
Process Simulation	Device Structure	TSUPREM4	TAURUS WORK BENCH (GUI)
Device Simulation	Electrical Characteristics	MEDICI(2D) DAVINCI(3D)	
Device Modeling	Device Model Parameters	AURORA	
Circuit Simulation	Functional Circuit	HSPICE	

TAURUSTSUPREM4: It is an advanced 1D & 2D process simulator for developing semiconductor process. It is used for fabricating semiconductor devices and has extensive stress modeling capabilities.

MEDICI (2D): It is a 2D device simulator from which we get the optical, electrical, thermal characteristics of semiconductor devices. The advanced version has a vast array that can perform accurate simulations.

TAURUS WORK BENCH: it can optimize IC fabrication process. It helps the market so well. Its main motive is to solve real technology problems in the shortest time possible and as well as maintaining lower cost.

HSPICE: It is a device level circuit simulator. It takes a spice file as input and produces output describing the requested simulation of the circuit.

3.4.2.2 TCAD simulation process

TCAD simulation is done by two processes. The modeling of the fabrication is termed Process TCAD, while the modeling of the device operation is termed Device TCAD.

- **Process Simulation:**

This simulation is for semiconductor process simulations. Modeling of the fabrication of semiconductor devices such as transistors is done by this. Semiconductor process simulation is the modeling of the fabrication of the semiconductor device.

The goal of process simulation:

- An accurate prediction of the active dopant distribution.
- The stress distribution.
- The device geometry

The procedure starts from the fabrication of IC devices. For this it requires series of processing steps. TCAD has traditionally focused mainly on the transistor fabrication part of the process flow ending with the formation of contacts-also known as front end of line manufacturing. TCAD has traditionally focused mainly on the transistor fabrication part of the process flow ending with the formation of contacts-also known as front end of line manufacturing. Back end like interconnect, dielectric, etc. are not considered.

- **Device Simulation:**

Device Simulation is a 2D and 3D device simulator that performs DC, AC, and transient analysis for silicon, binary, ternary, and quaternary material-based devices. It enables the both characterization and optimization of semiconductor devices for wide range of technologies.

It solves Poisson's equation, the electron and hole current continuity equations, the electron and hole energy balance equations, the lattice heat equation. The output can be optimized by steady state, transient and AC small signal analysis with automatic I-v curve tracing and time step algorithms. It uses Ray tracing to simulate transmission, reflection and refraction across interfaces, as well as absorption and emission. Now it also includes advanced adaptive mesh generation. It can simulate different materials such as Si, Ge, GaAs, SiGe, AlGaAs, InP, GaInAs, GaInGaPAs and SiC. It allows user to define and solve new physical models and partial differential equations.

3.4.2.3 TCAD work flow

The device simulation and process simulation worked together and make the TCAD simulation successful. In this section we will see that what actually happens during the simulation process in each sector. In general process simulation first do the fabrication and analyze the geometrical configuration. And then device simulation gives the output analysis through curves, different transient analysis as well as the parameters.

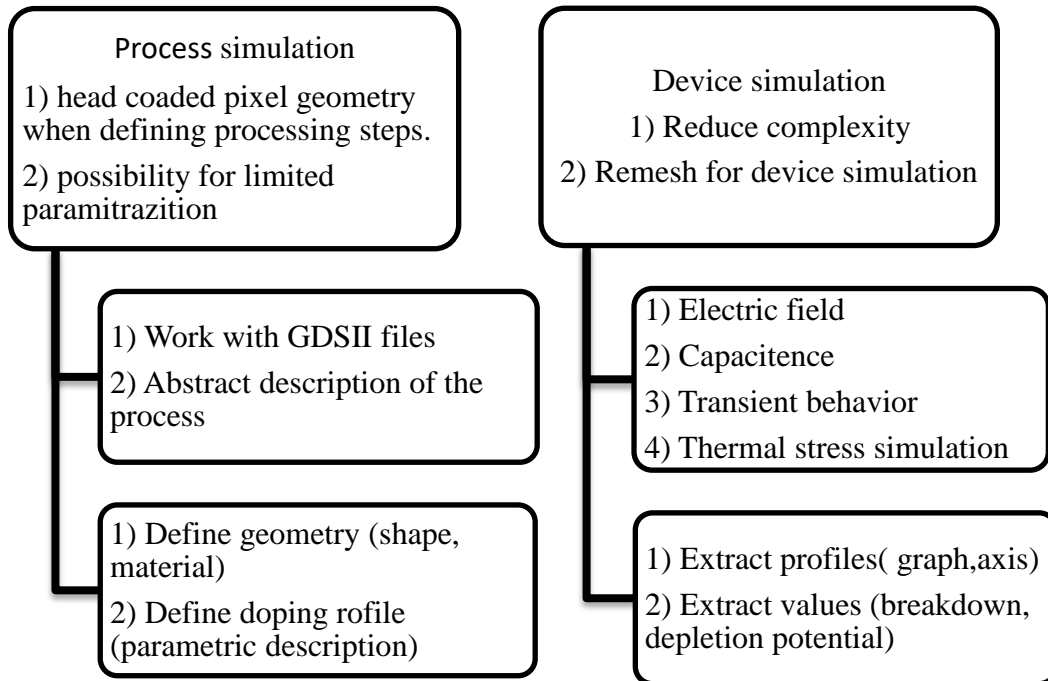


Fig 3.10 Simulation Work Flow

3.4.3 Parameters That Can be Changed

In case of simulation if we want to see the efficiency, change of properties, different curves there are certain parameters which values can be variable. Here some of the parameters are given below:

Table 3.2 Typical physical parameters that can changed as input [26]

Device parameters	Value
Device area (cm ²)	1
Front surface	Texture
Exterior front reflectance (%)	3
Exterior rear reflectance (%)	95
Light source	One sun (AM 1_5, 100 mW/cm ²)

Table 3.3 Typical layer parameters that can be changed as input [26]

Layer parameters	a-Si/n-a-Si	μ c-Si/n- μ c-Si	poly-Si/n-poly-Si	p-c-Si
Measured value				
Band gap	1.6/1.7	1.3/1.8	1.1/1.8	1.12
Electron mobility (cm ² /Vs)	0.2	10	20	1417
Hole mobility (cm ² /Vs)	0.1	5	10	470
Absorption (2.5 eV) (cm ⁻¹)	135015	68975	3390	405
Absorption (3 eV) (cm ⁻¹)	178959	176097	4364	396
Background doping (cm ⁻³)	1×10^{16}	1×10^{16}	1×10^{16}	1×10^{16}
Doping concentration (cm ⁻³)	-5×10^{18}	-5×10^{18}	-5×10^{18}	5×10^{18}
Assume value				
Dielectric constant	11.9	11.9	11.9	11.9
Electron affinity (eV)	3.4-4.05	3.4-4.05	3.4-4.05	3.4-4.05
Electron diffusivity (cm ² /s)	0.0051	0.22	0.31	28.6

Layer parameters	a-Si/n-a-Si	μ c-Si/n- μ c-Si	poly-Si/n-poly-Si	p-c-Si
Hole diffusivity (cm ² /s)	0.0026	0.03	0.08	10.96
Diffusion length (mm)	0.033	0.072	0.108	213.8
Front-surface recombination	10 ⁷	10 ⁷	10 ⁷	-
Rear-surface recombination	10 ⁶	10 ⁶	10 ⁶	-

3.5 EXPERIMENTAL ANALYSIS

Experimental analysis is a must in order to relate the theoretical knowledge with practical knowledge. Whether the information is or how accurate the calculation may be it cannot be used in the real life if it is not verify through any experimental procedure. For the behavioral characteristics of solar panel there are a number of experimental procedures.

3.5.1 For The Measurement of External Characteristics

Photovoltaic (PV) modules generate electricity when exposed to light, even when they are not connected in a circuit. Shocks and burns can result from contacts with output wiring and module itself. These hazards are increased when multiple modules are interconnected to increase array output current or voltage. Module of front surfaces is needed to be covered completely with an opaque cloth or other opaque material before performing any operation involving the module or electrical connections [27].

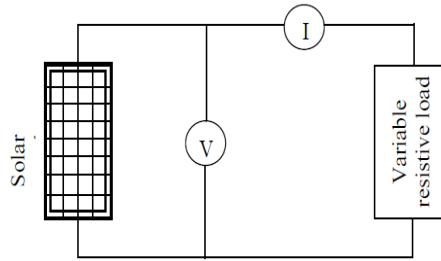


Figure 3.10 Experimental setup for the electric characteristics of solar panel

❖ **Material used**

A photovoltaic panel (BP Solar 10W, 12V), a solar panel rack (it supports and changes positions of a PV panel), 2 multimeters, insulated wires with alligator clips or other cables, a resistor panel.

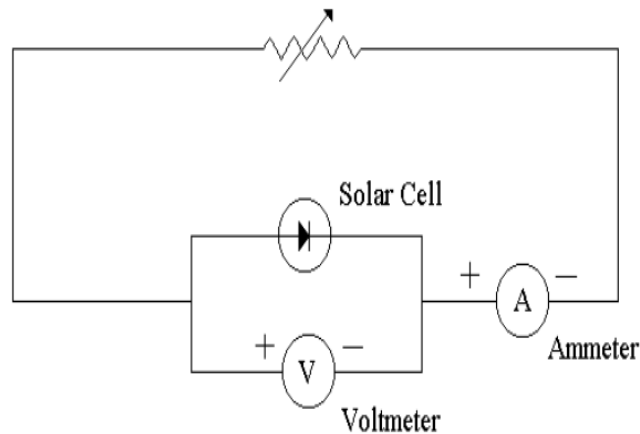


Figure 3.11 Schematic diagram for external characteristics of solar panel

❖ **Measurement of I-V characteristics:**

1. The output terminals of the PV panel are shorted with a wire. The short circuit current and panel output voltage are measured. The panel voltage will be small for this case. Both the voltage and current are recorded.

- The heavy-duty variable resistors are connected to the panel, starting from lower resistance to

- Higher one so that the panel voltage increases from zero toward open circuit. The voltage and current for each resistor are measured and recorded.
- The voltage and current are measured when the panel is open-circuit. The panel voltage and current are also recorded.
- All the data recorded are used to plot I versus V manually.

2. Step 1 in is repeated for different sunlight, i.e. different weathers or different time of a day.

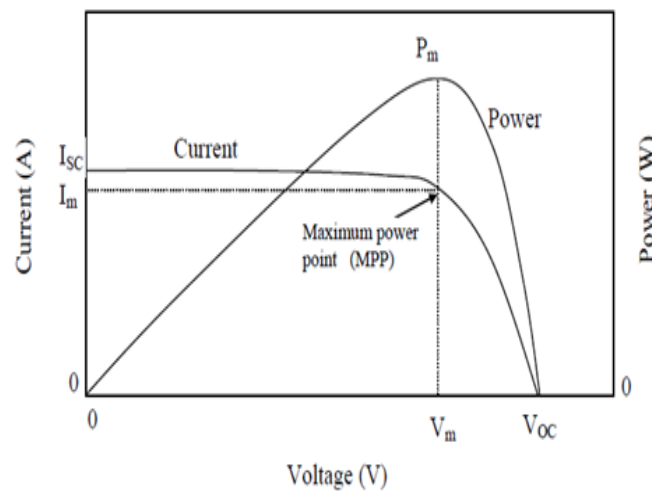


Figure 3.12 Characteristics of solar panel

3. Step 1 in is repeated and measured V-I curves at different tilting angles of the solar panel.

3.5.2 Measurement in Different Wavelengths

To observe the effects on solar cell in different weather, variable amount of sunlight and for different types of wavelengths we can use the same experimental setup which we have used for I-V characteristics. Here we are observing different changes in solar cell due to the effects of more and less light and different wavelengths of light on the PV cell and of the cell's temperature.

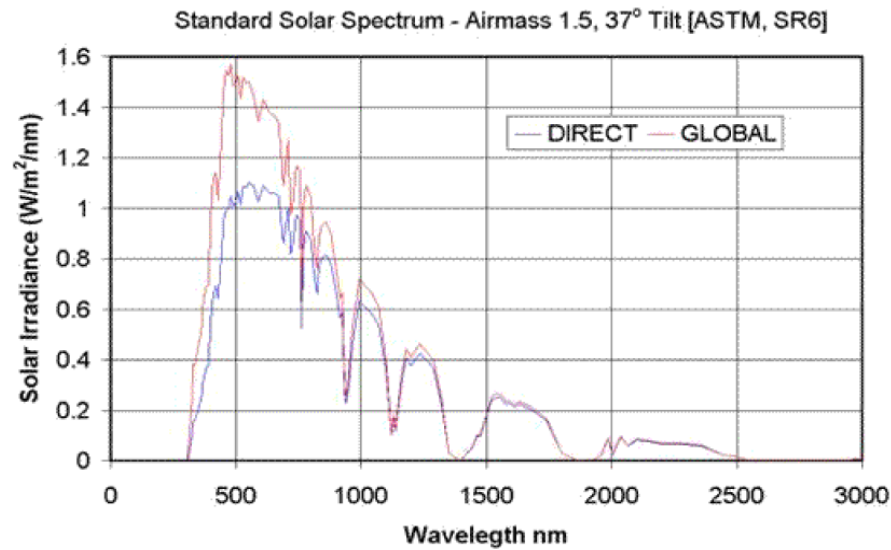


Figure 3.13 Solar irradiance vs wavelength curve[28]

Here we shall observe

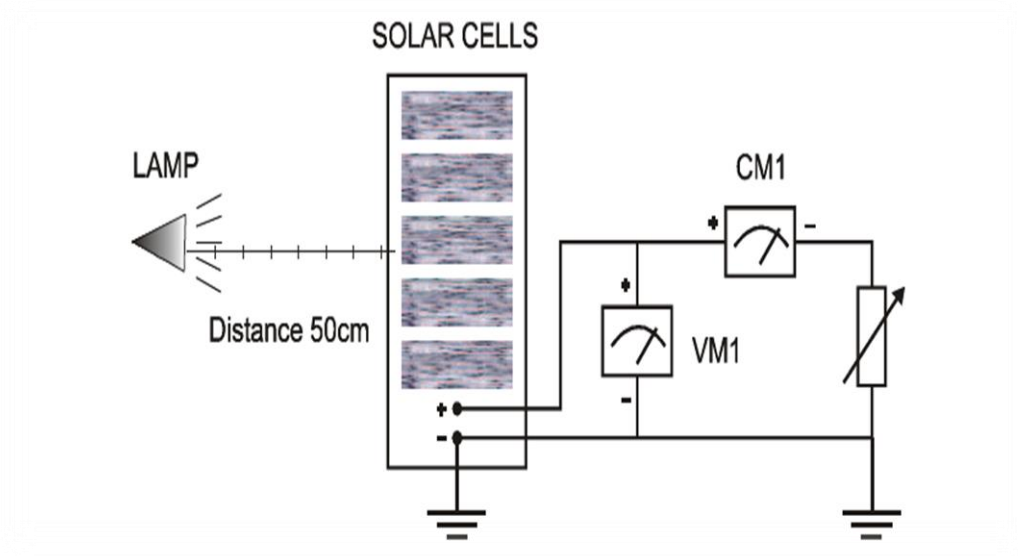
- Current readings will be larger when more light is absorbed.
- Open circuit voltage readings should be smaller when the PV cell is cold, though this temperature effect may be too minor to observe on a small scale.
- The decreasing angles from the sun (light source) result in lower current readings.

3.5.3 For the Measurement of Internal Characteristics

Solar cell works best in sun light. Some special featured solar can also operate in moonlight or even in infra-red light. If a solar cell is partly or fully shaded then the output can be drastically fall .That's why one needs to investigate the performance of solar cell in absence of light and measure its electrical characteristics to get insight of its internal characteristics.[29]

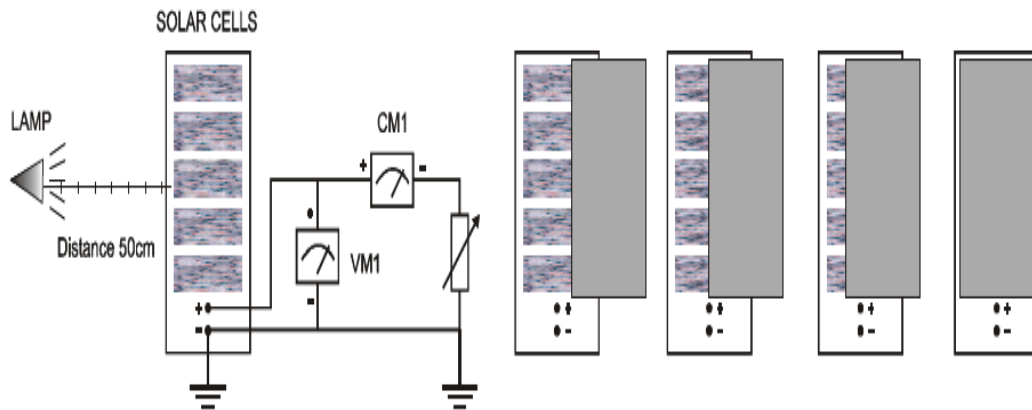
For the experiment we are observing the performance of solar cells under various shaded condition.

Initial alignment (without shading)



(a)

Horizontally shading (in segment)



(b)

Vertically shading (in segment)

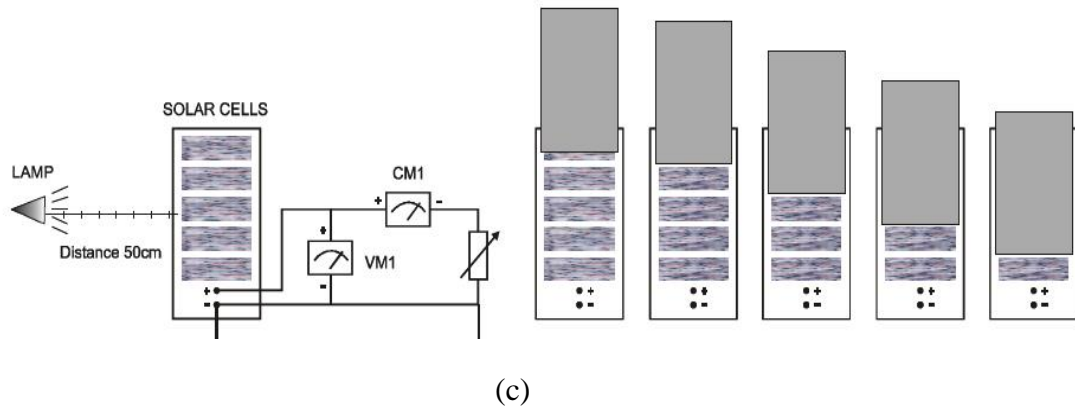


Figure 3.14 Internal characteristics of solar cell

In this experiment we observe that with the addition of the light the I-V curves shifts towards the fourth quadrant. In the first place a solar cell performs like a simple diode in absence of light. When sun light falls upon on solar cell the curve starts to move downward.

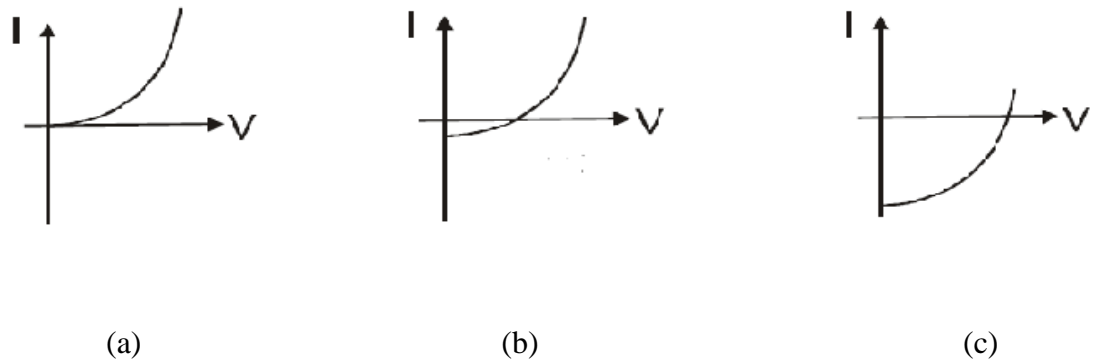


Figure 3.15 Change of I-V characteristics curve with increasing incident light

3.5.4 Measurement of Electro-luminiscence

It is also an important internal characteristic of any photo-voltaic element. The operation is done with or without injecting current. Here the external E-L quantum efficiencies of the sun cells are measured under the operation of LED as a function of injection current density. The E-L efficiencies can also be obtained through the integration of EL peaks in the EL spectra.

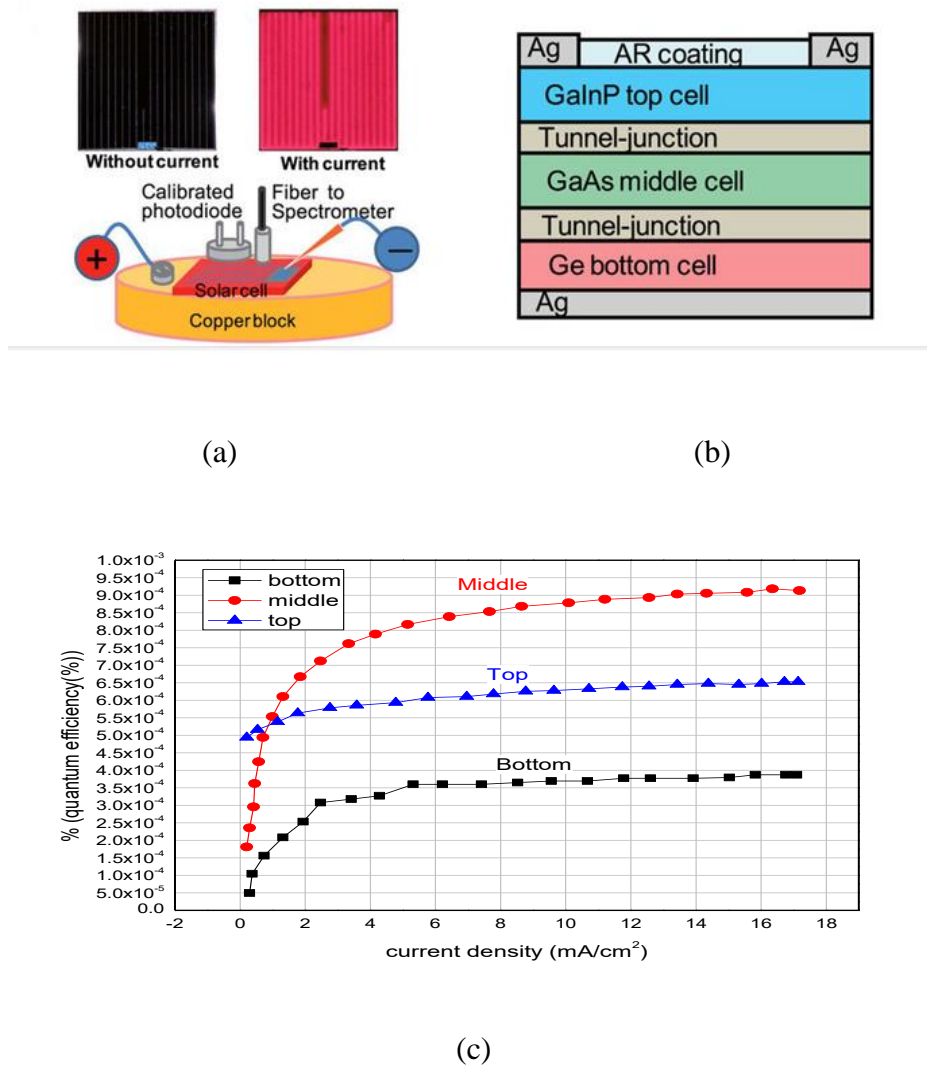


Figure 3.16 (a) Schematic of the experimental setup (b) Schematic structure of the GaInP/GaAs/Ge 3-junction solar cell (c) Output of the experiment EL Vs current density curve

3.6 RESULT FOUND FROM THESE METHODS:

In different analysis we observe that there is a variation of results for cells and modules made from different semiconductors and for subcategories within each semiconductor grouping like crystalline, polycrystalline, and thin film. Here we will see the results for different cell configuration under different supervision. The information are described for single junction cells and multiple junction cells.

The most important criterion for inclusion of results into the tables is they must have been independently measured by a recognized test centre listed elsewhere. A distinction is made. Table1 summerizes the best reported measurements for one sun non concentrator single junction cells and sub modules.

Table 2 summerizes the growing number of cell and sub module results involving high efficiency one sun multiple junction devices with these previously reported result.

Table 3.4 Confirmed single-junction terrestrial cell and submodule efficiencies measured under the global AM1.5 spectrum (1000 W/m) at 25°C) [30]

Classification	Efficiency(%)	V_{oc}(V)	J_{sc}(mA/cm²)	Fill Factor(%)
Silicon(crystalline cell)	26.7 ± 0.5	0.738	42.65	84.9
Si(multicrystalline cell)	21.9 ± 0.4	0.6726	40.76	79.7
Si (thin transfer)	21.2 ± 0.4	.687	38.50	80.3
GaAs (thin film cell)	28.8 ± 0.9	1.122	29.68	86.5
GaAs (multicrystalline)	18.4 ± 0.5	0.994	23.2	79.7
InP (crystalline cell)	24.2 ± 0.5	0.939	31.15	82.6

Classification	Efficiency(%)	V_{oc}(V)	J_{sc}(mA/cm²)	Fill Factor(%)
CIGS (cell)	21.7 ± 0.5	0.718	40.70	74.3
CdTe (cell)	21.0 ± 0.4	0.8759	30.25	79.4
CZTS (cell)	10.0 ± 0.2	0.7083	21.77	65.1
Si (amorphous cell)	10.2 ± 0.3	0.896	16.36	69.8
Si(microcrystalline cell)	11.9 ± 0.3	0.550	28.72	75.0
Perovskite (cell)	19.7 ± 0.6	1.104	24.67	72.3
Perovskite (minimodule)	16.0 ± 0.4	1.029	19.51	76.1
Dye (cell)	11.9 ± 0.4	0.744	22.47	71.2
Dye (minimodule)	10.7 ± 0.4	0.754	20.19	69.9
Organic (cell)	11.2 ± 0.3	0.780	19.30	74.2

Table 3.5 Confirmed multiple-junction terrestrial cell and sub module efficiencies measured under the global AM1.5 spectrum (1000 W/m) at 25°C [30]

Classifications	Efficiency (%)	V_{oc}(V)	J_{sc}(mA/cm²)	FillFactor(%)
5 junction cell (bonded)	38.8 ± 1.2	4.767	9.564	85.2
InGaP/GaAs/InGaAs	37.9 ± 1.2	3.065	14.27	86.7
GaInP/GaAs(monolithic)	31.6 ± 1.5	2.538	14.18	87.7
GaInP/GaAs/Si	35.9 ± 0.5	2.52/0.681	13.6/11.0	87.5/78.5
GaInP/GaAs/Si (wafer)	31.3 ± 1.1	3.046	11.7	87.5
GaInP/GaAs/Si(monolithic)	19.7 ± 0.7	2.323	10.0	84.3
Perovskite/Si(monolithic)	23.6 ± 0.6	1.651	18.09	79.0

3.7 CONCLUSION

The three basic procedures of analytical, simulation and experimental methods for the development and analysis of solar cell have been illustrated in the chapter. The current-voltage characteristic is measured by monitoring the current from the solar cell point by point from zero to the short circuit current using an electrical load regulator. The actual analysis begins with the determination of the physical variables that are responsible for the solar cell parameters. Solar cell device fabrication and device operation are implemented in simulation package TCAD by executing the process of data analysis and output transient analysis respectively. The measurement of photovoltaic cell characteristics both in presence and absence of light is done by experimental setup. The observed result is found to vary with different semiconductor subcategorized in crystalline, polycrystalline, thin film etc.

CHAPTER FOUR

TCAD SIMULATION SOFTWARE

4.1 INTRODUCTION

The thesis is based on solar cell simulation working. The simulations were carried out using TCAD Simulation Software. The TCAD enables one to design and predict the performance of semiconductor devices based on physics-based simulation. This tool is helpful in modeling the semiconductor device initially before fabricating it. This is very helpful in many research and development projects.

TCAD (Computer Aided Design) has included new physical models which use efficient numerical methods and algorithms. It also uses new meshing techniques, optimized linear solvers, etc., which helps in getting the simulation results very close to the practical results.

TCAD products are used either for:

- Process simulations which use tools like ATHENA, SSupreme4 etc.
- Device Simulations which use the Atlas Framework. Atlas has several simulators like S-Pisces, Luminous, Mixed Mode, TFT, Laser, Blaze etc.
- Virtual Wafer Fab to automate and emulate physical manufacturing and not limited to running only a single simulator but can combine any of the simulation tools available allowing the user to optimize full flow simulations.

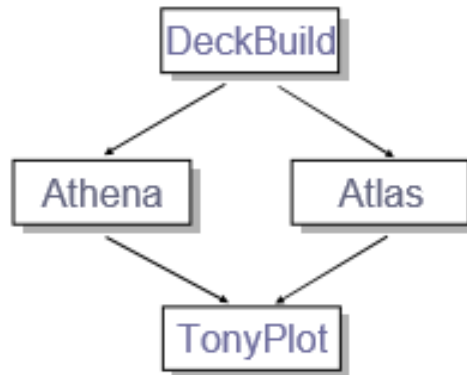


Fig. 4.1 TCAD software [31]

The VWF (Virtual Wafer Fab)

Framework consists of two different sets of tools:

- core tool
- auxiliary tools

ATHENA

- process simulation tool.
- predicts the physical structure that results from the processing steps.
- treats process simulation as a serial flow of events.

ATLAS

- device simulation tool.
- performs physically-based 2D/3D device simulations.
- predicts the electrical behavior of specified semiconductor structures and provides insight into the internal physical mechanisms associated with the device operation.
- various tools that comprise ATLAS include: S-PISCES, BLAZE, GIGA, TFT, LUMINOUS, LASER, MIXEMODE, DEVICE3D, INTERCONNECT3D, THERMAL3D.

4.2 VIRTUAL WAFER WEB (VWF)

TCAD International provides several software tools to perform process and device simulation. From Figure 2, it can be seen that Silvaco TCAD offers powerful simulation software.

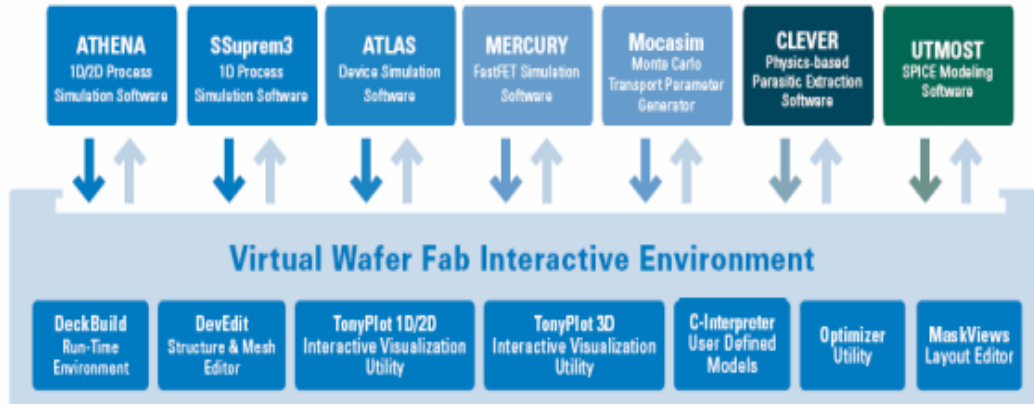


Fig.4.2 Virtual Wafer Fabrication Environment[32]

In this thesis, Silvaco Atlas was extensively used. The DeckBuild run-time environment received the input files. Within the input files, Silvaco Atlas was called to execute the code. And finally, TonyPlot was used to view the output of the simulation. Additionally, output log files were produced. The data extracted from the log files could then be displayed using Microsoft Excel or Matlab scripts.

4.3 ATLAS

Atlas provides general capabilities for physically-based two (2D) and three-dimensional (3D) simulation of semiconductor devices. It predicts the electrical behavior of specified semiconductor structures and provides insight into the internal physical mechanisms associated with device operation [33].

4.3.1 Functions of Atlas

ATLAS is a standalone tool for predicting the impact of process variables on circuit performance. Device simulation fits between process simulation and SPICE model extraction. ATLAS enables one to choose from the large selection of silicon, III-V, II-VI, IVVI or polymer/ organic technologies including, CMOS, bipolar, high voltage power device, VCSEL, TFT, optoelectronic, LASER, LED, CCD, sensor, fuse, NVM, ferroelectric, SOI, Fin-FET, HEMT and HBT.

Typical applications include MOS, bipolar and BiCMOS technologies. BLAZE simulates III-V, II-VI materials, and hetero-junction structures. It has built-in models for simulating abrupt and graded hetero-junctions for structures like MESFET, HEMT and HBT.

QUANTUM with its models simulates the effects of quantum confinement of carriers in semiconductor devices. TFT 2D/3D with its advanced physical models and numerical techniques simulates amorphous and polysilicon devices, including thin film transistors.

LUMINOUS 2D/3D is used to simulate light absorption and photo-generation in semiconductor devices. Luminous, when used with the S-Pisces or Blaze device simulators, calculates the optical intensity within the semiconductor device and converts these profiles into photo-generation rates in the device simulator. It works in conjunction with other ATLAS simulators.

LASER is used for simulating semiconductor laser diodes. The other simulators include VCSEL, OTFT, FERRO and NOISE for simulating vertical cavity surface emitting lasers, organic and polymer based devices, static I-V characteristics of ferroelectric films, and accurate characterization of small-signal noise sources, respectively.

4.3.2 Atlas Inputs and Outputs

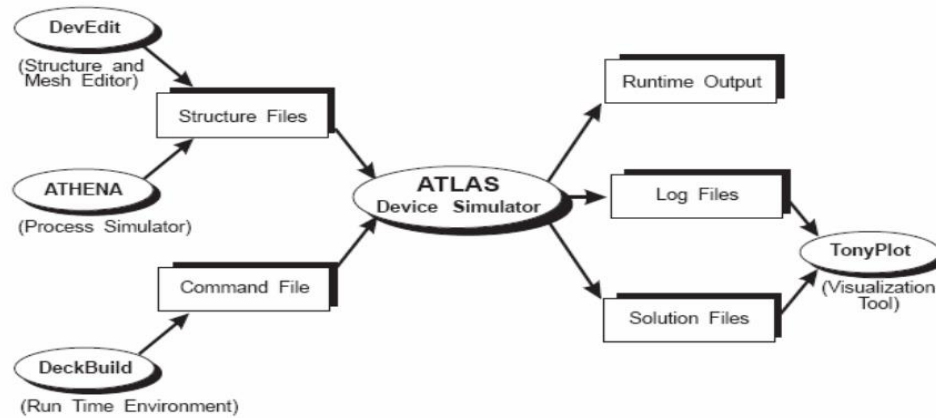


Fig 4.3 Flow of simulation

Simulations generally use two inputs which are: a text file that has commands for ATLAS to execute and a structure file that defines the structure of the device. The text file with simulator-specific commands is created with DECKBUILD. Structure files are created with DEVEDIT and ATHENA. ATLAS has three types of output. The progress of the simulation and error or warning messages are called the run-time output. Log files are generated with the currents and terminal voltages applied during device analysis. Finally the solution files store the two and three dimensional data relating to the values of solution variables within the device for a single bias point. The log files and the solution files are visualized using TONYPLOT [34].

4.4 DECKBUILD

Deckbuild is a powerful interactive run-time environment tool that allows user to transparently go from process simulation to device simulation to spice model extraction. It is easy to use run time environment for running core simulators such as ATLAS. Deckbuild helps in creating the input files to ATLAS. Multiple windows provide menu based or text-based input decks for the information entered. The deck

can be modified any time. Multiple decks are also created if there is any information that is being repeated. Multiple simulators can be called from the input deck, and the transfer of information is transparent to the user.

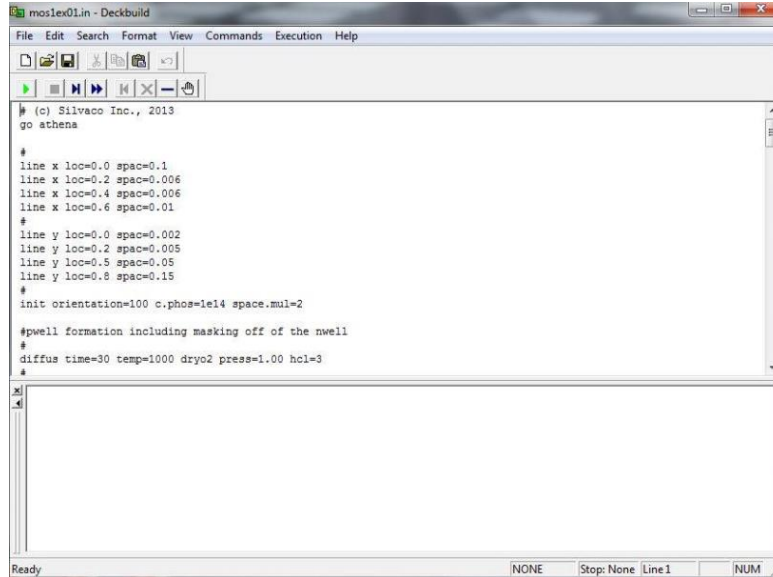


Fig 4.4 Deckbuild Commands Menu

It offers complete control of run, kill, pause, and stop-at, restart, single-step and history initialization operation, i.e., we can back-track to a previous point in the deck and run it from that instance. It also includes a large number of examples for all types of technologies. In simulation it displays runtime output with the errors or warnings and the progress of the simulations. Necessary changes can be made to the input deck according to the run time output. Besides using the interactive mode, one can also give simulator-specific statements.

The code also has a provision to incorporate the user-defined functions from the C-interpreter. Other simulator tools, such as TONYPLOT, DEVEDIT and MASKVIEW can also be invoked from Deckbuild. Deckbuild's optimizer helps in optimizing targets like structural dimensions and device parameters after complicated electrical tests and intermediate outputs.

4.5 DEVEDIT

Devedit is an interactive tool for defining and altering structures. It uses SILVACO's Master structure file format to communicate with process and device simulators. Analytic functions in Devedit are helpful in defining and altering the doping profiles. It could be a stand-alone for defining structures and later invoked by Deckbuild to perform ATLAS simulation of the device structure. This tool is valuable as a pre-processor for 2D device simulators. A new mode of DEVEDIT supports the definition and meshing of 3D structures. So basically it performs tasks as follows:

- Defining a device interactively on the screen for subsequent device or process simulations.
- Remeshing a device structure between process simulation and device test simulations, when the process simulator does not create a good grid for the device simulator.
- Remeshing a device structure during a process or device simulation, when the mesh is no longer adequate for the next simulation step.

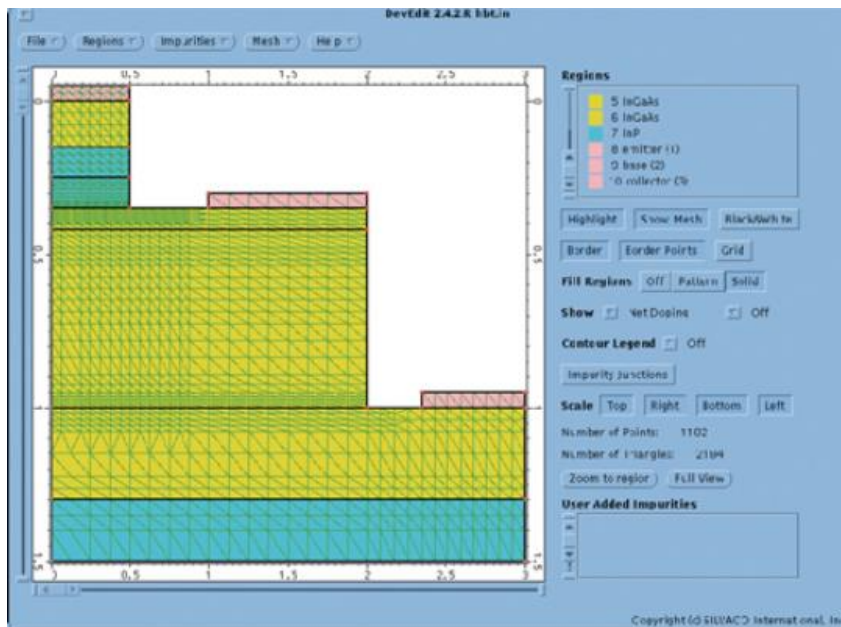


Fig 4.5 DevEdit Base Window Display

4.6 TONYPLOT

This is the common visualization tool in Silvaco TCAD products. It provides comprehensive capabilities for viewing and analyzing simulator output. The data can be plotted as desired by the user either in 1D x-y data, 2D contour data, Smith charts or polar charts. Measured data can also be imported and plotted in the above-mentioned types. The overlays feature helps in comparing the multiple simulation runs. It annotates plots to create meaningful figures for reports and presentations. It can plot to files, postscript printers, and other printer formats in sharp colors. It enables 2D structure plots to be cut by multiple, independently controlled 1D slices.

TonyPlot is a powerful tool designed to visualize TCAD 1D and 2D structures produced by TCAD simulators. It provides visualization and graphic features such as pan, zoom, views, labels and multiple plot support.

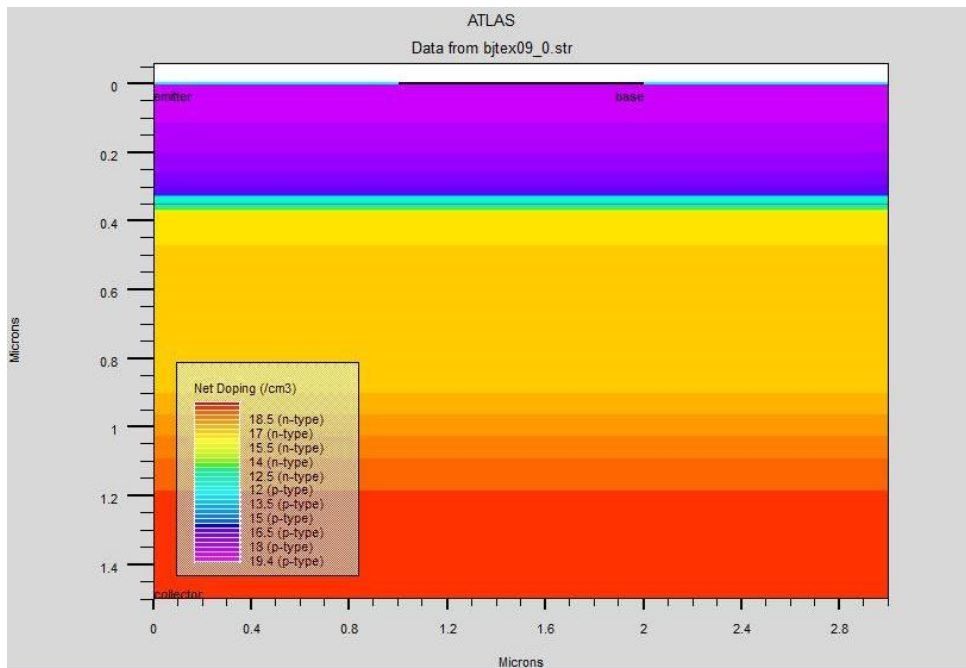


Fig 4.6 Atlas Tonyplot output

4.7 ATLAS PROCEDURE OVERVIEW

4.7.1 Modes of Operation Of Atlas

There are three different modes of operation of ATLAS [31]. These are given below:

1) Interactive mode with DeckBuild

```
deckbuild -as <input_filename>
```

2) Batch mode with DeckBuild

With X-Windows operation:

```
deckbuild -run -as <input_filename> -outfile<output_filename>
```

Without X-Windows operation:

```
deckbuild -run -ascii -as <input_filename> -outfile<output_filename>
```

3) Batch mode without DeckBuild

```
atlas<input_filename> -logfile<output_filename>
```

4.7.2 Starting With Deckbuild

To start DeckBuild, one needs to type: deckbuild. When DeckBuild starts, the following happens:

File control buttons:

Control room:

- commands for defining the problem
- switching between simulations
- plotting
- data optimization

File control buttons are used for:

- importing previously saved ASCII files describing a structure of interest
- Main control button contains: Optimizer and Examples

Run time control buttons:

These are used for controlling the way the simulator is run:

- **next** - sends current line to simulator
- **run** - runs deck from top to bottom
- **quit** - sends a quit statement to the simulator
- **restart** - restarts the current simulator
- **kill** - kills the simulator

4.7.3 Atlas Syntax

The form of the input file statements is:

<STATEMENT><PARAMETER> = <VALUE>

The parameter can be: real, integer, character and logical. The order in which the ATLAS commands occur is the following:

- A) Structure specification: MESH, REGION, ELECTRODE, DOPING
- B) Material models specification: MATERIAL, MODELS, CONTACT, INTERFACE
- C) Numerical method selection: METHOD
- D) Solution specification: LOG, SOLVE, LOAD, SAVE
- E) Results analysis: EXTRACT, TONYPLOT

The input file can be created using the DeckBuild Command Menu.

4.7.4 Structure Specification

(1)MESH statement specification:

INFILE, OUTFILE- file with previously saved mesh, new file

SPACE.MUL- scale factor applied to all specified grid spacing

CYLINDRICAL, RECTANGULAR- describes mesh symmetry

NX, NY- number of nodes along the x- and y-direction.

(2) X.MESH, Y.MESH statements:

Specify the location of grid lines along the x and y-axes.

NODE- specifies mesh line index

LOCATION- specifies the location of the grid line

RATIO- ratio to be used when interpolating grid lines between given locations

SPACING- specifies mesh spacing at a given location

(3)ELIMINATE statements:

Eliminates every second mesh point in a rectangular grid specified by X.MIN, X.MAX, Y.MIN and Y.MAX

COLUMNS, ROWS- columns, rows elimination

(4)REGION statement:

Specifies regions and materials. Material can be SILICON, OXIDE

NUMBER - denotes region number

POSITION - defines the location of the region in terms of (1) actual position and (2) grid nodes

(5)ELECTRODE statement:

Must specify at least one electrode within the simulation domain.

NAME - defines the name of the electrode: SOURCE, DRAIN, GATE

position parameter - BOTTOM, LEFT, RIGHT, TOP, SUBSTRATE, IX.LOW, IX.HIGH, X.MIN, X.MAX, LENGTH

(6) DOPING statement:

It can be used to set the doping profile analytically. Analytical doping profiles can be defined with the following parameters:

Distribution type -Uniform and Gaussian.

Doping type-n type and p type.

Concentration-peak concentration specification for Gaussian profiles.

Characteristics- principal characteristic length of the implant (standard deviation). One can specify junction depth instead.

Peak- specifies the location of a peak of a Gaussian profile

(7)Comments on the mesh setup

(1) Defining a good mesh is a crucial issue in device simulations. There are several factors that need to be taken into account when setting the mesh:

- Fine mesh is needed to properly resolve the structure.
- Efficiency for the simulation to finish in a reasonable time, fewer grid points must be used.

(2) Critical areas where fine mesh is needed include the followings:

Depletion regions: high-field regions

Si/SiO₂ interface: high transverse electric field region

(8) REGRID statement

It allows fine mesh generation in critical device areas. This statement is used after the MESH, REGION, MATERIAL, ELECTRODE, and DOPING statements. Regridding can be done by doping.

(9) CONTACT statement

NAME - specifies the name of the contact: GATE, DRAIN, ANODE

WORKFUNCTION - specifies workfunction of a metal, or if specifies N.POLYSILICON, then it implicitly assumes one.

(10) Material statement

Atlas also supplies a default list of parameters for the properties of the material used in the simulation. The parameters specified in the MATERIAL statement include, for example: electron affinity, energy bandgap, density of states function, saturation velocities, minority carrier lifetimes, Auger and impact ionization coefficients, etc. REGION specifies the region number to which the above-described parameters apply parameters . Some of the most commonly used parameters include: AFFINITY, EG300, MUN, MUP, NC300, NV300, PERMITTIVITY, TAUN0, TAUP0, VSATN, VSATP.

(11) INTERFACE statement

Specifies interface charge density and surface recombination velocity and amount of interface charge density, surface recombination velocity for electrons and holes.

(12) MODELS and IMPACT statements

The physical models that are specified with the MODELS and IMPACT statements include: mobility model CONMOB, ANALYTIC, ARORA, FLDMOB, TASCH, etc. recombination models SRH, CONSRH, AUGER, OPTR carrier statistics BOLTZMANN, FERMI, INCOMPLETE, IONIZ, BGN impact ionization CROWELL, SELB tunneling model FNORD, BBT.STD (band to band - direct

transitions), BBT.KL (direct and indirect transitions), HEI and HHI (hot electron and hot hole injection)

(13) METHOD statement

Allows for several different choices of numerical method selection. The numerical methods that can be specified within the METHOD statement include

GUMMEL De-coupled Gummel scheme which solves the necessary equations sequentially, providing linear convergence. Useful when there is weak coupling between the resultant equations.

NEWTON Provides quadratic convergence, and needs to be used for the case of strong coupling between the resultant equations.

BLOCK NEWTON more efficient than NEWTON method

method gummel block newton method carriers=0

(14) DC solution procedures and statements:

A stable DC solution is obtained with the following two-step procedure:

- Find good initial guess by solving equilibrium case (initial guess is found based on the local doping density)

solveinit - Step the voltage on a given electrode for a convergent solution:

solve vcollector=2.0 solve vbase=0.0 vstep=0.05 vfinal=1.0 name=base

- To overcome the problems with poor initial guess, one can use the TRAP statement, where MAXTRAPS is the maximum allowed number of trials (default value is 4)

method trap solve init solve vdrain=2.

(15) AC solution procedures and statements:

The AC simulation is simply an extension to the DC simulation procedure. The final result of this analysis is the conductance and capacitance between each pair of

electrodes. The two types of simulations are: - Single frequency solution during a DC Ramp solve.

(16) Transient solution procedures and statements:

For transient solutions, one needs to use piecewise-linear, exponential and sinusoidal bias functions. For a linear ramp, one needs to specify the following parameters: TSTART, TSTOP, TSTEP and RAMPTIME.

4.7.5 Result Analysis

Three types of outputs are produced by the ATLAS tool: run-time outputs, log files and solution files.

Run-time outputs:

The various parameters displayed during the SOLVE statement are listed below:

Initial guess methodology used (previous, local)

Iteration numbers of the solution and the solution method
i = outer loop iteration
number j = inner loop number for decoupled solutions
m = solution method used:
G=Gummel, B=Block, N=Newton, norms of the equations being solved, the error measure has met its tolerance.

Log files:

The LOG parameter is used to store the device characteristics calculated using ATLAS:

log outfile=<file_name

Solution files:

The syntax to produce the solution files that can be used in conjunction with TonyPlot is:

```
save outfile=<file_name> solve . . . . outfile=<file_name>.sta master [onefileonly]
```

Invoking TonyPlot

To create overlaid plots with TonyPlot, one needs to use the following command: `tonyplot -overlay file1.log file2.log`. To load structure files, containing mesh, doping profile information, etc., one can use the following statement:

The parameters extraction can be accomplished in two different ways:

- 1) Using the EXTRACT command that operates on previously solved curve or structure file.
- 2) Using the Functions Menu in TonyPlot that allows one to use saved data for post-computation.
- 3) Using the LOG statement for AC parameter extraction.

4.7.6 Atlas Extract Description

(1) The extract statement can be used in conjunction with:

Process extraction, after running Silvaco ATHENA simulator

Device extraction, after obtaining the electrical characteristics of the device structure being simulated.

Log-files: contain the electrical information, more precisely, the IV-data obtained via the ATLAS simulation process
¾ Structure files: contain the additional electrical information, such as electric field, electrostatic potential, etc.

(2) One can construct a curve using separate X and Y-axes. For each of the electrodes, one can choose one of the following: Voltage (v), Current (i), Capacitance (c), Conductance (g), Transient time for AC simulations (time), Frequency for AC simulations (frequency), Temperature (temperature) etc.

4.8 CONCLUSION

Thus TCAD tools provide researchers with the electrical properties of solar cells under illumination in both two and three dimensional domains. The simulated properties include IV characteristics, spectral response, quantum efficiency, photo generation rates, potential distribution etc. in advanced solar cell technology simulation solutions. The process flow of simulation composed of device simulation and process simulation through Atlas and Athena respectively have been elaborated in the chapter. Two inputs of simulation consisting of text file and simulation file are executed using Deckbuild and Devedit. Athena enables researchers for integration and manufacturing process whereas Atlas enables to simulate electrical, optical and thermal behavior of semiconductor devices.

CHAPTER FIVE

TYPE OF SOLAR CELLS SELECTED FOR SIMULATION

5.1 INTRODUCTION

Solar cell is a vast platform to make the cell efficient. So far we studied different kind of solar cells evolution theoretically, experimentally and also observed through simulation. Here we are analyzing two specific solar cell- single junction solar cell and multi junction solar cell. Multi junction solar cell consists more than one junction. We have used dual junction solar cell as a reference model for multi junction solar cell.

5.2 SILICON SOLAR CELL

A silicon solar cell is an electrical device that converts the energy of light into electricity by the photovoltaic effect, which is a physical and chemical phenomenon. The operation of a Si solar cell requires three basic attributes:

- The absorption of light, generating either electron-hole pairs or excitations.
- The separation of charge carriers of opposite types.
- The separate extraction of those carriers to an external circuit.

The basic structure of a Si solar cell consist of:

1. Metal contact
2. Anti-reflective coating
3. Glass
4. n doped Si & p doped Si(create p n junction)

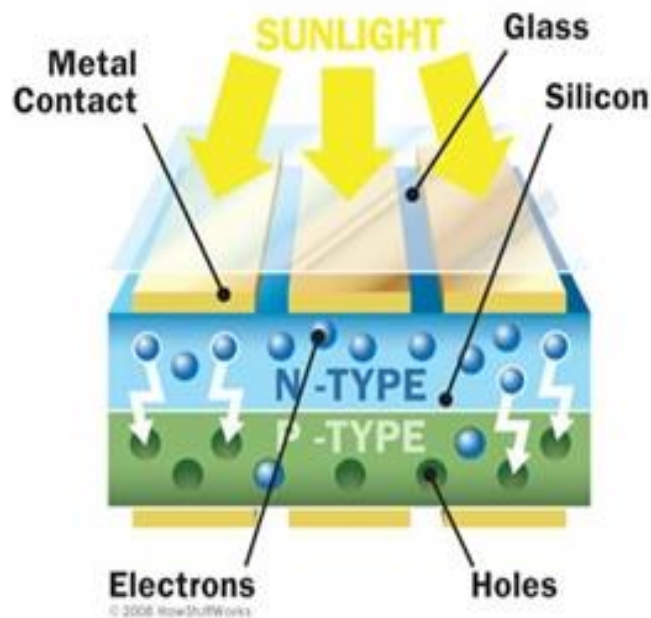


Figure 5.1 Structure of silicon solar cell

5.3 WORKING PRINCIPLE

The working of a Si solar cell is simple.it works in several steps:

- Photons in sunlight hits the solar panel and absorbed by silicon.
- Electrons are excited because of the incident photon.

- Excited photon can either dissipate the energy as heat and return to its orbital or travel through the cell until it reaches an electrode. The chemical bonds of the material are vital for this process to work.
- Si is used in two layers that is p dopes & n doped. In general one layer being doped with boron, the other phosphorus.
- These layers have different chemical electric charges and subsequently both drive and direct the current of electrons [35].
- The power generation happened by an array of solar cells convert solar energy into an usable amount of direct current (DC) electricity. An inverter can convert the power to alternating current (AC).

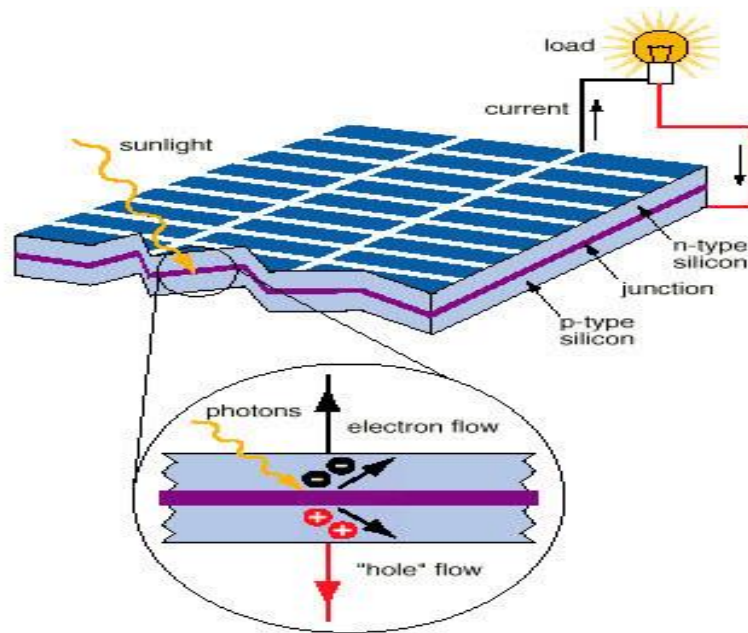


Figure 5.2 Cross-sectional view of Si solar cell

There are many ways to improve Si solar cell. We select this model as our reference model for initial analysis. We develop the model with further modification by changing its different parameter.

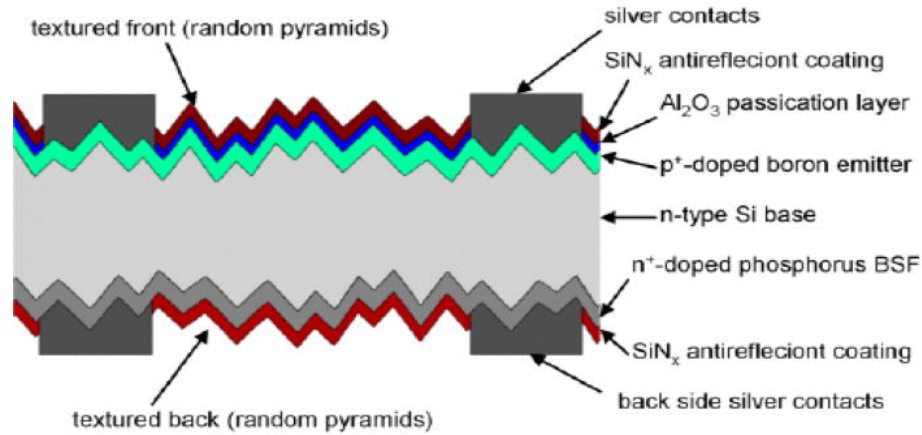


Figure 5.3 Referenced model for Si solar cell

5.4 DUAL JUNCTION SOLAR CELL

Multi-junction (MJ) solar cells are solar cells with multiple p-n junctions made of different semiconductor materials. Each material's p-n junction will produce current for different wavelengths of light. The use of multiple semiconductor materials allows the absorbance of a wide range of wavelength [36].

Multi-junction solar cells have been studied since 1960. The first multi-junction device was demonstrated in early 1980s, and it converted 16% of the solar energy into electricity. In 1994, US National Renewable Energy Laboratory (NREL) broke the 30% barrier. The maximum theoretical limit efficiency of multi-junction solar cells is 86.8% [37].

Basic Principles of Multi-Junction Solar Cells The highest-efficiency solar cells use multiple materials with bandgaps that span the solar spectrum. Multi-junction solar cells consist of some single-junction solar cells stacked upon each other, so that each layer going from the top to the bottom has a smaller bandgap than the previous, and so it absorbs and converts the photons that have energies greater than the bandgap of that layer and less than the bandgap of the higher layer [38].

5.5 PARAMETERS TO BE CONSIDERED

5.5.1 Lattice Match:

Figure 5.4 represents the bandgap E_g and the lattice parameter 'a' is the quaternary III-V alloy system. A line joining two points represents the changes in E_g and 'a' with composition in ternary alloy composed of the compound at the end of that line. For example GaAs alloy with $E_g=1.42\text{eV}$ and $a=0.565\text{nm}$ and E_g decreases and increases as GaAs is alloyed with InAs and we move along the line joining GaAs to InAs.

Alloys of groups III and V of the periodic table are good candidates for fabricating such multi junction cells are being shown in the figure 5.4 to make the whole scenario more acceptable.

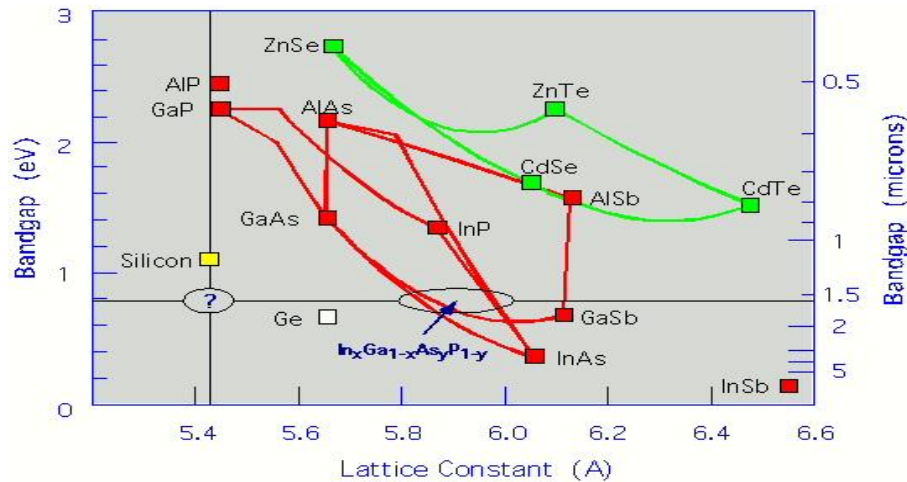


Figure 5.4 Graph of Bandgap Vs Lattice Constant

Eventually at InAs, $E_g=0.35\text{eV}$ and $a=0.606\text{nm}$ point x in figure is composed to InAs and GaAs and it is the ternary alloy $\text{In}_x\text{Ga}_{1-x}\text{As}$. It has $E_g=0.7\text{eV}$ and $a=0.587\text{nm}$, which is the same a as that for InP, $\text{In}_x\text{Ga}_{1-x}\text{As}$ as at X is therefore lattice matched to InP and hence can be grown on an InP substrate without creating defects at the interface.

Further $\text{In}_x\text{Ga}_{1-x}\text{As}$ at X can be alloyed with InP to obtain a quaternary alloy $\text{In}_x\text{Ga}_{1-x}\text{As}_y\text{P}_{1-y}$, whose properties lie on the line joining X and InP and therefore all have the same lattice parameter as InP but different bandgap layers of $\text{In}_x\text{Ga}_{1-x}\text{As}_y\text{P}_{1-y}$ with composition between X and InP can be grown exponentially on InP substrate by various technique such as liquid phase epitaxy or molecular beam epitaxy.

The hatched area between solid lines represents the possible values of E_g and a for frequently III-V alloy system in which the bandgap is direct and hence suitable for direct electron and hole recombination.

5.5.2 Bandgap:

In order to optimize conversion efficiency of a photovoltaic cell, the solar cell should absorb as much of the spectrum as possible, and so bandgaps should cover a wide range. Besides, bandgaps of adjacent layers should differ by as small amount as possible, because the amount of excess energy from light converted to heat is equal to the difference between the photon energy and the bandgap of the absorbing material [39]. The band gap of the semiconductor material determines how the solar cell reacts to light.

Table 5.1 Bandgap of some semiconductor

Material	Bandgap (eV at 300k)
Si	1.12
Ge	0.67
GaAs	1.43
GaP	2.26
InP	1.35
GaN	3.44
InAs	0.36
InSb	0.17
$\text{In}_x\text{Ga}_{1-x}\text{P}$	1.8-2.26
$\text{Al}_x\text{Ga}_{1-x}\text{As}$	1.42-2.16

The band gap of the semiconductor material determines the wavelength of light that meet the requirements to generate electrical energy. The conversion formula between band gap and wavelength is:

$$\lambda(\mu\text{m}) = \frac{hc}{E_g(\text{eV})}$$

Where,

λ = wavelength in micrometers

h =Planck's constant

c =speed of light in vacuum

E_g = band gap in eV (1eV is approximately equal to 1.6×10^{-19} J of energy)

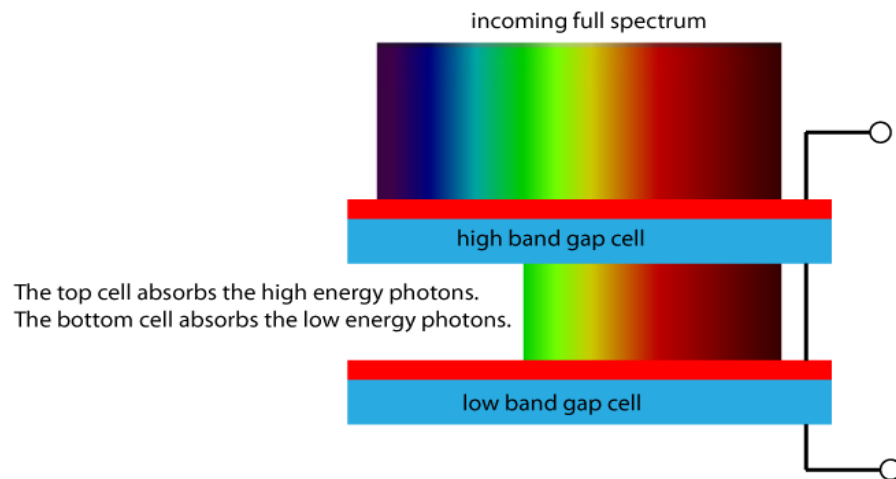


Figure 5.5 Irradiance on different bandgap cell

Figure 5.5 shows irradiance on cell with different bandgap. Higher energy photons are absorbed followed by low energy photons.

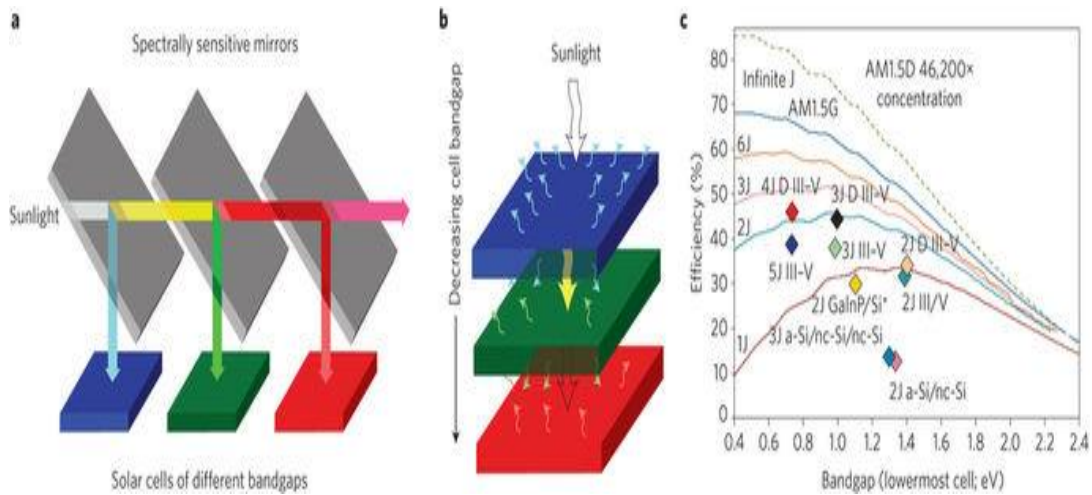


Figure 5.6 Design of multijunction solar cell & the efficiency vs Bandgap

Top cell has a highest bandgap and bottom cell has the lowest. The motto behind such design is absorbing huge amount of light.

5.5.2.1 Structure:

The first problem about the structure of multi-junction solar cell is the layering. Designing the materials layer by layer in a best way is the most challenging part. Multi-junction solar cells made from multiple materials, layers and various bandgap.

Solar Junction's multi-junction solar cell is comprised of multiple individual solar cells grown on top of each other. Each sub-cell is composed of a unique material that absorbs a specific portion of the solar spectrum. The top cell absorbs lower wavelength light, while the bottom cell absorbs higher wavelength light. Solar Junction's multi-junction technology enables a roadmap to ever-increasing efficiency gains. By adding additional sub-cells designed to absorb increasingly narrow segments of the solar spectrum efficiency gets higher.

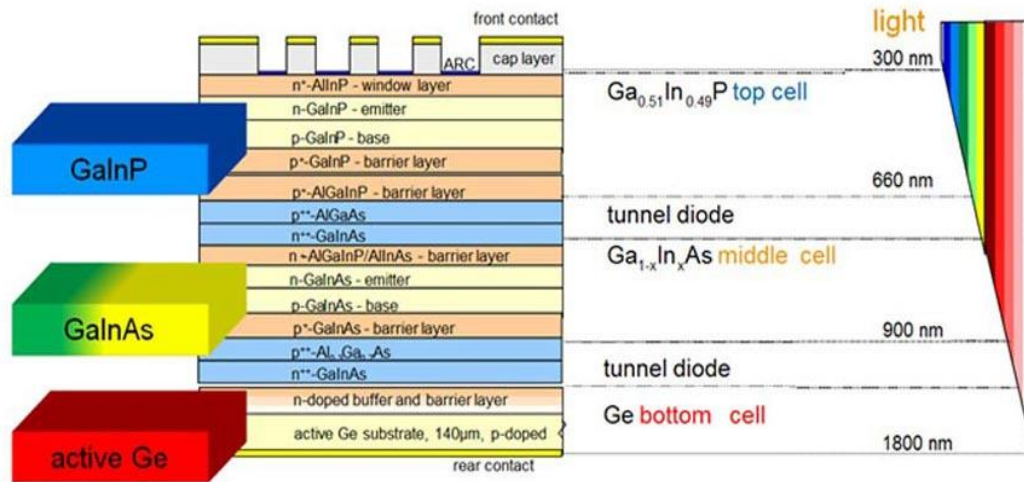


Figure 5.7 Structure of multi junction solar cell

5.5.2.2 Metal contacts:

The metallic contacts are usually on two sides of the cell. They are important to be on the back surface so that shadowing on the lighting surface is reduced. The metallic contacts are mainly low resistivity electrodes that make contact with the semiconductor layers. They are often Aluminium [35]. This provides an electrical connection to a load or other parts of a solar cell.

5.5.2.3 Window layer & back surface layer:

A window layer is used in order to reduce the surface recombination velocity. Similarly, a back-surface field (BSF) layer reduces the scattering of carriers towards the tunnel junction. The structure of these two layers is the same.

It is a hetero junction which catches electrons. The electrons cannot jump above the barrier formed by the hetero junction because they don't have enough energy. Hence, electrons cannot recombine with holes and cannot diffuse through the barrier. By the way, window and BSF layers must be transparent to wavelengths absorbed by the next p-n junction. And the doping concentration must be greater than 10^{18} cm^{-3} [36]

So we can say,

$$E_{g_{\text{window}}} > E_{g_{\text{emitter}}} \& E_{g_{\text{BSF}}} > E_{g_{\text{base}}}$$

The back surface field or BSF consists of a higher doped region at the rear surface of the solar cell. The interface between the high and low doped regions behaves like a p - n junction and an electric field forms at the interface which introduces a barrier to minority carrier flow to the rear surface. The minority carrier concentration is thus maintained at higher levels in the bulk of the device and the BSF has a net effect of passivating the rear surface.

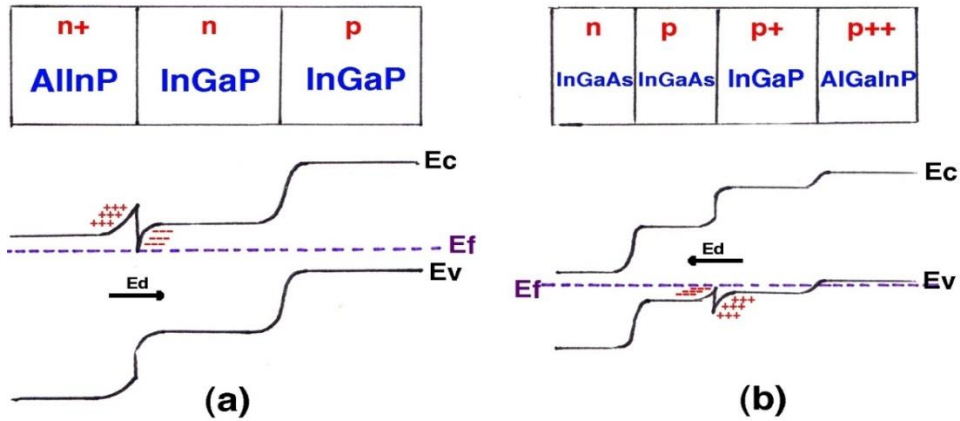


Figure 5.8 (a) Layers and band diagram of a window layer. The surface recombination is reduced. (b) Layers and band diagram of a BSF layer. The scattering of carriers is reduced.

5.5.2.4 Anti-reflective (AR) coating:

Anti-reflective (AR) coating is generally composed of several layers in the case of MJ solar cells. The top AR layer has usually a NaOH surface texturation with several pyramids in order to increase the transmission coefficient. On the one hand, the thickness of each AR layer is chosen to get destructive interferences. Therefore, the reflection coefficient R decreases to 1% [35].

5.5.2.5 Tunnel junction:

The main goal of tunnel junctions is to provide a low electrical resistance and optically low loss connection between two sub-cells. Without it, the p-doped region of the top cell would be directly connected with the n-doped region of middle cell. Hence, a p-n junction with opposite direction to the others would appear between the top cell and the middle cell.

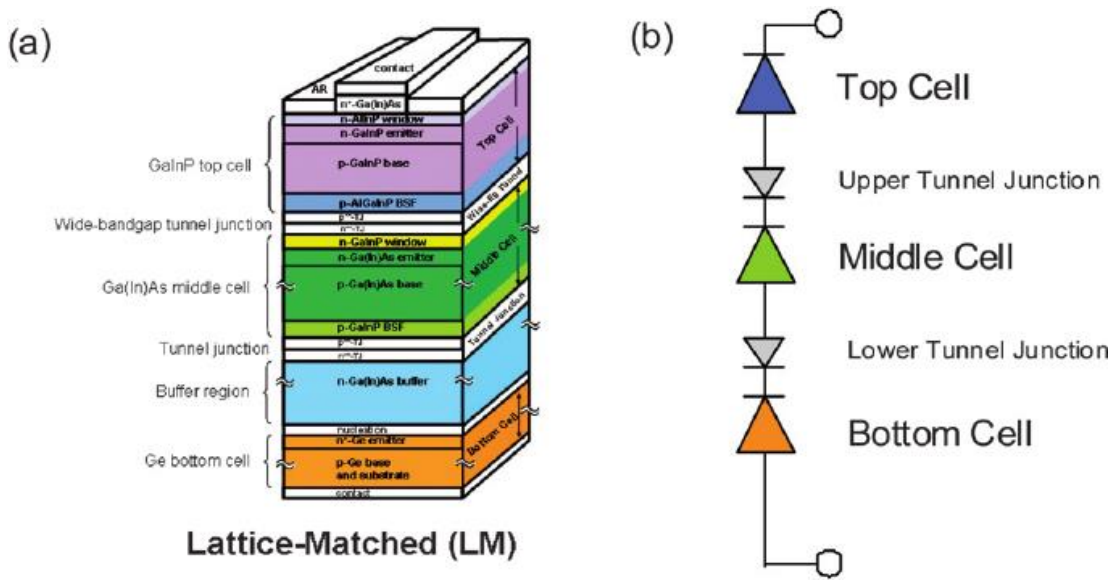


Figure 5.9 a) structure of MJ solar cell b) diode sequence of the junctions

Consequently, the photo voltage would be lower than if there would be no parasitic diode. In order to decrease this effect, a tunnel junction is used. It is simply a wide band gap, highly doped diode. The high doping reduces the length of the depletion region and electron can easily tunnel through depletion region as follows:

$$l_{depletion} = \sqrt{\left\{ \frac{2\epsilon(\phi - v)(N_A + N_D)}{qN_A N_D} \right\}}$$

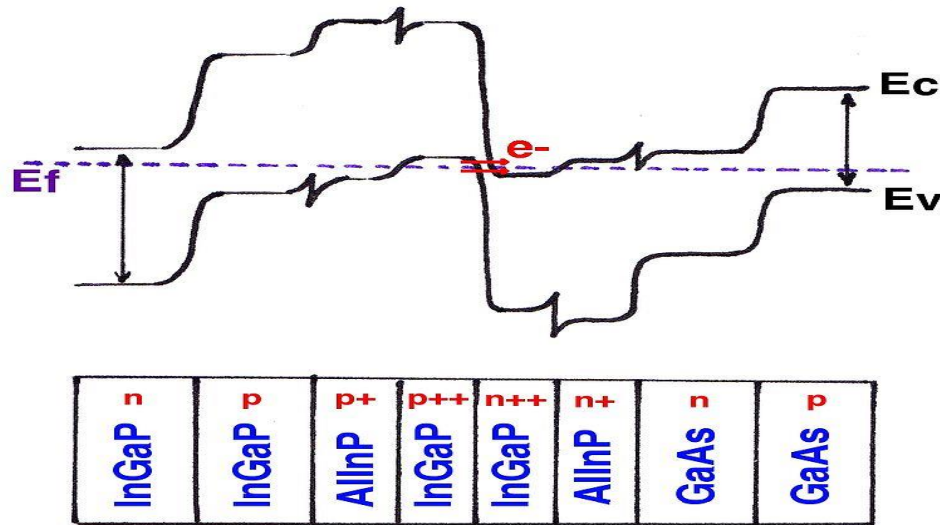


Figure 5.10 Layers and band diagram of the tunnel junction. Because the length of the depletion region is narrow and the band gap is high, electrons can tunnel.

Figure 5.10 shows three different regions: the tunneling region, the negative differential resistance region and the thermal diffusion region. The region where electrons can tunnel through the barrier is called the tunneling region.

There, the voltage must be low enough so that energy of some electrons who are tunneling is equal to energy states available on the other side of the barrier. Consequently, current density through the tunnel junction is high.

Then, the resistance is extremely low and consequently, the voltage too. This is why tunnel junctions are ideal for connecting two p-n junctions without having a voltage drop. When voltage is higher, electrons cannot cross the barrier because energy states are no longer available for electrons.

Therefore, the current density decreases and the differential resistance is negative. In order to avoid the reduction of the MJ solar cell performances, tunnel junctions must be transparent to wavelengths absorbed by the next photovoltaic cell.

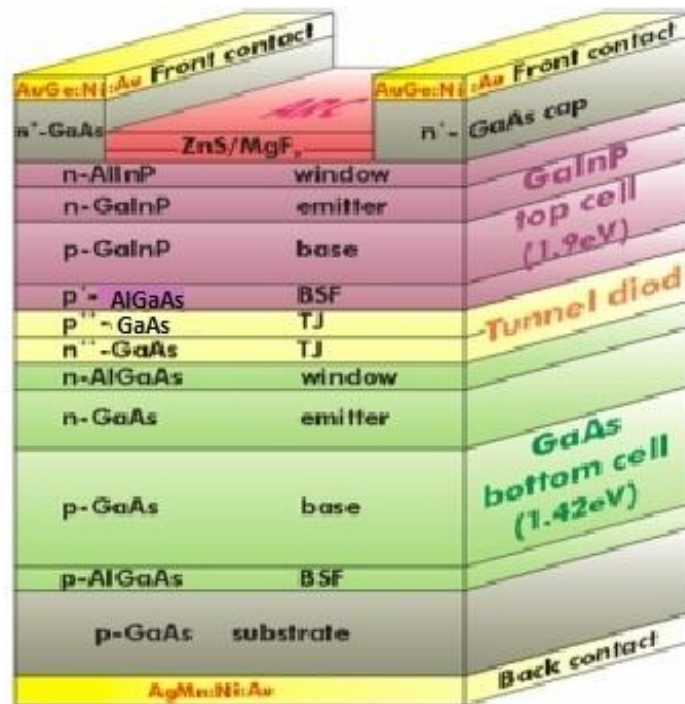


Figure 5.11 Reference model of dual junction solar cell

Multi-junction can be dual, triple or quadrant. Here we are working on dual junction solar cell. And try to improve it by changing the doping concentration and back surface material.

5.6 CONCLUSION

In this chapter we studied the structure of both single and multi-junction solar cells. The working principle and different important parameters for the understanding of both the solar cells have been described here. For the purpose of simulation we used reference model. For single junction solar cell we will work on concentration of doping. And for dual junction we will concentrate on the material properties as well as the concentration.

CHAPTER SIX

RESULT AND DISCUSSION

6.1 INTRODUCTION

Photovoltaics is the process of converting the solar energy into electrical energy. The rapidly growing and increasingly important renewable alternative to conventional fossil fuel electricity generation, but compared to other electricity generating technologies, it is a relative newcomer. But in the near future it is going to take the leading role as the source of power. So the techniques are being improved day by day.

The primary device was a single junction solar cell in 1980s research which have ended up to hetero-junctions with complex material alloy combination. Now a days there are various research is going on in regard of improving the efficiency. There are a wide variation of material variance along with technical difference.

So we have initially started our analysis from the primary device single junction silicon solar. For silicon single junction solar cell we have used three different materials (boron, arsenic, silicon) as the n-layer.

Then we have further moved by taking account the dual-junctions. It is the improved system in the field of solar cells. Here different junction layers are made by different alloys. It is a vast field to explore where there are combination of alloys can be done.

Further variety can be done by changing the thickness of the layers or the concentration acceptor and donor layers one at a time or together can be done. There is also a wide scope for the window and the back-surface layers to be manipulated. In

a word it the hetero-junctions are a interesting field to be worked with. For our analysis we have chosen two combinations InGaP-GaAs ,AlGaAs-GaAs.

In our whole analysis we have approached versatile techniques as we seem right at the moment. Sometimes we focused on the semiconductor material . Sometimes it was all about concentration. Even we have considered both the conditions sometimes.

So our whole analysis can be summarized as:

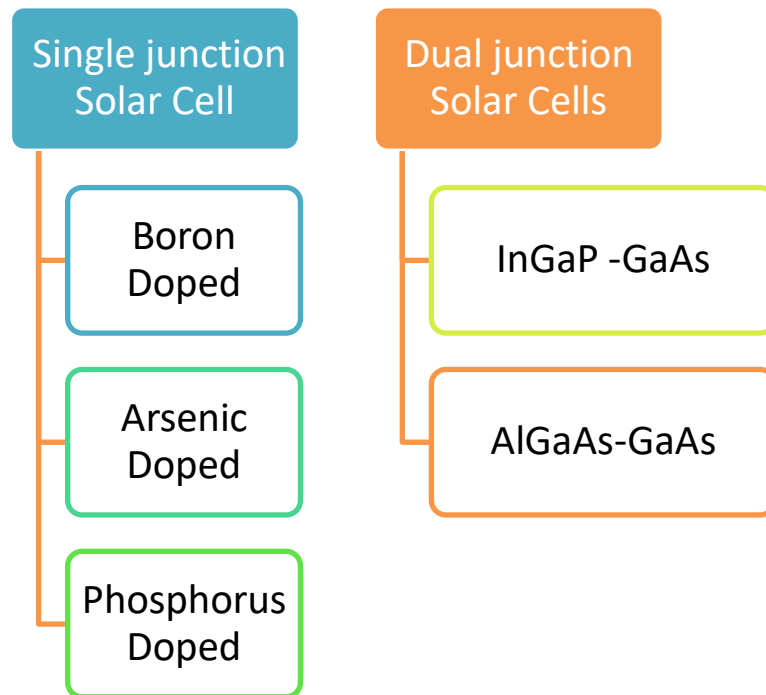


Figure 6.1 Summary of the analysis

Our main objective is to find out the most efficient solar cell from our analysis. So we have always tried to get the highest efficiency and fill factor by applying different measures.

a) For silicon solar cell we have changed the doping material along with concentration

b) For the dual-junctions we have applied a number of approaches as follows

- i) changing the concentration
- ii) changing the material of the back-surface
- iii) changing concentration for new back-surface

6.2 SINGLE JUNCTION SOLAR CELL

It has the most simple structure among all the solar devices. It represents a simple p-n junction device where silicon is the substrate material and p-type doped. And there is a very thin layer of another n-doped material. That's how the p-n junction is created. For the substrate material crystalline silicon is used. The fill-factor range for this type of solar cells vary from 70-80%. And the efficiency fluctuates between 16-24%. [40,41]

6.2.1 Boron Doped Silicon Solar Cell

For the calculation we have changed the n-doped boron layer from $(10^{15} - 10^{21}) \text{ cm}^{-3}$. Where the fill-factor varied from **82~83%** and the varied from **16~18%**.

The characteristics of multi-junction devices such as the short circuit current (I_{sc}), open circuit voltage (V_{oc}), maximum power (P_{max}), and fill factor (FF) depend on the photocurrent generated by the component cells and their I-V curves. Therefore, study the information on the I-V curve of each component cell to characterize the devices precisely.

I-V Curve (for concentration 10^{15} cm^{-3})

I-V Characteristic Curves are graphs of output voltage versus current for different levels of isolation and temperature and ability to convert sunlight into electricity. The most important values for calculating the fill factor, efficiency and generating p-v curve is obtained with the help of I-V curve.

We get I-V graph from simulation. At first we obtain I v curve to get the electrical characteristics of the cell which summarize in the relationship between the output current and voltage. The amount and intensity of solar insolation (solar irradiance) controls the amount of output current (I), and the operating temperature of the solar cells affects the output voltage (V) of the PV array.

From the I-V curve, P-V curve and the V_{oc} , I_{sc} parameters we further obtain curves to study fill factor and efficiency of the cells.

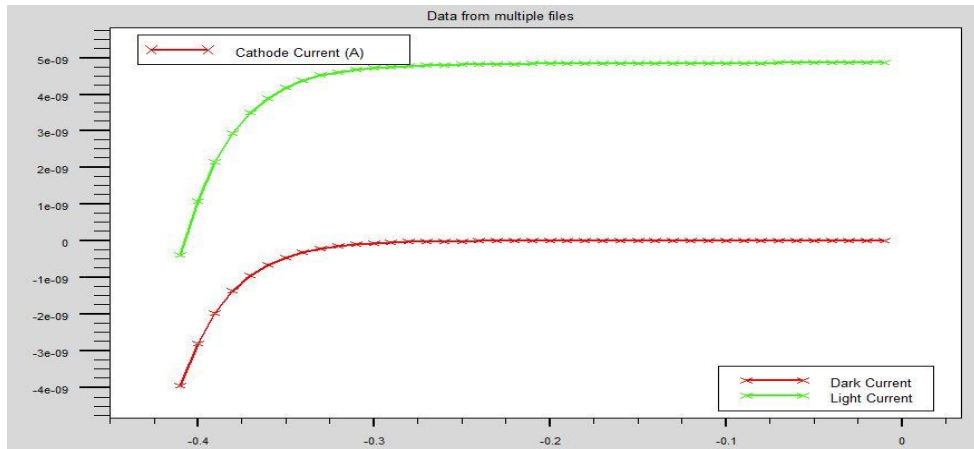


Figure 6.2 I-V Characteristics Curve Boron Doped Silicon Solar Cell

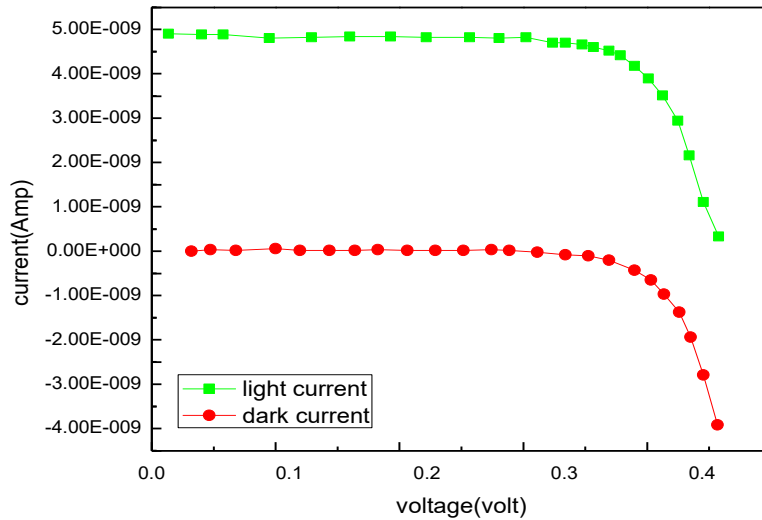


Figure 6.3 I-V Characteristics Curve Boron Doped Silicon Solar Cell (mirrored for calculation)

P-V Curve (for concentration 10^{15}cm^{-3})

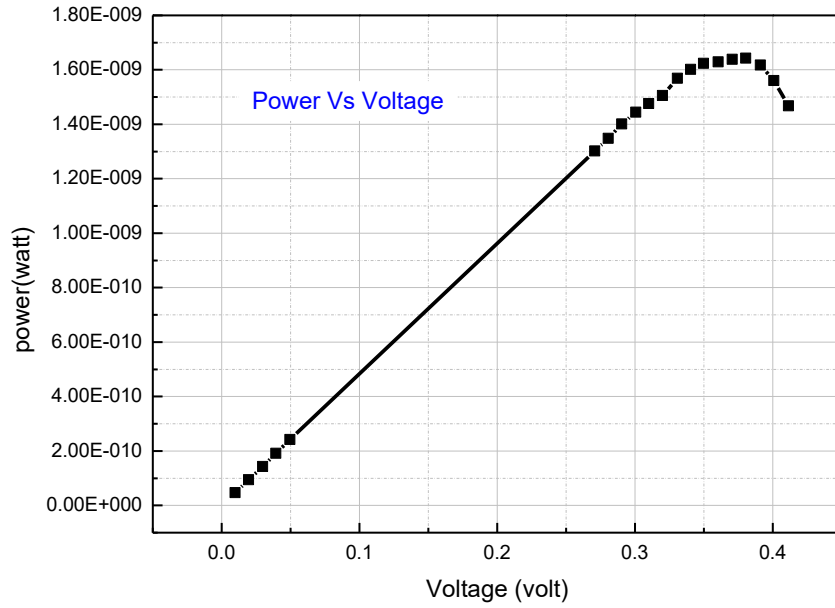


Figure 6.4 P-V curve of Boron Doped Silicon Solar Cell

Table 6.1 Important parameters for boron doped silicon solar cell

Concentration	Open-circuit Voltage, V_{oc} (volt)	Short-circuit Current, I_{sc} (amp)	Fill-Factor (%)	Efficiency (%)
10^{15}	0.4115	4.8×10^{-9}	83.08	18.2
10^{16}	0.4106	4.78×10^{-9}	82.53	18
10^{17}	0.4099	4.74×10^{-9}	82.715	17.88
10^{18}	0.4103	4.64×10^{-9}	83.53	17.66
10^{19}	0.4107	4.58×10^{-9}	85.33	17.33
10^{20}	0.4103	4.55×10^{-9}	83.19	17
10^{21}	0.41055	4.48×10^{-9}	82.623	16.88

Efficiency

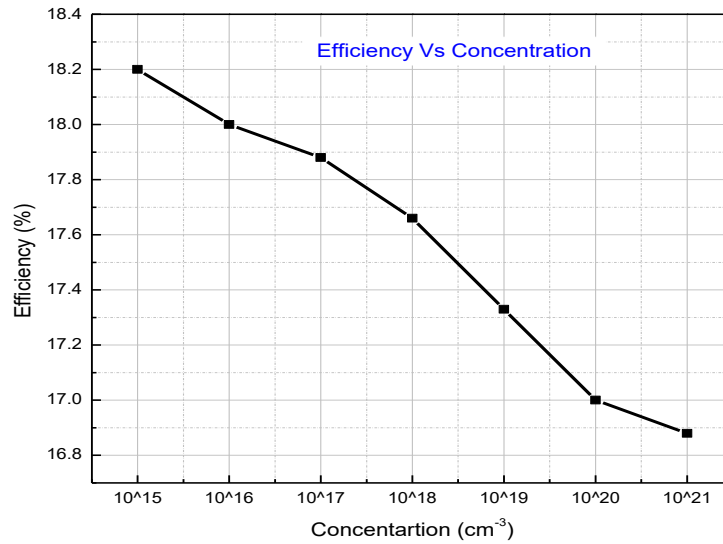


Figure 6.5 Graph of efficiency for different concentration

For figure 6.5 we got the highest efficiency of 18.2% at 10^{15} cm^{-3} and the lowest efficiency 16.88% at 10^{21} cm^{-3} . And with the increasement of concentration the efficiency has decreased.

Fill-Factor

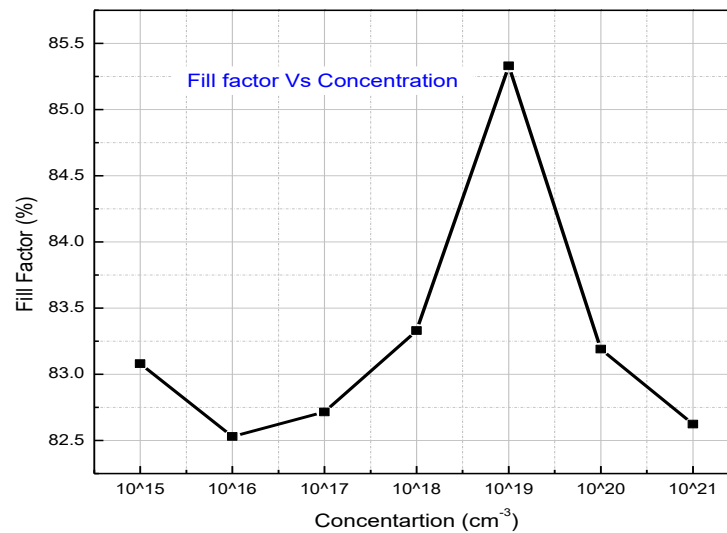


Figure 6.6 Graph of fill factor for different concentration

For figure 6.6 we got the highest efficiency of 83.53 % at 10^{18} cm^{-3} and the lowest efficiency 82.53% at 10^{16} cm^{-3} . But we could not find any significant change of fill factor with concentration as the curve appeared to be random.

6.2.2 Arsenic Doped Silicon Solar Cell

For the calculation we have changed the n-doped arsenic layer from

$(10^{12} - 6 \times 10^{22}) \text{ cm}^{-3}$. Where the fill-factor varied from **82~84%** and the varied from **16~18%**.

I-V Curve (for concentration $3 \times 10^{16} \text{ cm}^{-3}$)

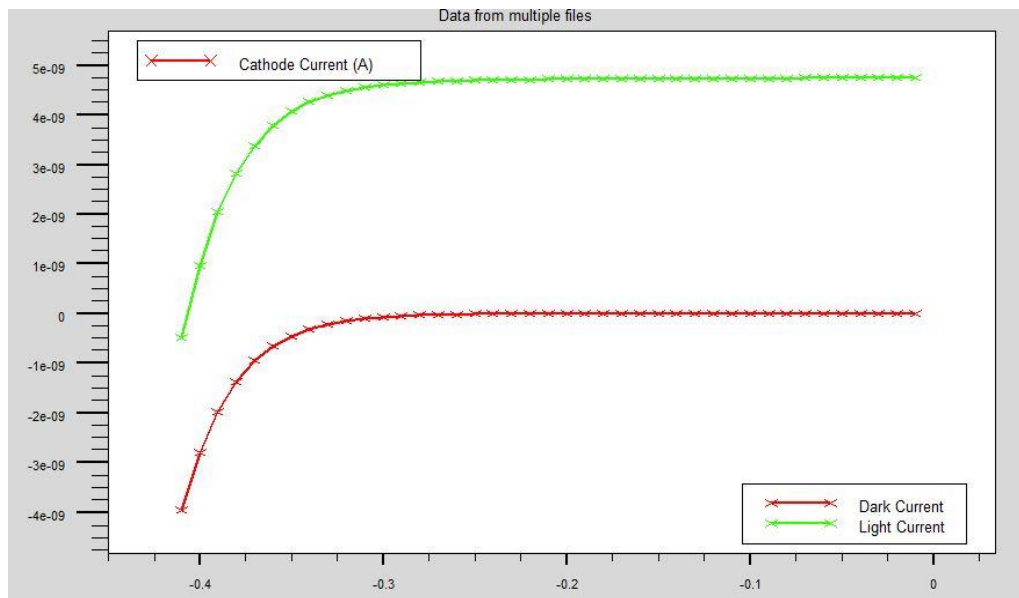


Figure 6.7 I-V characteristics of Arsenic doped Si solar cell

This I-V characteristics curve was mirrored again (like the boron doped silicon solar cell) for further calculation.

P-V Curve (for concentration $3 \times 10^{16} \text{ cm}^{-3}$)

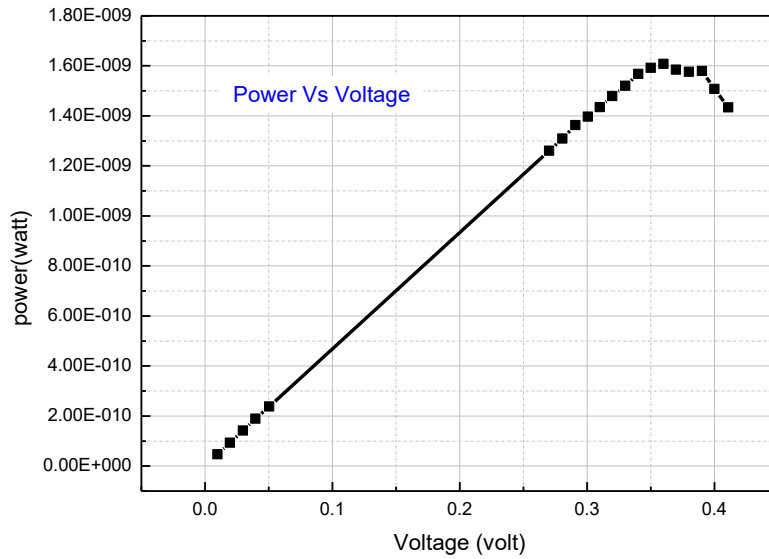


Figure 6.8 P-V characteristics of Arsenic doped Si solar cell

Table 6.2 Important parameters for arsenic doped silicon solar cell

Concentration	Open-circuit Voltage, V_{oc} (volt)	Short-circuit Current, I_{sc} (amp)	Fill-Factor (%)	Efficiency (%)
10^{12}	0.411	4.84×10^{-9}	82.34	18.27
2×10^{14}	0.4104	4.84×10^{-9}	83.245	18.38
3×10^{16}	0.4108	4.77×10^{-9}	82.099	17.88
4×10^{18}	0.40015	4.58×10^{-9}	84.347	17.33
5×10^{20}	0.4105	4.49×10^{-9}	82.1248	16.77
6×10^{22}	0.4105	4.39×10^{-9}	82.063	16.44

Efficiency

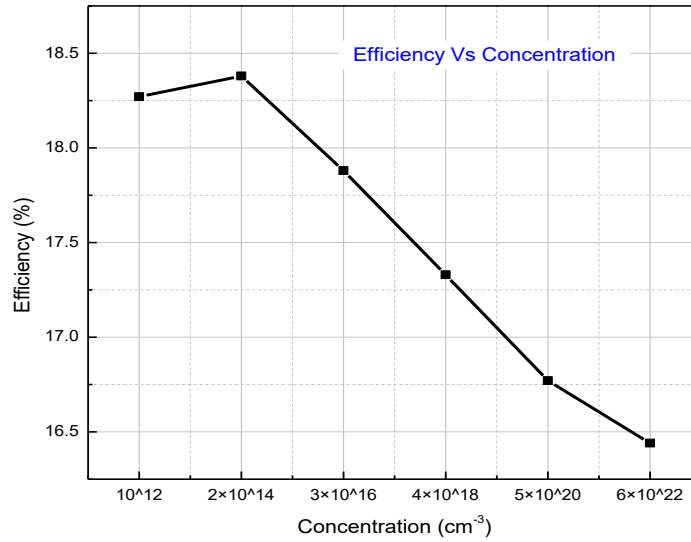


Figure 6.9 Efficiency for different concentration

For figure 6.9 we got the highest efficiency of 18.38% at $2 \times 10^{14} \text{ cm}^{-3}$ and the lowest efficiency 16.44% at $6 \times 10^{22} \text{ cm}^{-3}$. At first it the efficiency increased but later with the increasing concentration the efficiency has decreased.

Fill-Factor

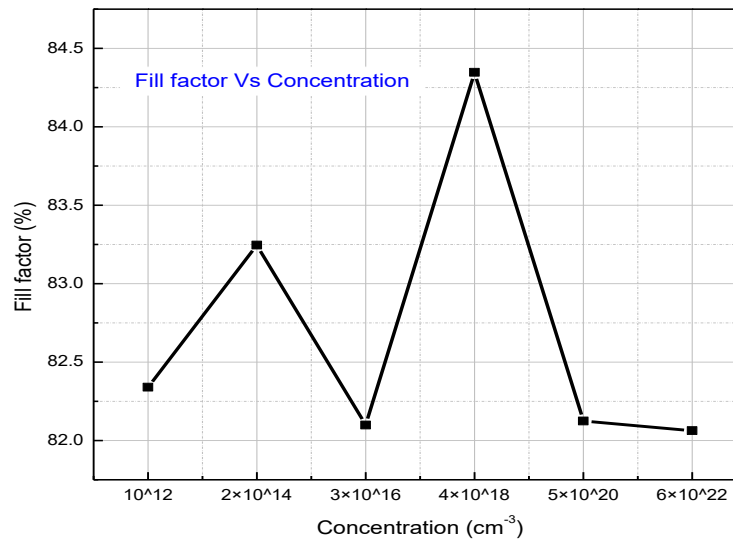


Figure 6.10 Fill Factor for different concentration

For figure 6.10 we got the highest efficiency of 84.347 % at $4 \times 10^{18} \text{ cm}^{-3}$ and the lowest efficiency 82.063% at $6 \times 10^{22} \text{ cm}^{-3}$. The curve is a random one maintaining a sequence of increment and decrement of fill factor with the increase of concentration.

6.2.3 Phosphorus Doped Silicon Solar Cell

For the calculation we have changed the n-doped phosphorus layer from $(10^{12} - 6 \times 10^{22}) \text{ cm}^{-3}$. Where the fill-factor varied from **82~84%** and the varied from **17~18%**.

I-V Curve (for concentration $4 \times 10^{19} \text{ cm}^{-3}$)

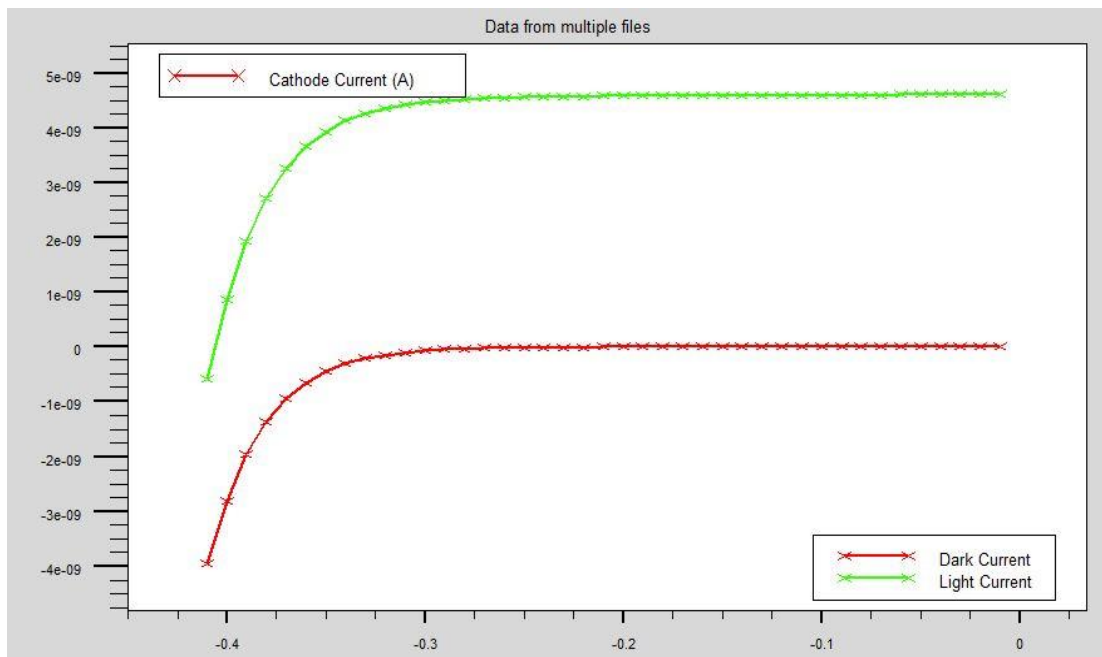


Figure 6.11 I-V curve for phosphorus doped Si solar cell

This I-V characteristics curve was mirrored again (like the boron doped silicon solar cell) for further calculation.

P-V Curve (for concentration $4 \times 10^{19} \text{ cm}^{-3}$)

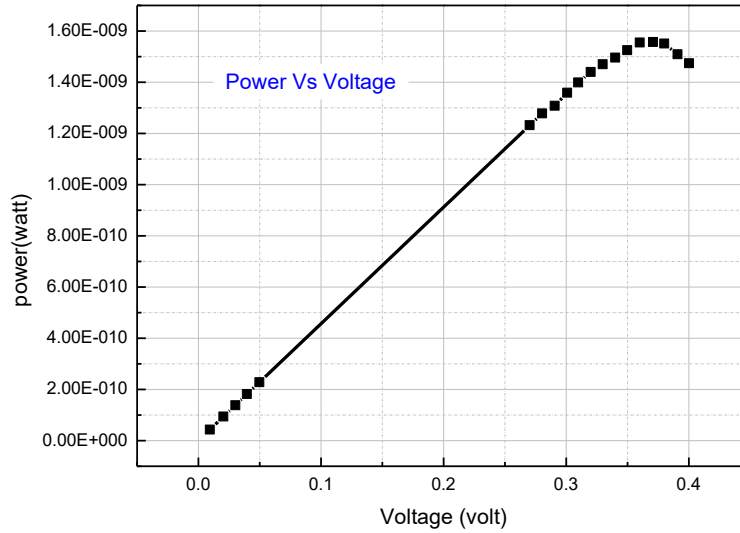


Figure 6.12 P-V curve for phosphorus doped Si solar cell

Table 6.3 Important parameters for phosphorus doped silicon solar cell

Concentration	Open-circuit Voltage, V_{oc} (volt)	Short-circuit Current, I_{sc} (amp)	Fill-Factor (%)	Efficiency (%)
1.5×10^{13}	0.4096	4.87×10^{-9}	82.40	18.25
2×10^{15}	0.411	4.84×10^{-9}	82.34	18.24
2.5×10^{15}	0.4108	4.86×10^{-9}	81.64	18.11
3×10^{17}	0.4104	4.84×10^{-9}	83.245	18.55
3.5×10^{17}	0.4104	4.82×10^{-9}	81.35	17.55
4×10^{19}	0.4108	4.77×10^{-9}	82.099	17.88
4.5×10^{19}	0.4103	4.54×10^{-9}	83.24	17.22
5×10^{21}	0.40015	4.58×10^{-9}	84.35	17.33

Efficiency

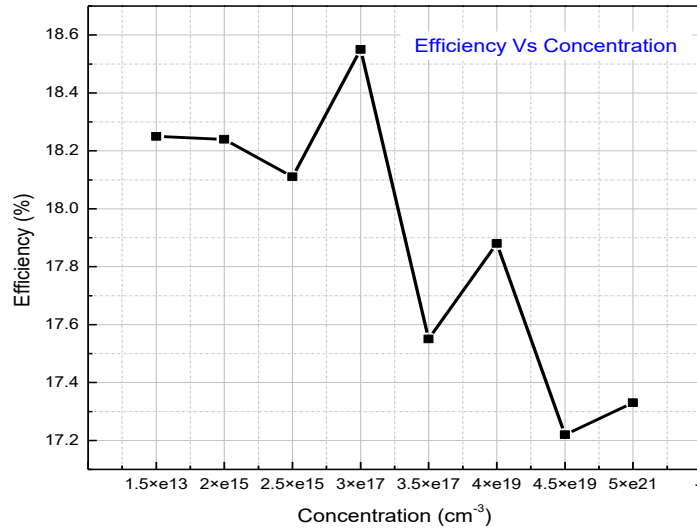


Figure 6.13 Efficiency for different concentration

For figure 6.13 we got the highest efficiency of 18.55% at $3 \times 10^{17} \text{cm}^{-3}$ and the lowest efficiency 17.22% at $4.5 \times 10^{19} \text{cm}^{-3}$. There is no regularity maintained in the curve.

Fill-Factor

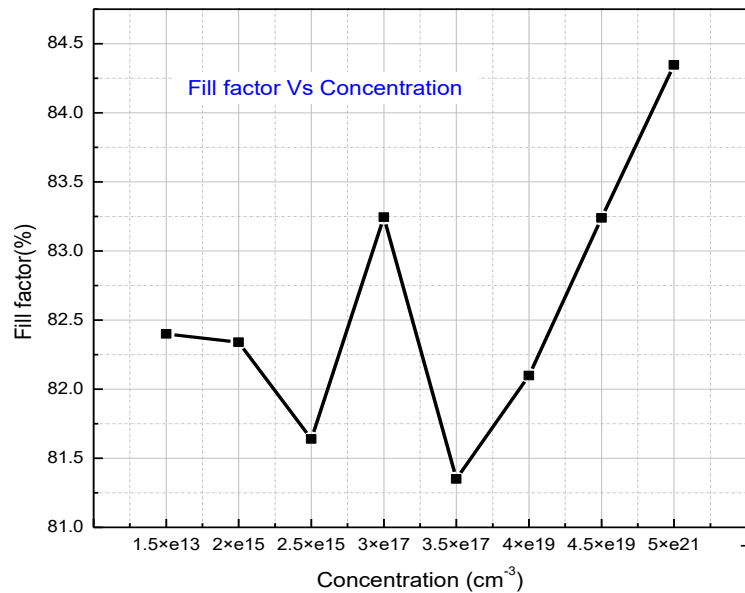


Figure 6.14 Fill factor for different concentration

For figure 6.14 we got the highest efficiency of 84.35 % at $5 \times 10^{21} \text{cm}^{-3}$ and the lowest efficiency 81.35% at $3.5 \times 10^{17} \text{cm}^{-3}$. No sequence is maintained in the curve.

6.3 COMPARISON BETWEEN DIFFERENTLY DOPED SILICON SOLAR CELL

Efficiency and fill factor are the one of the most important parameter in order to compare the overall performance and quality of solar devices. So we are considering both the parameters in order to compare between the differently doped single junction solar cells.

Comparison of efficiency

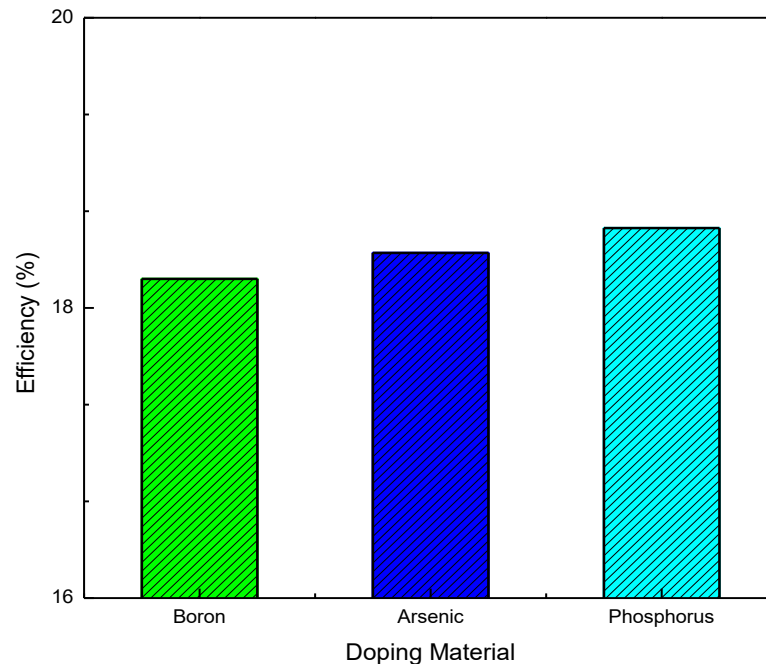


Figure 6.15 Efficiency for different material doped Si solar cell

We got the highest efficiency for phosphorus doped silicon solar cell (18.55%) and lowest for the boron doping (18.2%).

Comparison of fill factor

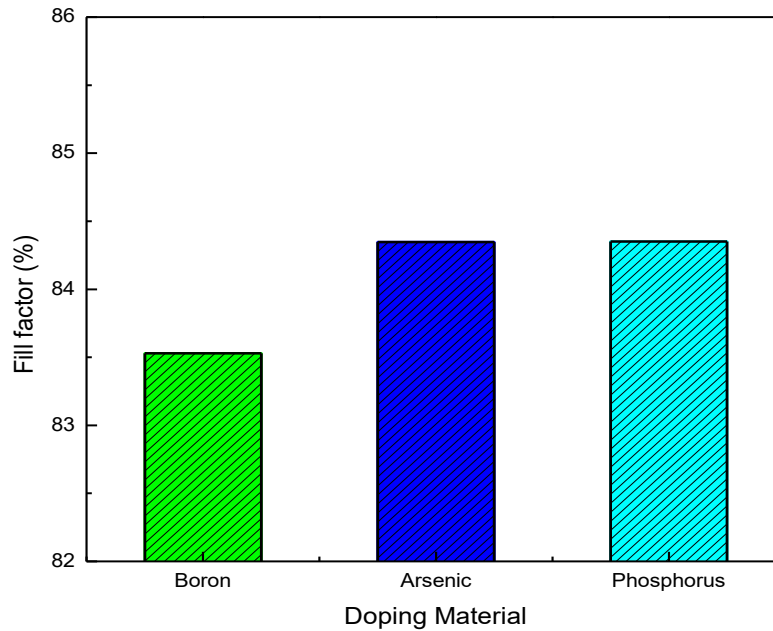


Figure 6.16 Fill factor for different material doped Si solar cell

We also got the highest fill factor for phosphorus doped silicon solar cell (84.35%). We got almost same fill factor (84.347%) for arsenic doped solar cell and eventually lowest for the boron doping (83.53%).

6.4 DUAL JUNCTION SOLAR CELL

We have further moved our analysis from single junction to dual junction. We have observed that the efficiency is much more higher than the single junction solar cell. So the rest of our evaluation is on the basis of dual-junction, varying different variables of it which includes concentration, materials, layering etc. In the recent research work the efficiency of the tandem cells have been achieved up to 45%. Here we have conducted our assessment on two DJs which is InGaP-GaAs and AlGaAs-GaAs.

6.4.1 InGaP-GaAs Dual Junction Solar Cell

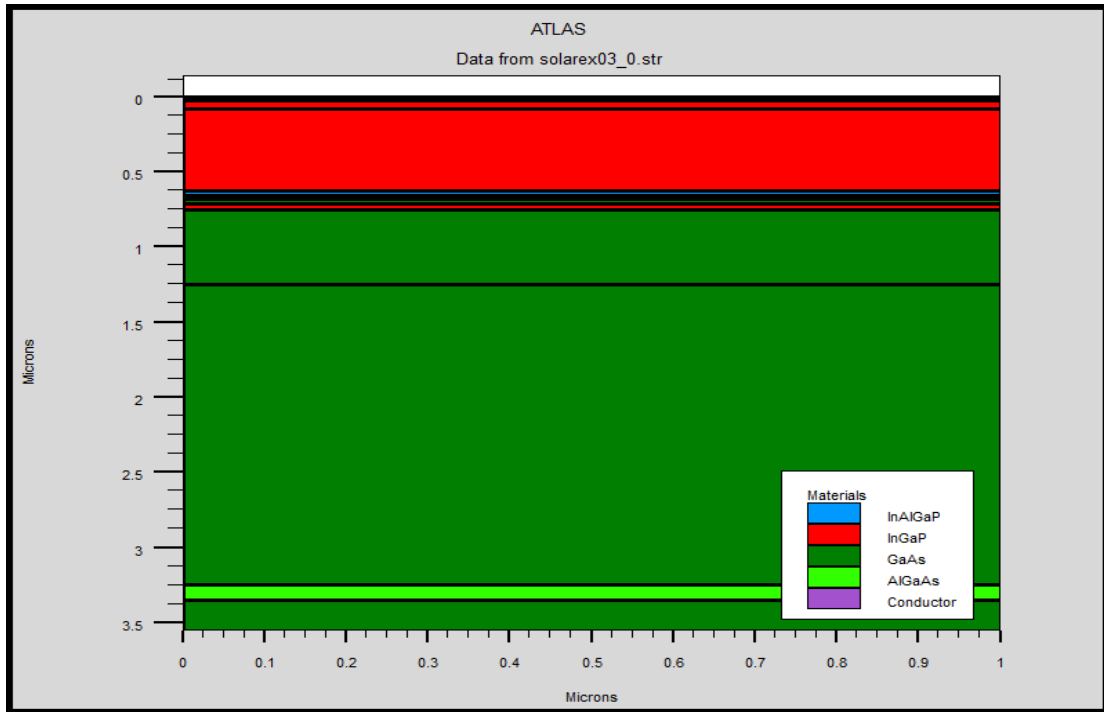


Figure 6.17 Schematic diagram of InGaP-GaAs solar cell

I-V Curve

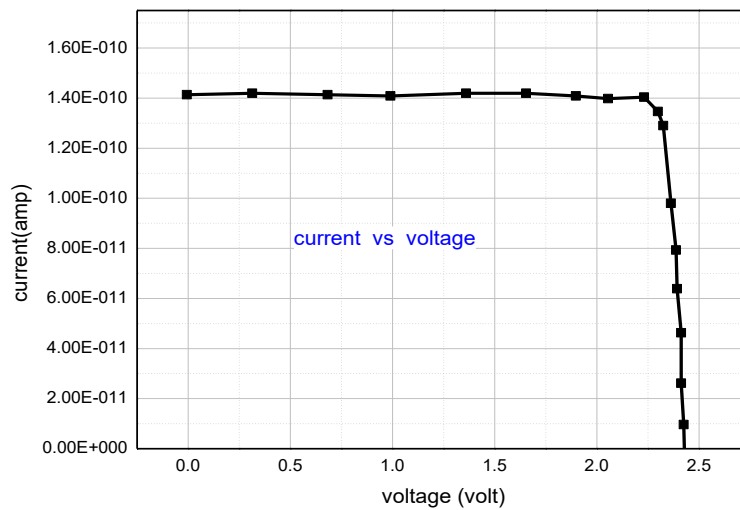


Figure 6.18 I-V characteristic of InGaP-GaAs dual junction solar cell

From figure 6.18 after analyzing we get, $V_{oc}=2.44V$, $I_{sc}=1.41 \times 10^{-10} A$ and $P_{max}=3.13 \times 10^{-10} W$.

P-V Curve

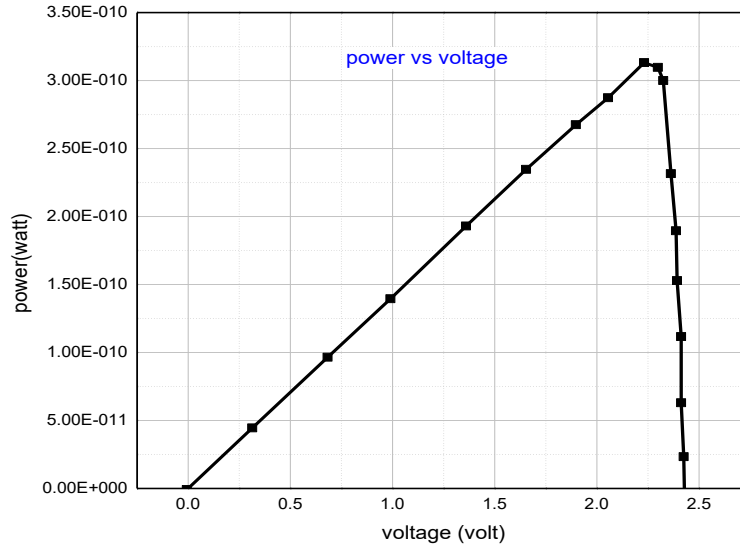


Figure 6.19 P-V characteristic of InGaP-GaAs dual junction solar cell

From figure 6.19 after analyzing we get, $FF=90.98\%$ and $\eta=37.085\%$

6.4.2 AlGaAs-GaAs Dual Junction Solar Cell

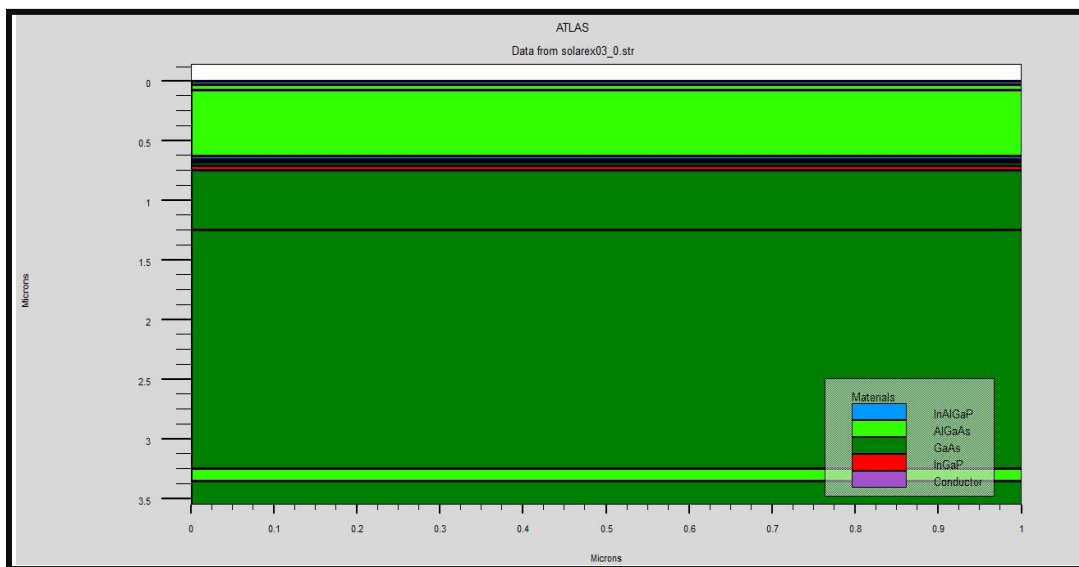


Figure 6.20 Schematic diagram of AlGaAs-GaAs dual junction solar cell

I-V Curve

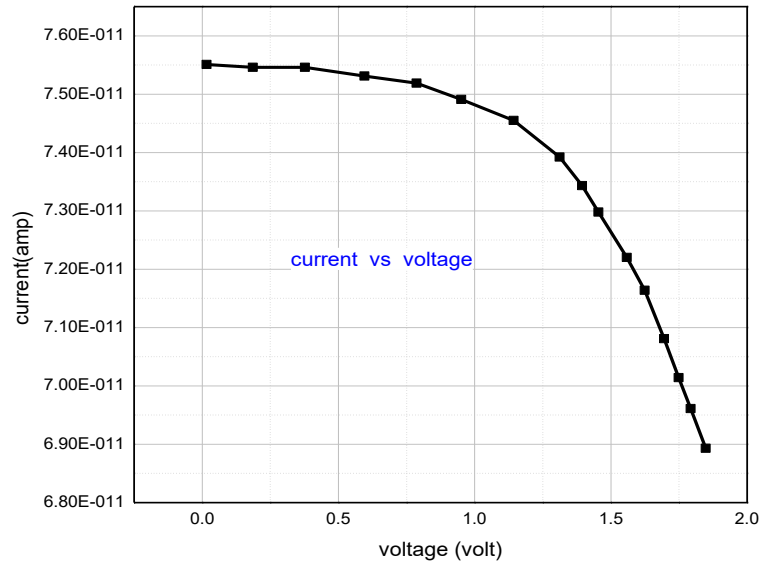


Figure 6.21 I-V characteristics of AlGaAs-GaAs dual junction solar cell

From figure 6.21 after analyzing we get $V_{oc}=1.75V$, $I_{sc}=7.55 \times 10^{-11}A$ and $P_{max}=6.11 \times 10^{-9}W$.

P-V Curve

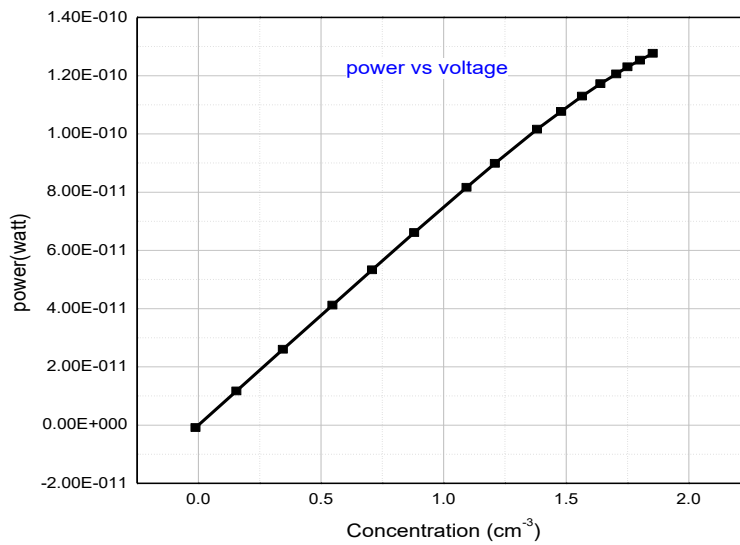


Figure 6.22 P-V characteristics of AlGaAs-GaAs dual junction solar cell

From figure 6.22 after analyzing we get $FF=91.258\%$ and $\eta=15.16\%$.

Comparison between different cells Efficiency

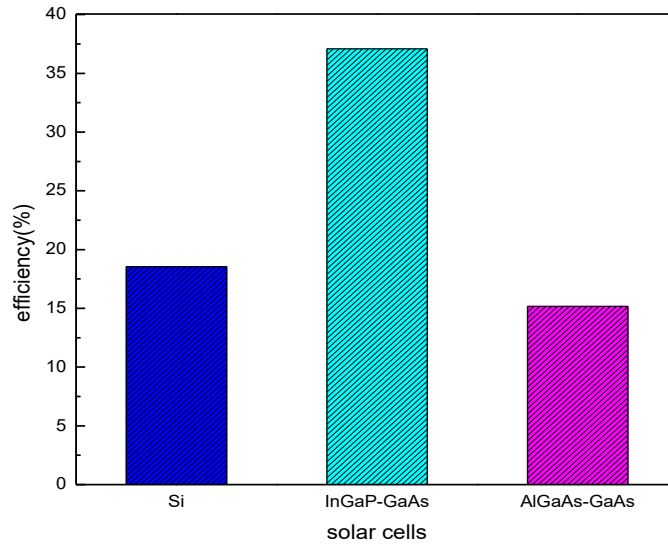


Figure 6.23 Efficiency for different solar cell

From figure 6.23 We got the highest efficiency for InGaP-GaAs solar cell (37.08%) and lowest for the AlGaAs-GaAs (15.36%). Though both of them are DJ but the cell with higher bandgap difference got the highest efficiency.

Comparison between different cells fill factor

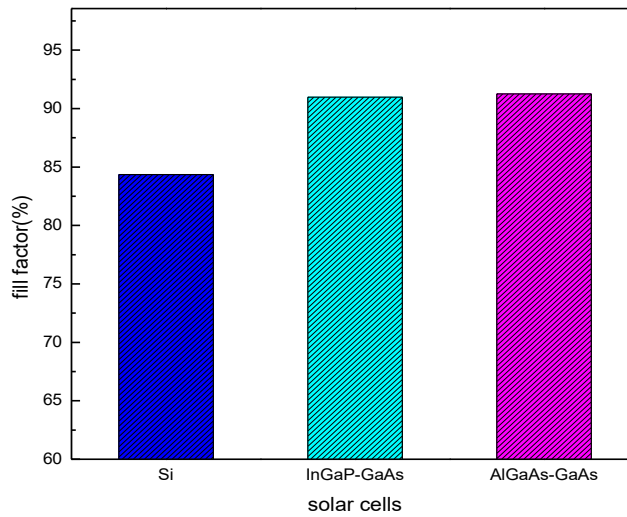


Figure 6.24 Fill factor for different solar cells

From figure 6.24 we observe that the highest fill factor is for AlGaAs-GaAs(91.25%) and lowest for silicon solar cell(83.08%). There is a slight difference of fill factor between InGaP-GaAs & AlGaAs-GaAs solar cell.

From the above discussion we came up with the decision that InGaP-GaAs has the best efficiency (37.08%). In our next section we have tried to improve InGaP-GaAs solar cell by either by changing the concentration or by replacing the back surface material. Sometimes we have changed the both.

6.5 InGaP-GaAs DUAL JUNCTION SOLAR CELL

This is the most highly efficient solar cell among all the reference cells we have been working with. So to get our desired high efficient solar device our main focus is to make this cell as much efficient as possible.

6.5.1 Concentration Increasing

In this step we have increased the concentration of both junctions.

- **1st attempt (increasing concentration for both junctions initially)**

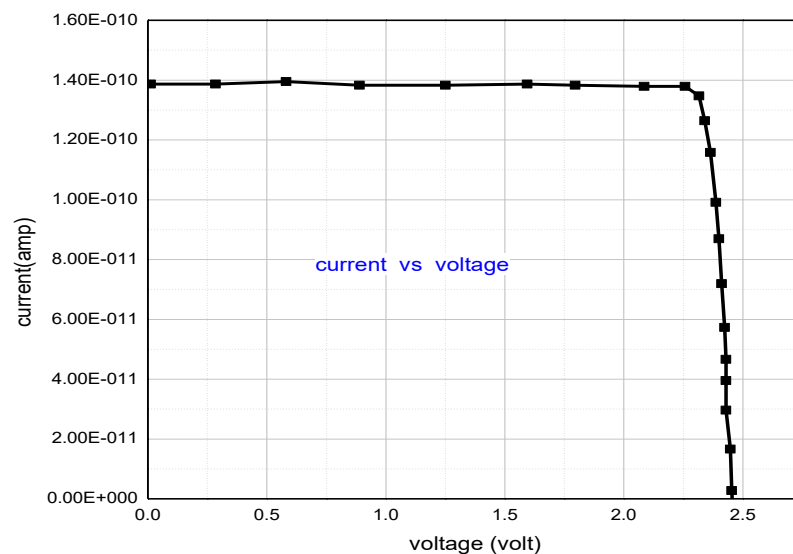


Figure 6.25 I-V curve for high concentration

From figure 6.25 after analyzing we get, $V_{oc}=2.46V$, $I_{sc}=1.39\times 10^{-10}$ A and $P_{max}=3.12\times 10^{-10}$ W.

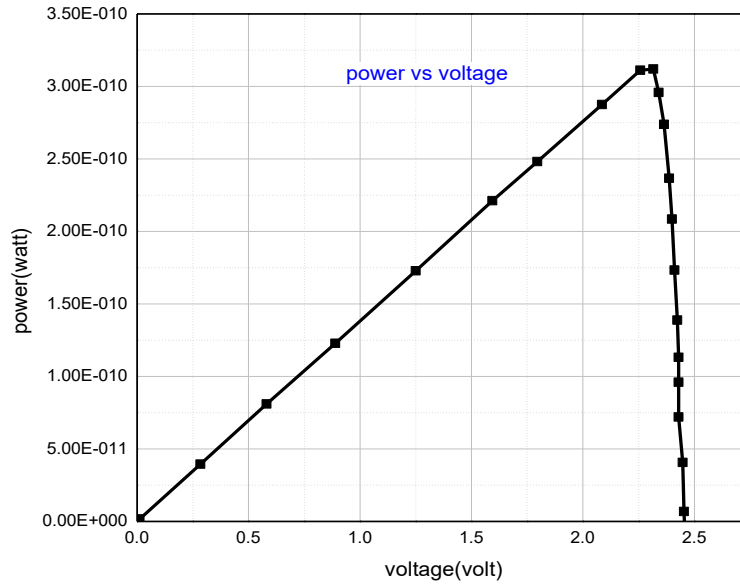


Figure 6.26 P-V curve for high concentration

From figure 6.26 after analyzing we get, $FF=91.24\%$ and $\eta=36.96\%$.

- **2nd attempt (further increasing concentration)**

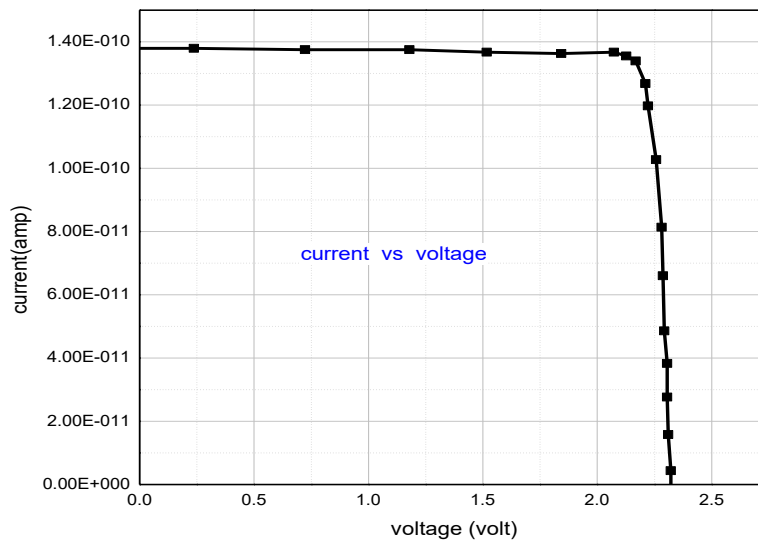


Figure 6.27 I-V characteristics for higher concentration

From figure 6.27 after analyzing we get, $V_{oc}=2.32V$, $I_{sc}=1.38\times 10^{-10}$ A and $P_{max}=2.90\times 10^{-10}$ W.

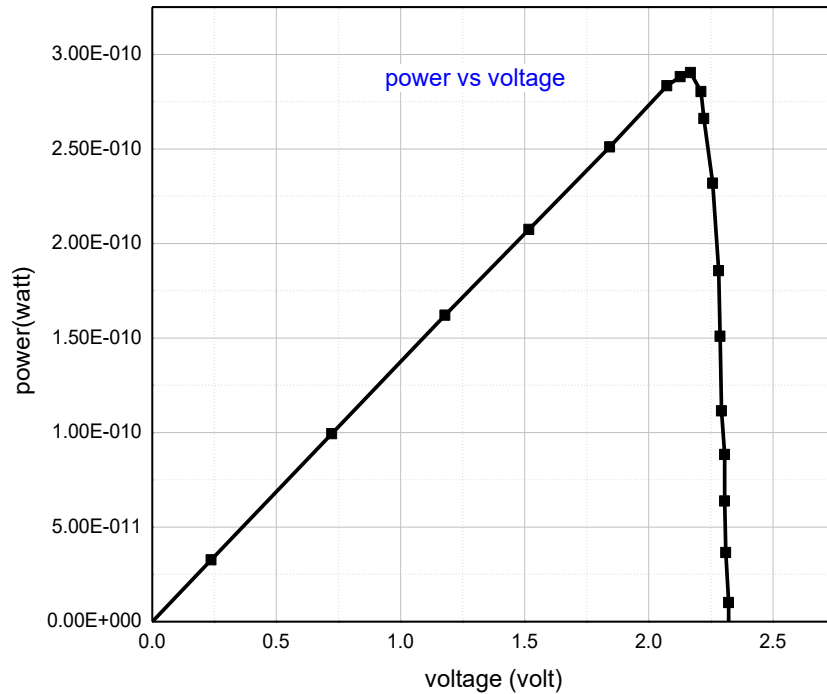


Figure 6.28 P-V characteristics for higher concentration

From figure 6.28 we get, $FF=90.57\%$ and $\eta=34.36\%$.

So from the analysis we can see that the more we increase the concentration of the junctions of the two junctions of our cell we will not be able to get any higher frequency. As the more concentration it becomes more tough for the photon to get through the layers. So for further analysis we must adapt another method in order to get a higher effective cell for further assessment.

From the above discussion we can form a table where we can summarize and show the change of efficiency for increasing concentration of InGaP & GaAs.

Table 6.4 Efficiency for increasing concentration

MATERIAL	THICKNESS (μm)	$\eta=37.08\%$	$\eta=36.96\%$	$\eta=34.36\%$
		CONCENTRATION (cm^{-3})	CONCENTRATION (cm^{-3})	CONCENTRATION (cm^{-3})
InAlGaP	0.0300	$N_A=2\times 10^{18}$	$N_A=2\times 10^{18}$	$N_A=2\times 10^{18}$
InGaP	0.0500	$N_A=2\times 10^{18}$	$N_A=5\times 10^{18}$	$N_A=8\times 10^{18}$
InGaP	0.5500	$N_D=7\times 10^{16}$	$N_D=9\times 10^{16}$	$N_D=10\times 10^{16}$
InAlGaP	0.0300	$N_D=2\times 10^{18}$	$N_D=2\times 10^{18}$	$N_D=2\times 10^{18}$
GaAs	0.0250	$N_D=5\times 10^{19}$	$N_D=5\times 10^{19}$	$N_D=5\times 10^{19}$
GaAs	0.0250	$N_A=3\times 10^{19}$	$N_A=3\times 10^{19}$	$N_A=3\times 10^{19}$
InGaP	0.0400	$N_A=3\times 10^{18}$	$N_A=3\times 10^{18}$	$N_A=3\times 10^{18}$
GaAs	0.5000	$N_A=2\times 10^{18}$	$N_A=4\times 10^{18}$	$N_A=8\times 10^{18}$
GaAs	2.00	$N_D=2\times 10^{17}$	$N_D=4\times 10^{17}$	$N_D=8\times 10^{17}$
AlGaAs	0.100	$N_D=5\times 10^{18}$	$N_D=5\times 10^{18}$	$N_D=5\times 10^{18}$
GaAs	0.200	$N_D=1\times 10^{18}$	$N_D=1\times 10^{18}$	$N_D=1\times 10^{18}$

6.5.2 Concentration Decreasing

In this step we have decreased the concentration of both junctions.

- 1st attempt (decreasing concentration for both junctions initially)

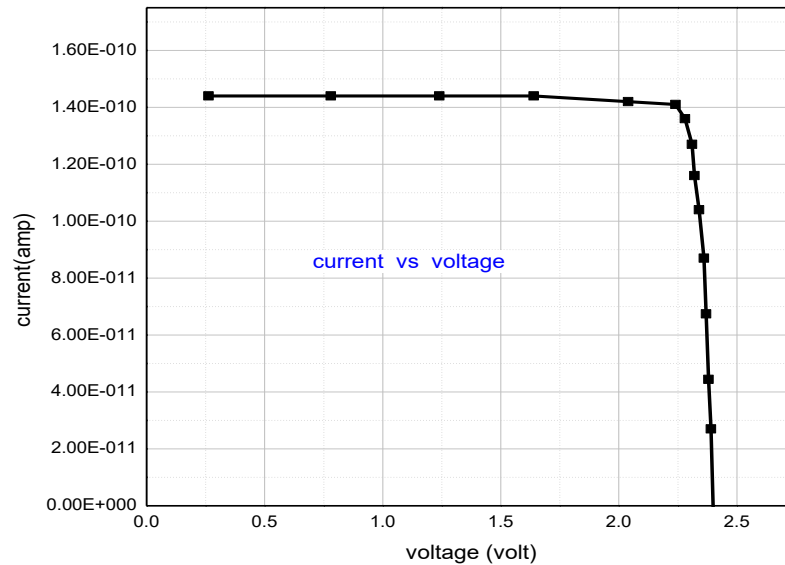


Figure 6.29 I-V curve for decreasing concentration

From figure 6.29 after analyzing we get, $V_{oc}=2.42\text{V}$, $I_{sc}=1.44\times 10^{-10}\text{ A}$ and $P_{max}=3.15\times 10^{-10}\text{ W}$.

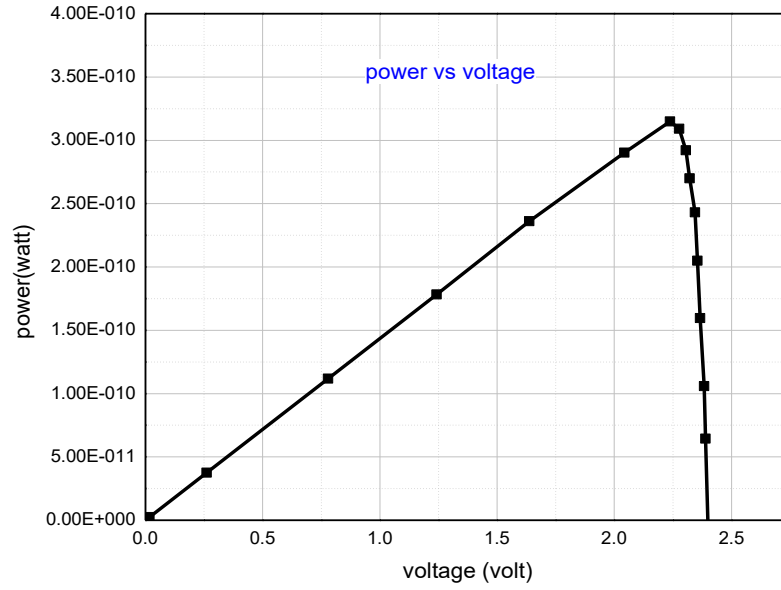


Figure 6.30 P-V curve for decreasing concentration

From figure 6.30 after analyzing we get, FF=90.38% and $\eta=37.32\%$.

- **2nd attempt (further decreasing concentration)**

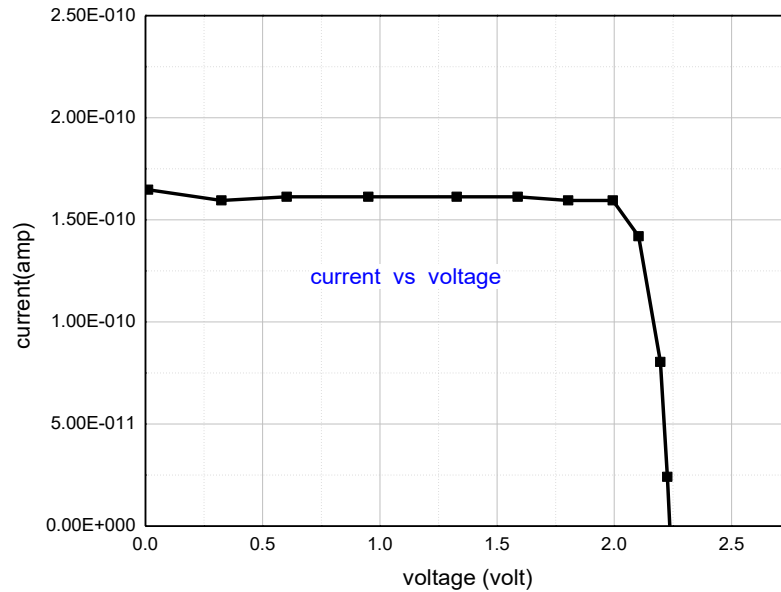


Figure 6.31 I-V curve for lower concentration

From figure 6.31 after analyzing we get, $V_{oc}=2.34V$, $I_{sc}=1.65 \times 10^{-10} A$ and $P_{max}=3.18 \times 10^{-10} W$.

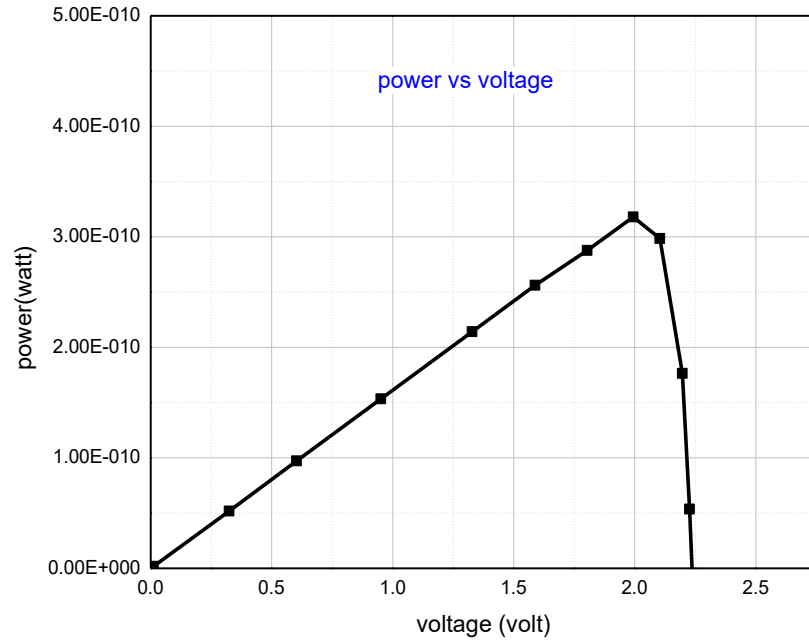


Figure 6.32 P-V curve for lower concentration

From figure 6.32 after analyzing we get, $FF=82.36\%$ and $\eta=38.86\%$.

From our all the calculation we observe a totally opposite situation like our previous case. In this case the more we are decreasing the concentration of the junctions we are getting higher efficiency. So it is the better way of approach.

From the above graph for decreasing concentration we see that for lower concentration efficiency will be high. So we can demonstrate the whole phenomena simply by a table which is demonstrate later.

Table 6.5 Efficiency for decreasing concentration

MATERIAL	THICKNESS (μm)	$\eta=37.08\%$	$\eta=37.32\%$	$\eta=38.86\%$
		CONCENTRATION (cm^{-3})	CONCENTRATION (cm^{-3})	CONCENTRATION (cm^{-3})
InAlGaP	0.0300	$N_A=2\times 10^{18}$	$N_A=2\times 10^{18}$	$N_A=2\times 10^{18}$
InGaP	0.0500	$N_A=2\times 10^{18}$	$N_A=1\times 10^{18}$	$N_A=1\times 10^{18}$
InGaP	0.5500	$N_D=7\times 10^{16}$	$N_D=5\times 10^{16}$	$N_D=3\times 10^{16}$
InAlGaP	0.0300	$N_D=2\times 10^{18}$	$N_D=2\times 10^{18}$	$N_D=2\times 10^{18}$
GaAs	0.0250	$N_D=5\times 10^{19}$	$N_D=5\times 10^{19}$	$N_D=5\times 10^{19}$
GaAs	0.0250	$N_A=3\times 10^{19}$	$N_A=3\times 10^{19}$	$N_A=3\times 10^{19}$
InGaP	0.0400	$N_A=3\times 10^{18}$	$N_A=3\times 10^{18}$	$N_A=3\times 10^{18}$
GaAs	0.5000	$N_A=2\times 10^{18}$	$N_A=1\times 10^{18}$	$N_A=1\times 10^{18}$
GaAs	2.00	$N_D=2\times 10^{17}$	$N_D=1\times 10^{17}$	$N_D=1\times 10^{17}$
AlGaAs	0.100	$N_D=5\times 10^{18}$	$N_D=5\times 10^{18}$	$N_D=5\times 10^{18}$
GaAs	0.200	$N_D=1\times 10^{18}$	$N_D=1\times 10^{18}$	$N_D=1\times 10^{18}$

6.5.3 Changing Back Surface

We have approached another way of analysis by changing the materials of back surface. For InGaP the BSF material in reference model is AlInGaP, but we change it to AlGaAs.

I-V Curve

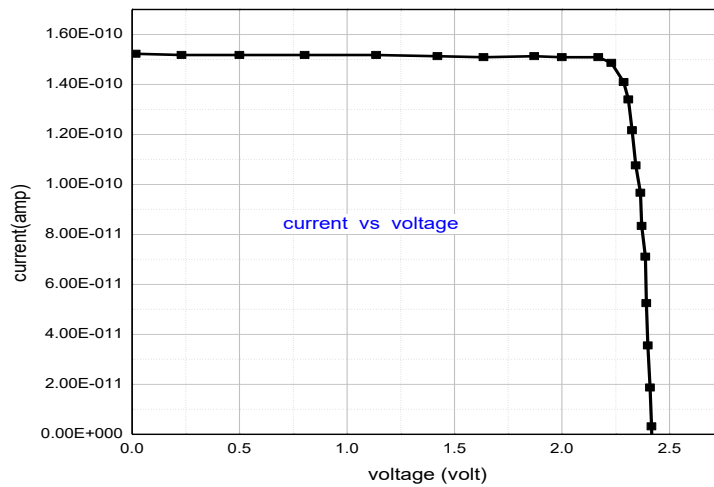


Figure 6.33 I-V curve for new BSF

From figure 6.33 we get, $V_{oc}=2.42V$, $I_{sc}=1.52\times 10^{-10}$ A and $P_{max}=3.31\times 10^{-10}$ W.

P-V Curve

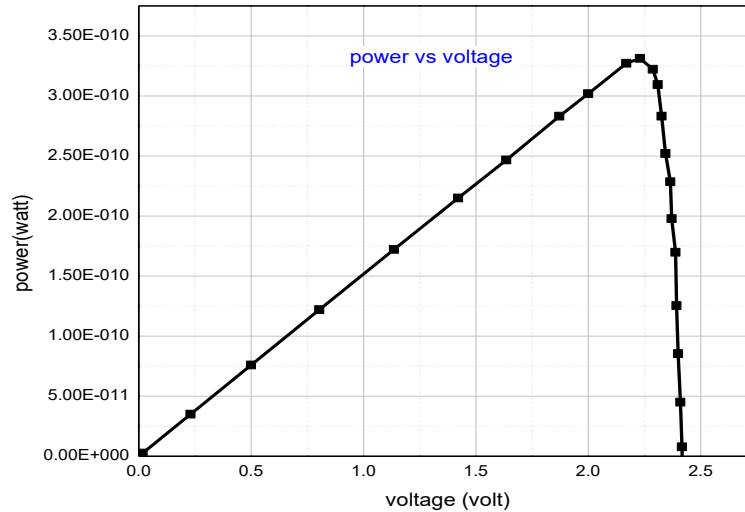


Figure 6.34 P-V curve for new BSF

From figure 6.34 after analyzing we get, $FF=89.98\%$ and $\eta=39.21\%$.

From this data we can see we are getting better efficiency for this new model keeping the reference thickness and concentration. So changing the BSF layer is more effective for InGaP-GaAs solar cell.

Table 6.6 Efficiency between new BSF & reference model

THICKNESS (μm)	CONCENTRATION (cm^{-3})	MATERIAL $\eta=37.08\%$	MATERIAL $\eta=39.21\%$
0.0300	$N_A=2\times 10^{18}$	InAlGaP	InAlGaP
0.0500	$N_A=2\times 10^{18}$	InGaP	InGaP
0.5500	$N_D=7\times 10^{16}$	InGaP	InGaP
0.0300	$N_D=2\times 10^{18}$	InAlGaP	AlGaAs
0.0250	$N_D=5\times 10^{19}$	GaAs	GaAs
0.0250	$N_A=3\times 10^{19}$	GaAs	GaAs
0.0400	$N_A=3\times 10^{18}$	InGaP	InGaP
0.5000	$N_A=2\times 10^{18}$	GaAs	GaAs
2.00	$N_D=2\times 10^{17}$	GaAs	GaAs
0.100	$N_D=5\times 10^{18}$	AlGaAs	AlGaAs
0.200	$N_D=1\times 10^{18}$	GaAs	GaAs

6.5.4 Increasing Concentration for New BSF

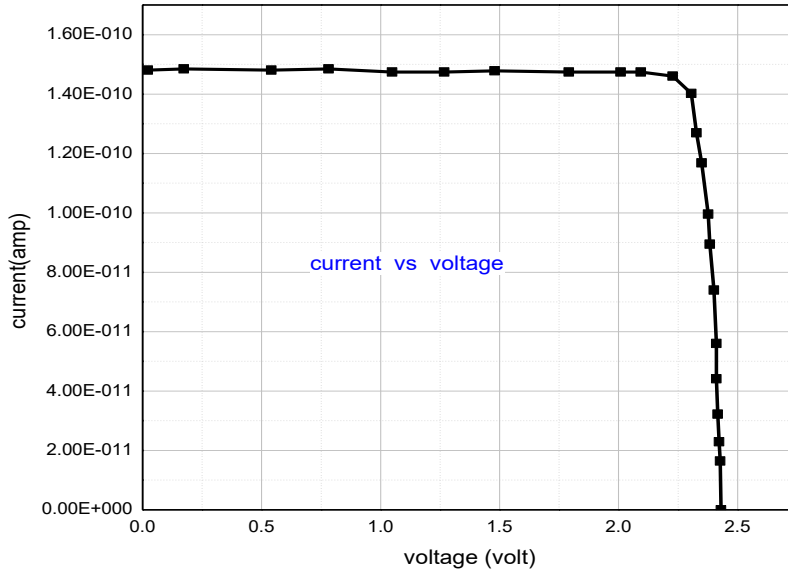


Figure 6.35 I-V curve for increasing concentration in new BSF model

From figure 6.35 after analyzing we get, $V_{oc}=2.42V$, $I_{sc}=1.52\times 10^{-10}$ A and $P_{max}=3.31\times 10^{-10}$ W.

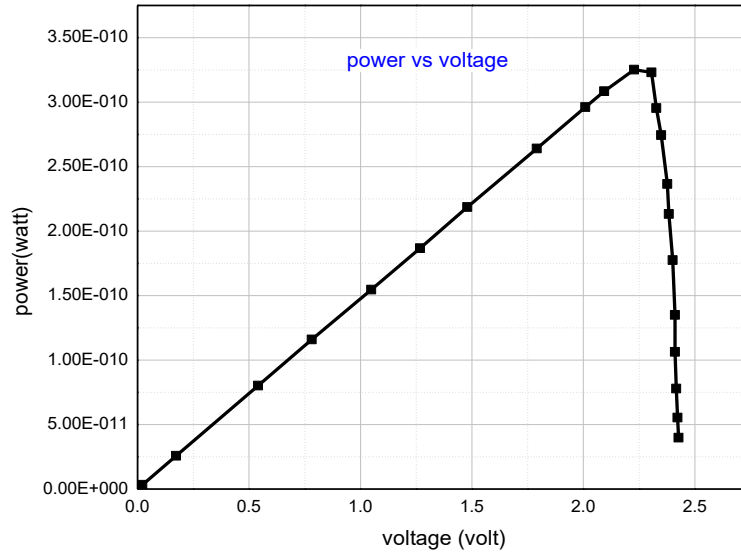


Figure 6.36 P-V curve for increasing concentration in new BSF model

From figure 6.36 after analyzing we get, $FF=90.36\%$ and $\eta=38.5\%$.

6.5.5 Decreasing Concentration for New BSF

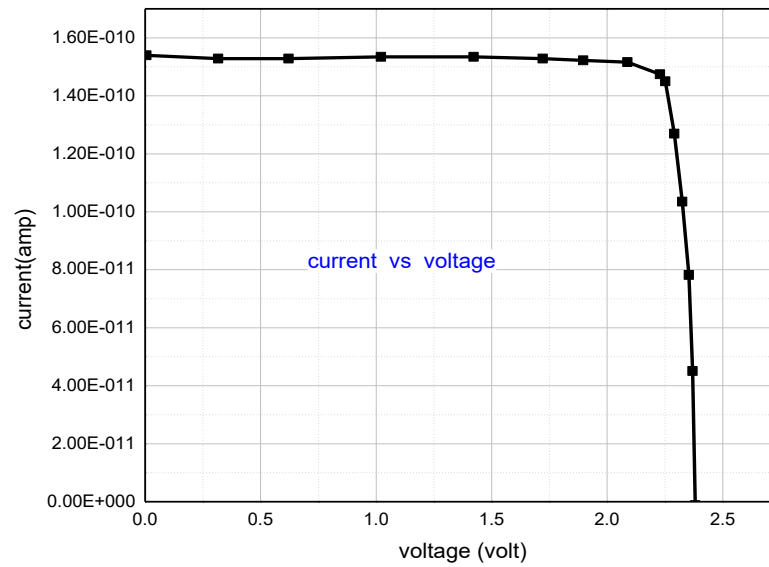


Figure 6.37 I-V curve for decreasing concentration in new BSF model

From figure 6.37 after analyzing we get, $V_{oc}=2.38V$, $I_{sc}=1.54\times 10^{-10}A$ and $P_{max}=3.30\times 10^{-10}W$.

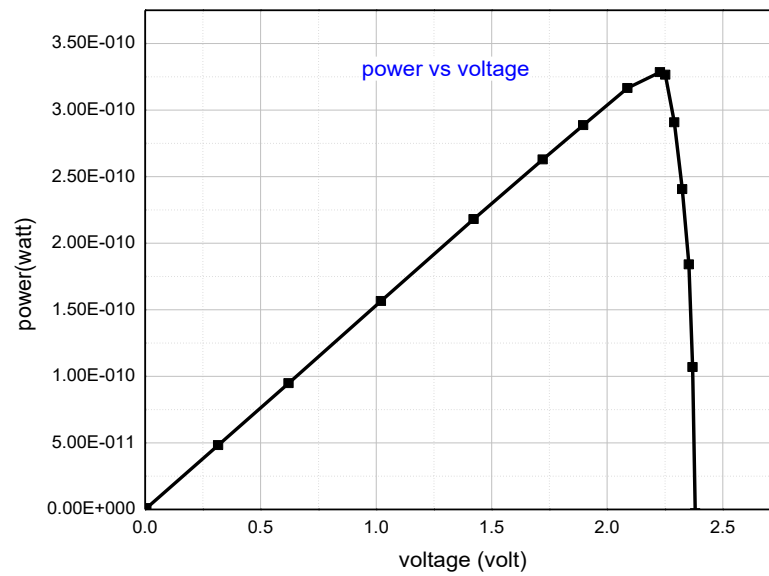


Figure 6.38 P-V curve for decreasing concentration in new BSF model

From figure 6.38 after analyzing we get, $FF=90.15\%$ and $\eta=38.98\%$.

Table 6.7 Efficiency for both increasing & decreasing concentration of new BSF model

MATERIAL	THICKNESS (μm)	η=39.21%	η=38.5%	η=38.98%
		CONCENTRATION (cm ⁻³)	CONCENTRATION (increasing) (cm ⁻³)	CONCENTRATION (decreasing) (cm ⁻³)
InAlGaP	0.0300	$N_A=2\times 10^{18}$	$N_A=2\times 10^{18}$	$N_A=2\times 10^{18}$
AlGaAs	0.0500	$N_A=2\times 10^{18}$	$N_A=4\times 10^{18}$	$N_A=1\times 10^{18}$
AlGaAs	0.5500	$N_D=7\times 10^{16}$	$N_D=9\times 10^{16}$	$N_D=5\times 10^{16}$
AlGaAs	0.0300	$N_D=2\times 10^{18}$	$N_D=2\times 10^{18}$	$N_D=2\times 10^{18}$
GaAs	0.0250	$N_D=5\times 10^{19}$	$N_D=5\times 10^{19}$	$N_D=5\times 10^{19}$
GaAs	0.0250	$N_A=3\times 10^{19}$	$N_A=3\times 10^{19}$	$N_A=3\times 10^{19}$
InGaP	0.0400	$N_A=3\times 10^{18}$	$N_A=3\times 10^{18}$	$N_A=3\times 10^{18}$
GaAs	0.5000	$N_A=2\times 10^{18}$	$N_A=4\times 10^{18}$	$N_A=1\times 10^{18}$
GaAs	2.00	$N_D=2\times 10^{17}$	$N_D=4\times 10^{17}$	$N_D=1\times 10^{17}$
AlGaAs	0.100	$N_D=5\times 10^{18}$	$N_D=5\times 10^{18}$	$N_D=5\times 10^{18}$
GaAs	0.200	$N_D=1\times 10^{18}$	$N_D=1\times 10^{18}$	$N_D=1\times 10^{18}$

6.5.6 Concentration Change for Wider Bandgap for New BSF

Here we have moved on with the device with lower concentration as it has showed the highest efficiency till now. We now have changed the concentration of the junction consist of InGaP which has wider bandgap than the junction made of GaAs.

I-V Curve

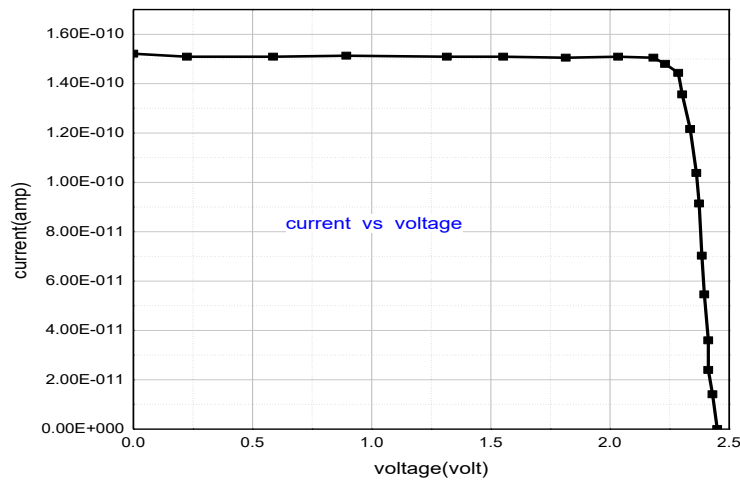


Figure 6.39 I-V curve for new BSF high concentration of InGaP

From figure 6.39 after analyzing we get, $V_{oc}=2.49V$, $I_{sc}=1.51\times 10^{-10}$ A and $P_{max}=3.38\times 10^{-10}$ W.

P-V Curve

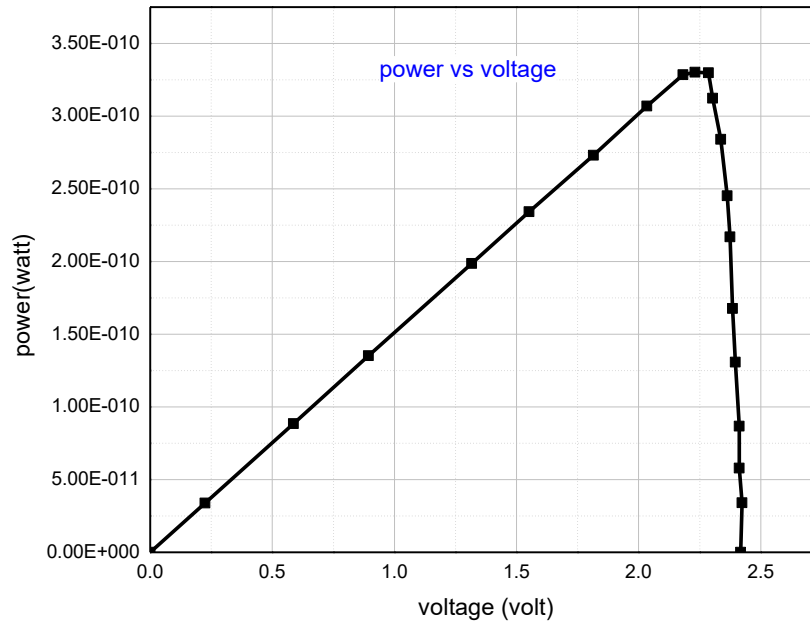


Figure 6.40 P-V curve for new BSF high concentration of InGaP

From figure 6.40 after analyzing we get, $FF=89.89\%$ and $\eta=40.02\%$

So from the whole analysis we can come to our final statement about getting the highest efficiency by mainly approaching two methods. The first way was by changing the back surface. The second method was by increasing the concentration of the junction which is formed by the comparatively wider bandgap materials among the other junctions.

So after combining our two approaches by simulation we have been able to represent a double junction solar cell showing an efficiency of 40.02% .

Table 6.8 Model proposed for highest efficiency

$\eta=40.02\%$		
MATERIAL	THICKNESS (μm)	CONCENTRATION (cm^{-3})
InAlGaP	0.0300	$N_A=2\times 10^{18}$
InGaP	0.0500	$N_A=6\times 10^{18}$
InGaP	0.5500	$N_D=10\times 10^{16}$
AlGaAs	0.0300	$N_D=2\times 10^{18}$
GaAs	0.0250	$N_D=5\times 10^{19}$
GaAs	0.0250	$N_A=3\times 10^{19}$
InGaP	0.0400	$N_A=3\times 10^{18}$
GaAs	0.5000	$N_A=2\times 10^{18}$
GaAs	2.00	$N_D=2\times 10^{17}$
AlGaAs	0.100	$N_D=5\times 10^{18}$
GaAs	0.200	$N_D=1\times 10^{18}$

6.6 CONCLUSION

After the whole analysis we have come up with some certain decisions. Firstly, dual junction solar cells are more efficient than the single junction ones in every condition. Secondly, in case of single junction solar cells the phosphorus doped silicon solar cell is better (for both efficiency and fill factor) than any other single junction cells.

Thirdly, by introducing new BSF the efficiency of dual junction can be significantly increased. Fourthly, increased concentration of the junction of wider bandgap plays a vital to make the device more efficient.

CHAPTER SEVEN

CONCLUSION AND RECOMMENDATION

7.1 CONCLUSION

With the advancement of photovoltaic technology and growing importance of renewable energy based electricity production system the photovoltaic devices have become the most promising field of application. The photovoltaic conversion is the direct transformation of electromagnetic energy of solar radiation to continuous electrical energy. PV market is one of the fastest flourishing industries growing at annual rate of 35-40%. Many researches have been done in the field of efficiency improvement and still under process. The analysis is based on the parameters influencing efficiency through theoretical and practical approach.

We have analyzed and observed all the data using TCAD simulation tools. We carried out the simulation process and made calculation of efficiency, fill factor of number of single and multi junction solar cells by changing different variables. Different values were taken and compared for various types of multijunction solar cells and maximum efficiency was observed for the case of InGaP-GaAs dual junction cell.

A dual junction solar cell model of InGaP-GaAs have been proposed. The concentration and BSF layer of InGaP was changed to achieve maximum conversion efficiency. The optimized solar cell provided efficiency of 40.02% and fill factor of 89.89%. Thus we have demonstrated the importance of the material and concentration of BSF layer on the performance of solar cell.

7.2 RECOMMENDATION FOR FUTURE

We have worked on single junction solar cell using three materials P,As,B for doping purpose. In future many other materials can also be used in case of doping to improve efficiency.

- We used crystalline silicon substrate in case of single junction solar cell. Amorphous silicon substrate can be used for future prospect to achieve better efficiency due to its high bandgap, environmental friendly structure.
- The observations found from single and dual junction solar cell, the latter provide better efficiency. So more importance can be given to the dual junction pv cells for further developments.
- Concentrations can be changed to make the device more economical and cost effective.
- In future the BSF layer of higher bandgap can be used than we have used.
- By bandgap engineering in future, we can improve the dual junction to triple and quadrant junction solar cells.